Summer 2015

The development of cationic polymers for non-viral gene delivery system

Amaraporn Wongrakpanich
University of Iowa

THE DEVELOPMENT OF CATIONIC POLYMERS FOR NON-VIRAL GENE DELIVERY SYSTEM

by

Amaraporn Wongrakpanich

A thesis submitted in partial fulfillment
of the requirements for the Doctor of
Philosophy degree in Pharmacy
in the Graduate College of
The University of Iowa

August 2015

Thesis Supervisor: Professor Aliasger K. Salem

Graduate College
The University of Iowa
Iowa City, Iowa

CERTIFICATE OF APPROVAL

PH.D. THESIS

This is to certify that the Ph.D. thesis of

Amaraporn Wongrakpanich

has been approved by the Examining Committee
for the thesis requirement for the Doctor of Philosophy
degree in Pharmacy at the August 2015 graduation.

Thesis Committee:
Aliasger K. Salem, Thesis Supervisor

Maureen D. Donovan

Peter S. Thorne

Lewis L. Stevens

Nicole K. Brogden

To my parents

ACKNOWLEDGMENTS

My deep gratitude goes first to my advisor, Dr. Aliasger K. Salem for giving me the opportunity to do research in his lab and teaching me how to design and carryout experiments independently. His ability to always recognize the positive side of any situation allowed me to have confidence in my work and encouraged me to stay motivated. This helped a lot in my research as things don't always go as expected. I hope to repay his gratitude towards me and show him how much I learned during the time spent in his lab. I look forward to our collaboration in the future.

I would also like to show appreciation to my thesis and comprehensive exam committee, including Dr. Peter Thorne, Dr. Maureen Donovan, Dr. Lewis Stevens, Dr. Nicole Brogden, Dr. Jennifer Feigel and Dr. Mahfoud Assem for their insightful suggestions and discussion during the progress of this work that has made me a better researcher. I would like to thank Dr. Douglas Flanagan, from whom I took two courses that enhanced my ability to not only learn and think on my own but to really understand difficult concepts rather than just using memorization alone.

I would like to thank Dr. Peter Thorne, Dr. Lyse Norian, Dr. Vicki Grassian, Dr. Aloysius Klingelhurtz and Dr. Douglas Spitz for their helpful suggestions during our collaboration over various projects. I'm also grateful to Dr. Andrea Adamcakova-Dodd, Dr. Meng Wu and Dr. Mei-ling Joiner for teaching and guiding me with their expertise in in vivo pulmonary delivery methods, High-Content Screening and mitochondria model in heart diseases, respectively. I thank Kathy Walters and Chantal Allamargot of Central Microscopy Research Facility for teaching me useful microscopy techniques. Also, the graduate students who worked closely with me; Brett Gross, Imali Mudunkotuwa, Kranti Mapuskar, Amani Makkouk, Kristan (Sorensen) Worthington, Xin Qi and others that are not mentioned here.

All of this work would not have been possible without my labmates. I would like to thank Dr. Sean Geary (who helped me tremendously with writing, taught me to think like a scientist and who is a great friend), Vijaya Joshi (who taught me everything in the lab from pipetting, handling biohazardous waste to making complicated fancy particles), Sheetal D'mellow, Kawther Ahmed, Dahai Jiang, Caitlin Lemke, Kareem Ebeid, Nattawut Leelakanok, Keerthi Atluri, Angie Morris, Anh-Vu Do, Behnoush Khorsand, Khanidtha Chitphet, Cristina Maria de Barros and Emad Wafa with the wonderful scientific discussions and helping me with anything I needed. I will never forget the great times I had during lab gatherings, chit chatting during group lunches, sipping coffee on the deck or even fighting for space in the cell culture hood. I am looking forward to reading about your guys' work in the big journals later!

I also want to acknowledge Lois Baker, Rita Schneider, Debra Goodwin and Brenda Zobeck for helping me with administrative work during my PhD program.

I would like to thank two professors in Thailand, Dr. Doungdaw Chantasart and Dr. Varaporn Junyaprasert. Without them, I wouldn't love Pharmaceutics and wouldn't have had the opportunity to study here at the University of Iowa.

Very special thanks to Eric Foster for always being by my side, sharing my happiness when I got awesome lab results and sharing my sadness when the results were unexplained. He makes Iowa City the happiest place to live. Furthermore, I would like to acknowledge all my friends here in Iowa City and Thai Student Association. I love you all.

Most importantly, none of this could have happened without my family. The love and support of my father, mother and younger sister has been essential in my successes. Thank you Mom, Dad and Gam.

ABSTRACT

Gene therapy involves the delivery of nucleic acid material to target cells in order to alter expression of an important protein, leading to the alleviation of symptoms of a disease. Using vehicles or vectors to carry the genetic material dramatically enhances its successful delivery to the target cells. These vectors can be divided into two main categories, viral and non-viral systems. For the work performed here, the focus was on improving the efficacy of non-viral vectors (made of cationic polymers) in terms of improving transgene expression and reducing cytotoxicity in both in vitro and in vivo systems.

When cationic polymers are mixed with plasmids (pDNA), they form polyplexes which protect pDNA from hash environments and deliver pDNA to target cells. In Chapter 2, polyplexes comprising chitosan and pDNA were formed and two types of pDNA (with and without CpG sequences) were investigated. It was found that chitosan polyplexes containing pDNA without CpG sequences exhibited higher transfection efficiencies and lower inflammatory responses in mice lungs than polyplexes containing pDNA with CpG sequences present. Thus it was apparent that, in order to obtain optimal gene expression with minimal cytotoxicity, the presence of CpG sequences in the pDNA of the polyplexes played an important role.

In Chapter 3, a novel cationic co-polymer, poly(galactaramidoamine), or PGAA, was tested for its transfection efficiency and cytotoxicity in vitro. PGAA/pDNA polyplexes generated high transfection efficiencies in two types of cell lines, HEK293 and RAW264.7. Cytotoxicity of PGAA/pDNA polyplexes increased as the nitrogen to phosphate (N/P) ratios increased.

High-content screening (HCS) has gained interest in cellular imaging because of its ability to provide statistically significant data from multiple parameters simultaneously in cell-based assays. In Chapter 4 HCS was used to measure transfection efficiencies

and cytotoxicities of polyplexes made from fluorescently labeled polyethylenimine (PEI) and pDNA encoding EGFP in HEK293 cells. We also showed that there were 4 – 5 polyplexes found in the cytoplasm of successfully transfected cells, while there was less than 1 polyplex, on average, within the cytoplasm of non-transfected cells. Our findings suggest that HCS has the potential to be used as a tool in the field of gene delivery. HCS does not only simultaneously measure transfection efficiency and cytotoxicity of various non-viral gene vectors; it can also be used to track such vectors through various subcellular compartments.

Our research goal was to develop polyplex formulations made from cationic polymers that generate high transfection efficiencies and low toxicities. We found that pDNA composition was an important parameter with respect to its influence on transgene expression and inflammatory responses. We also introduce a new system to the gene delivery field (high-content screening) with the hope that this could help elucidate and overcome pathways of, and barriers to, successful non-viral based gene delivery systems, respectively.

PUBLIC ABSTRACT

Gene therapy is the process of delivering genetic material, such as DNA (encoding for an important protein) into a patient's cells in order to treat a particular disease such as a genetic disorder or heart disease. This process of DNA delivery into cells is known as "transfection" and it is important that the efficiency of transfection be optimized such that a patient can obtain maximum therapeutic benefit from such a treatment. DNA is susceptible to being destroyed by harsh physiological environments prior to reaching its target. This problem can be diminished with the use of vectors that not only protect against harsh conditions but also encourage entry into cells. By mixing 1) DNA with 2) positively charged polymers, "polyplexes" form which protect DNA from degradation and increase transfection efficiency.

The development of effective polyplex formulations requires optimization. In the work presented here, it was discovered that when polyplexes contained specific sequences within the DNA called "CpG", this lowered transfection efficiencies and increased inflammatory responses compared to DNA without CpG, as measured using a mouse lungs model. Thus, DNA composition played an important role in influencing DNA transfection efficiency of polyplexes. Another aspect to take into account is the degree of positive charge of the polymer. We tested a new polymer called poly(galactaramidoamine) or PGAA. We found that this PGAA can form polyplexes with DNA and could be used in gene therapy. At the present time, mechanisms by which the polyplexes get inside and transfect the cells are still unclear. We also introduced a new system called high-content screening to the gene delivery field. This system offers automated measurements of transfection efficiency and cytotoxicity and could be used to reveal the polyplexes trafficking inside cells.

TABLE OF CONTENTS

LIST OF TABLES

LIST OF FIGURES

PREFACE

Publications from this thesis research

1. Wongrakpanich, A.; Joshi, V. B.; Salem, A. K., Poly(galactaramidoamine) is an efficient cationic polymeric non-viral vector with low cytotoxicity for transfecting human embryonic kidney (HEK293) and murine macrophage (RAW264.7) cells. Pharmaceutical development and technology 2013, 18, (5), 1255-8.
2. Wongrakpanich, A.; Adamcakova-Dodd, A.; Xie, W.; Joshi, V. B.; Mapuskar, K. A.; Geary, S. M.; Spitz, D. R.; Thorne, P. S.; Salem, A. K., The absence of CpG in plasmid DNA-chitosan polyplexes enhances transfection efficiencies and reduces inflammatory responses in murine lungs. Molecular pharmaceutics 2014, 11, (3), 1022-31.
3. Wongrakpanich, A.; Wu, Meng; Salem, A. K., Correlating Intracellular Non-viral Polyplex Localization with Transfection Efficiency using High-Content Screening. Under review in Biotechnology Progress (BTPR-15-0183).

CHAPTER 1 INTRODUCTION

Gene therapy involves the intracellular introduction, in vivo, of nucleic acid material capable of altering expression of a specific protein(s) in order to alleviate the symptoms of a disease [1]. Normally, gene therapy involves DNA, encoding for a desired protein, which is introduced into target cells in order to restore expression of that vital protein [2, 3]. Although in the past, gene therapy has been focused on treating genetic disorders such as cystic fibrosis [4-7], hemophilia [8-10] and sickle cell anemia [11], now a range of other diseases are also targets for gene therapy [12], such as cancer [13-16], autoimmune diseases [17, 18], neurodegenerative diseases [19, 20] and cardiovascular diseases [21-23].

Usually, in gene therapy, the genetic material (or transgene) is delivered to target cells via vehicles, or vectors. Once inside the cells, the genetic material is released from the vector and then transcribed within the nucleus and then translated into the desired therapeutic protein within the cytosol [1, 12]. Vector systems for gene delivery can be divided into two categories, viral and non-viral. Viral vectors are viruses that have been modified to limit viral replication as well as to make room for insertion of the gene(s) of interest. Examples of viral vectors include adenoviruses, adeno-associated viruses, retroviruses, and lentiviruses, all of which are modified to prevent viral replication [24]. Non-viral vectors include inorganic substances (such as calcium phosphate), cationic lipids, as well as synthetic and natural polymers. Of the two, viral vectors are the more effective gene delivery vehicles, yielding high transfection efficiencies in vivo [2, 3, 25, 26]. However, viral vectors have issues with respect to their safety profiles, particularly since they can cause unwanted immunogenic responses and cytotoxicity [27]. Another concern for certain viral vectors is the risk of virus insertional mutagenesis which can interfere with critical cellular functions or be the cause of oncogenesis [28, 29]. The concept of gene therapy was promulgated in the 1970s when Friedmann and Roblin published a paper in

Science: “Gene therapy for human genetic disease?” [30]. Since then, gene therapy whether viral or non-viral, has been continuously in development. To date, there are more than 1800 clinical trials in gene therapy that have been completed or ongoing worldwide [31]. Currently, the first and only gene therapy treatment in the western world that has been approved by the European Commission is alipogene tiparvovec (Glybera®) using adeno-associated virus serotype 1 (AAV1)- viral vector for the treatment of lipoprotein lipase deficiency (LPLD) [32]. Although in clinical trials, this treatment showed promising efficacy and low immunogenicity [33-35], the cost for Glybera® is approximate $1.4 million per one patient and all patients receiving Glybera® are followed for 15 years in order to assess long-term efficacy and safety [36, 37]. Although viral vectors provide high transfection efficiencies and long-term gene expression and have been the dominant gene vector system in clinical trials, the safety concerns and the extremely high cost of therapy are still major barriers. Consequently, the use of viral vectors in clinical trials has decreased significantly over the past decade [1]. Recently, non-viral vectors have drawn attention in the gene therapy field. On the other hand, the use of alternative modes of gene delivery has gradually increased in clinical trials over the past 10 years (18.3% of all trials in 2013 compared to 14% in 2004 [38, 39]). When compared with viral vectors, non-viral vectors, especially polymer-based, have lower immunogenicity and toxicity [1, 40]. Another advantage of non-viral vectors is the ease of production which leads to lower costs. The main drawback of using non-viral vectors is their lower transfection efficiencies compared to viral vectors.

Of the non-viral vectors, cationic polymers have been used extensively at the pre-clinical stage. Cationic polymers condense the genetic material (plasmid DNA, pDNA), which is negatively charged, upon mixing to form polyplexes through an electrostatic interaction. These self-assembling polyplexes condense pDNA into small dense structures. The size, morphology and surface charge of these polyplexes depend on the characteristics of the cationic polymers as well as the formulation details, such as

pDNA concentration, buffer conditions, mixing order and the ratio of the cationic group in the polymer (amine) to the anionic group in pDNA (phosphate) [41, 42]. These polyplexes can protect pDNA from harsh environmental conditions, facilitate cell uptake and release DNA intracellulary close to or at the site of action (nucleus) [43, 44]. At the present time, the internalization mechanism of polyplexes is not well understood [45]. For cellular uptake, the cationic polyplexes bind to the plasma membrane (anionic) through electrostatic interactions and are internalized possibly by endocytic pathways such as clathrin-mediated endocytosis, caveolae-mediated endocytosis or micropinocytosis [46-48]. Moreover, it has been reported that uptake can occur through clathrin- and caveolin-independent endocytosis [46]. After internalization, the polyplexes stay in the endosomes which can fuse with lysosomes for degradation. Therefore, polyplexes have to escape from the endosome in order to successfully transfect cells. A hypothesis called “proton sponge” was proposed by Boussif et al. in 1995 [49]. They studied the cationic polymer, poly(ethylenimine) (PEI), for gene delivery purposes. According to the theory, the amine groups in cationic polymers can be protonated, offering a large buffering capacity during endosomal acidification. This protonation induces an influx of chloride ions and water. Finally, the osmotic swelling leads to endosomal rupture resulting in the release of polyplexes, vectors and/or pDNA into the cytoplasm [49, 50]. The proton sponge hypothesis is the most accepted mechanism in explaining endosomal escape in cationic polymers containing amine groups [50-52]. However, the legitimacy of this theory is still in debate [53-56]. After endosomal escape, the polyplexes should release the pDNA next to or inside the nucleus for transcription to occur. It is possible that polyplexes could travel through the cytoplasm toward the nucleus on microtubules via active transport [57]. The Nuclear membrane surface contains very small nuclear pores (approximately 10 nm in diameter) which are channels for transporting small proteins, ions and metabolites in and out of the nucleus [58, 59]. This is much smaller than the size of the polyplexes (100 – 500 nm in diameter). The mechanism of delivering pDNA to the nucleus by cationic non-viral

vectors is still unknown. The most widely accepted assumption is that nuclear translocation of pDNA occurs during mitosis when there is no nuclear membrane [48]. Although there have been many studies conducted in an attempt to investigate intracellular delivery of polyplexes, the knowledge in this area is still lacking.

Among the cationic polymers being used as non-viral vectors, PEI has been considered the gold standard for transfection in vitro and in vivo and is a promising alternative carrier to viral vectors [60-62]. The factors that contribute to the ability of PEI complexes to mediate efficient transfection include: enhanced protection of DNA from enzymatic degradation, enhanced internalization by cells, and the ability to mediate endosomal escape and then release the DNA [49]. A drawback of PEI is its toxicity and non-degradability [63]. Recently, biodegradable polymers have gained interest in the gene delivery field. Because of their biodegradability, these polymers show low toxicity and can be readily cleared from the body. Thus, these biodegradable polymers can be given to patients for repeated systemic therapeutic use. An example of a biodegradable and biocompatible cationic polymer used in gene therapy is chitosan [64-68]. Although chitosan has low toxicity, its transgene expression is also low. To overcome the problems of low transfection efficiency and high toxicity, various cationic polymers and polyplex formulations have been modified in the hope of creating efficient gene delivery systems.

Research Objective

The ultimate goal of this research was to develop and investigate polyplex formulations made from cationic polymers that were capable of mediating high transfection efficiencies and low cytotoxicities, therefore rendering them as strong candidates for use in non-viral gene delivery.

Rational

This research has been divided into three parts. The first section concerns an investigation of the transfection efficiency, toxicity and immunogenicity of polyplex

formulations as applied to both in vitro and in vivo situations. For this purpose, chitosan, one of the most studied non-viral vectors was chosen. Chitosan is well known as a biodegradable, biocompatible and low toxicity polymer when used as a non-viral vector [69]. Moreover, chitosan and modified chitosan have been shown to be effective transfection reagents in both in vitro and in vivo models [65, 68, 70-72]. Rather than optimizing transfection efficiency through comparisons of chitosan and modified chitosan formulations, which has already been extensively studied, it was instead chosen, in this study section, to investigate another less explored parameter influencing polyplex development and consequently transfection efficiency, which is pDNA composition. To explain, many pDNA vectors contain unmethylated 5'-cytosine-guanosine-3' dinucleotide (CpG) sequences, which can potentially induce inflammatory responses through the production of proinflammatory cytokines [73, 74]. This is because these CpG motifs are recognized as "foreign" in vertebrates by the innate immune system, as they are commonly found in bacterial DNA but rarely found in vertebrates [75]. The immunogenic nature of CpG motifs may reduce in vivo transfection efficiencies of plasmids that harbor them [76]. In this study, pDNA with or without CpG sequences were used to create chitosan polyplexes (CSpp). These polyplexes were tested for transfection efficiencies and cytotoxicity in both in vitro and in vivo models.

The second part of the overall research presented here was to test a recently invented cationic polymer, poly(galactaramidoamine) or PGAA [77-79]. PGAA is a member of the poly(glycoamidoamine)s family which was synthesized by the polymerization of a mixture of dimethyl-*meso*-galactarate and pentaethylenehexamine [77]. PGAA synthesis was influenced by chitosan and PEI. Amine density in polymer structures directly affects cytotoxicity and transfection efficiency. High amine density results in high transfection efficiency and high cytotoxicity. Reducing the amine content can reduce cytotoxicity but also results in low transfection efficiencies [78, 80]. Having amine densities higher than chitosan and lower than PEI, PGAA was designed to have low cytotoxicity and high

transfection efficiency [78]. Thus, PGAA has the potential to be a good cationic non-viral vector. In this study, the transfection efficiency and cytotoxicity mediated by polymeric PGAA non-viral vectors were evaluated. The study was conducted using previously untested cell lines, human embryonic kidney cells (HEK293) and mouse macrophage cells (RAW264.7)).

At the present time, there are more than 30 groups of polymers that are commonly being investigated in preclinical studies as non-viral gene delivery vectors [43, 81]. Since non-viral vectors are gaining more interest in the gene therapy field of late, it is expected that this number will increase. To find optimal transfection conditions for each cationic polymer, many optimization experiments need to be conducted. Although gene delivery has been in use for decades, intracellular trafficking and transfection mechanisms of cationic polymers are still unclear [45]. This knowledge is necessary to improve our understanding of the extracellular and intracellular barriers to transfection in order to design an ideal non-viral vector to overcome these barriers, thereby yielding high transfection efficiencies with minimal toxicity [82]. Using high-content screening (HCS), which is a combination of high-throughput techniques and multicolor fluorescent cellular imaging [83, 84], may help elucidate the mechanisms of, and barriers to, non-viral vector mediated transfection. For the last section of this research, HCS has been introduced as a tool in understanding gene delivery. In this section, PEI, the gold standard for non-viral gene vector was chosen because of its well characterized transfection efficiency and cytotoxicity.

Organization

This dissertation is divided into five chapters. This first chapter includes an introduction to the research, a research objective and rational, organization and peer collaborated efforts.

Chapter two provides the methodologies in making CSpp from purified low molecular weight chitosan and two types of pDNA (with and without CpG sequences) along with the full characterization of the polyplexes. These polyplexes were tested for transfection efficiencies and cytotoxicities in cell lines. These polyplexes have been tested for their capacity to promote inflammatory responses (such as total white blood cell count and cytokine levels obtained from bronchoalveolar lavages) along with transfection efficiencies in murine lung models.

Chapter three describes the methodologies in making PGAA polyplexes as well as polyplex characterizations. These polyplexes were tested for transfection efficiencies and cytotoxicities in two different cell lines.

Chapter four describes the methodologies of preparing polyplexes made from two types of PEI (fluorescently labeled branched-PEI and branched PEI) with pDNA encoding green fluorescent protein (pGEFP-N1) and transfecting them into a cell line (HEK293). The transfection efficiency and cytotoxicity was measured using a HCS instrument. Transfection efficiency and cytotoxicity results were confirmed with manual counting and CellTiter 96® AQueous One Solution Cell proliferation assay (MTS assay), respectively. Moreover, we attempted to investigate intracellular trafficking of these polyplexes by quantifing the number of polyplexes inside the nucleus and cytoplasm 24 hours post-transfection.

Chapter five is the conclusion of this research, what knowledge was gained and how this knowledge can be applied in the non-viral gene therapy field in the future.

Peer Collaborated Efforts

The content in Chapter 2 involved quantifying endotoxin in chitosan, intranasal instillation of the polyplexes into mice lungs, collecting and analysing lung lavages for assessment of inflammatory responses and was a collaborative effort with Professor Peter Thorne, Andrea Adamcakova-Dodd, Nervana Metwali and Wei Xie at Department

of Occupational and Environmental Health, University of Iowa. Detection of ROS precursors (superoxide anions) in vitro after cells were exposed to CSpp was guided by Professor Douglas Spitz and Kranti A. Mapuskar at Department of Radiation Oncology, Carver College of Medicine, University of Iowa.

The content in Chapter 4 involved HCS techniques and image analysis and was a collaborative effort with Meng Wu, Director of High Throughput Screening Facility, Division of Medicinal and Natural Products Chemistry, College of Pharmacy and Department of Biochemistry, Carver College of Medicine, University of Iowa.

CHAPTER 2 THE ABSENCE OF CPG IN PLASMID DNA-CHITOSAN POLYPLEXES ENHANCES TRANSFECTION EFFICIENCIES AND REDUCES INFLAMMATORY RESPONSES IN MURINE LUNGS

Introduction

Chitosan,an abundant linear polysaccharide derived from crustacean shells, is composed of random β-(1-4)-linked D-glucosamines (deacetylated units) and N-acetyl-D-glucosamines (acetylated units) where the number of N-acetyl-D-glucosamine units constitute < 50% (Figure 2-1) [85]. Chitosan has applications in many areas including water treatment, the food industry, and agriculture [86, 87]. And because of its biodegradability and biocompatibility, chitosan has been studied intensively for its therapeutic applications in drug and gene delivery systems [64, 65, 68, 85, 88]. Chitosan has a pK_a value of ~6.5. As the pH of the solvent decreases, below 6.5, the concentration of protonated amine groups in chitosan increases and therefore chitosan can be dissolved in most aqueous acids. Chitosan has gained interest as a cationic non-viral gene delivery vector because of its: (i) relative ease of preparation in aqueous acidic solutions; (ii) low toxicity; and (iii) ability to condense DNA which provides protection against nuclease degradation [89, 90]. The molecular weight and degree of deacetylation of chitosan influence its physical and chemical properties. For gene delivery purposes, low molecular weight chitosan having a degree of deacetylation higher than 80 percent yields high transfection efficiencies and low toxicities [64, 91, 92]. Chitosan can be degraded by various enzymes such as lysozyme, collagenase, *β*-glucosidase, N-acetylglucosaminidase and human chitinase [93-96]. This biodegradable property of chitosan could help in releasing pDNA from chitosan/pDNA polyplexes (CSpp) in physiological conditions.

Previous studies have shown that CSpp are particularly promising as gene delivery formulations for treatment of pulmonary pathologies [97, 98] such as cystic fibrosis

[99, 100], asthma [101] and lung cancer [102]. Although chitosan causes minimal cytotoxicity and is generally non-inflammatory, a drawback is its low transfection efficiency when compared to viral vectors and non-viral synthetic vectors such as polyethylenimine (PEI) [103, 104]. Thus, most of the studies involving CSpp delivery have been focused on strategies to improve transfection efficiency such as optimizing the molecular weight and the degree of deacetylation of chitosan [70, 105, 106], as well as establishing appropriate amine to phosphate ratios (N/P) of chitosan/DNA polyplexes [106]. Mixing chitosan with other cationic gene vectors [107, 108] and/or modifying the structure of chitosan has also resulted in enhanced transfection efficiencies [109-111].

The toxicity of pure or chemically modified chitosan has been investigated in its free form as well as in the form of micro and nanoparticles. It is well known that pure chitosan is considered non-toxic [112-115]. The LD_{50} of chitosan in mice has been shown to exceed 16 g/kg body weight when orally administered to mice [85]. Culturing chitosan nanoparticles, prepared by ionotropic gelation with pentasodium tripolyphosphate, with a cell line derived from human conjunctival epithelium, had no effect on cell viability compared to untreated cells [116]. In addition, it has been reported that CSpp have little or no significant impact on cell viability in vitro for a range of cell types [97, 117-119]. This is in contrast to commonly used transfection reagents such as LipofectAMINE™ 2000 which can be highly cytotoxic [120]. Despite showing promise in cytotoxicity assays in vitro, a thorough characterization of the cytotoxicity and inflammation induced by CSpp in vivo, particularly with respect to pulmonary delivery needs further investigation.

Aside from chitosan, pDNA itself may also play a critical role in the cytotoxicity and inflammation imparted by CSpp in vivo. In pDNA vectors, unmethylated 5'-cytosine-guanosine-3' dinucleotide (CpG) sequences, which are found in DNA from bacteria and rarely in vertebrates [121], can potentially induce inflammatory responses through the production of proinflammatory cytokines. This may result in lowered transfection efficiencies [76]. Schwartz et al. found that intratracheal instillation of bacterial DNA

(containing abundant CpG motifs) to mice induced higher influxes of neutrophils and increased proinflammatory cytokine production in mouse bronchoalveolar lavage (BAL) fluids than intratracheal instillation of calf thymus DNA (containing low numbers of CpG motifs) [73]. Yew et al. reported that nasal instillation of complexes comprised of cationic lipids and CpG-depleted pDNA resulted in lower proinflammatory cytokine levels in BAL fluid when compared to the complexes comprising CpG-rich pDNA [122]. Additionally, Hyde et al. compared pulmonary inflammatory responses to complexes comprising cationic liposomes and various plasmids containing varying numbers of unmethylated CpG sequences per plasmid. It was found that intranasal administration of complexes made with CpG-free plasmids produced no inflammatory responses while the presence of one unmethylated CpG sequence per plasmid was enough to trigger inflammatory responses [123]. Lesina et al. showed that PEI complexes with a CpG-free plasmid administered in aerosolized form resulted in 60 times higher luciferase expression in the lung than that of PEI complexes containing plasmid with unmethylated CpG sequences [124]. Although both types of PEI complexes increased inflammatory cytokine levels at 1 hour after administration, the cytokine levels of mice treated with PEI complexes with CpG-free plasmid reverted back to normal after 24 hours while the others remained elevated [125].

Specific aims for this study are:

1. To characterize chitosan/pDNA polyplexes (CSpp), evaluate their cytotoxicity in vitro and determine the degree of pulmonary inflammation following delivery to mouse lungs using intranasal instillation
2. To determine whether unmethylated CpG sequences in plasmid DNA influence transfection efficiency and inflammation in vivo by comparing CSpp containing unmethylated CpG [CpG(+)] with CSpp containing methylated CpG [CpG(-)]

Materials and Methods

Chitosan purification

Low molecular weight chitosan from Blue waters crab shells was purchased from Sigma-Aldrich, Co. (St. Louis, MO), Product number 448869, Lot# MKBF2754V. According to the manufacturer's certificate of analysis, the deacetylation degree was 96.1%. The viscosity of 1% (w/w) chitosan in 1% (v/v) acetic acid was 35 cps. Based on the viscosity, the molecular weight is approximately 50,000 – 190,000 daltons. Chitosan was purified according to a previously published method with some modifications [126, 127]. Chitosan, 2 g, was dissolved in 200 ml of 1% (v/v) acetic acid (to generate a 1% w/v chitosan solution) by dispersing slowly onto the surface of the acetic acid solution with continuous stirring, and unwanted insoluble substances were filtered out with Whatman™ 541 filter paper (GE Healthcare, Amersham Place Little Chalfont, Buckinghamshire, UK). Small insoluble particles such as residual chitin, protein, polysaccharides and polysaccharide conjugates from chitosan starting materials [126] that went through the filter paper were separated out from chitosan solution by centrifugation of the chitosan solution at 10,016 x *g* for 1 hour (accuSpin™ 400, Thermo Fisher Scientific Inc., Rockford, IL). The supernatant was titrated with 1 N NaOH to pH ~ 8.5 to create insoluble chitosan. Precipitated chitosan was collected by filtration using Whatman™ 541 filter paper. Insoluble chitosan was redispersed in 0.1 M sodium bicarbonate solution, pH 8.3. Deproteinization and demetallization were performed by adding 0.5% (w/v) sodium dodecyl sulfate (SDS) and 20 mM ethylenediaminetetraacetic acid (EDTA) disodium salt. At this stage, it is important to keep the pH between 7.0 – 8.5 to avoid an interaction between chitosan and SDS [126]. Insoluble chitosan was collected via filtration through a Whatman™ 541 filter paper , dialyzed (SnakeSkin® dialysis tubing; 10K MWCO, Thermo Fisher Scientific Inc., Rockford, IL) and lyophilized using a

FreeZone 4.5-L Benchtop Freeze Dry System (Labconco Corporation, Kansas City, MO).

Purified chitosan and unpurified chitosan in the soluble and insoluble form were tested for endotoxin by Peter S. Thorne's laboratory, University of Iowa, using a modification of the kinetic chromogenic Limulus Amebocyte Lysate (LAL) assay (Lonza, Walkersville, MD) according to the company protocol [128].

Plasmid amplification and purification

Two types of plasmids used in this study were pCpG-Luc (CpG(-)) (InvivoGen™, San Diego, CA) and VR1255 (CpG(+)) (Vical®, San Diego, CA). CpG(-) was completely devoid of CpG motifs (4696 bps). CpG(-) encoded firefly luciferase and the Zeocin™ resistance gene. The CpG(+) plasmid contained CpG motifs (6413 bps). CpG(+) encoded firefly luciferase and the kanamycin resistance gene. CpG(-) and CpG(+) was transformed into *Eschrichia coli* (*E. coli*) GT115 and *E. coli* DH5α, respectively. Both plasmids were amplified by first streaking E.coli containing the plasmid of interest in Lennox L Agar (875 mg in 25 ml of nanopure water, RPI Research Products International Corp, Mt. Prospect, IL) and incubated overnight at 37°C, inverted. Lennox L Broth was prepared by dissolving Lennox L Broth powder 20 g in 1 L of nanopure water, (RPI Research Products International Corp, Mt. Prospect, IL). A single colony was added into 5 ml of Lennox L Broth medium. This was incubated in a shaker at 37°C, 300 rpm for 6 hours. After the culture started to become turbid, the medium containing bacteria was added into 500 ml of Lennox L Broth medium and incubated in a shaker (300 rpm) at 37°C overnight. Both Lennox L Agar and Lennox L Broth contain 50 µg/ml of Zeocin™ (Invitrogen life technologies, Carlsbad, CA) for CpG(-) selection and 100 µg/ml of kanamycin (RPI Research Products International Corp, Mt. Prospect, IL) for CpG(+) selection.

All plasmids were purified using a GenElute™ HP Endotoxin-Free Plasmid Maxiprep Kit (Sigma-Aldrich Co., St. Louis, MO), according to the manufacturer's protocol. pDNA concentrations were determined using a NanoDrop 2000 spectrophotometer (Thermo Fisher Scientific Inc., Waltham, MA). An absorbance ratio of 260 nm to 280 nm was used to access the quality of extracted pDNA. The 260/280 ratio of approximately 1.8 indicated a pDNA preparation free of protein contamination [129].

Preparation of CSpp

The CSpp were prepared by ionic interaction between positively charged chitosan and negatively charged pDNA molecules [117]. In this study, dextran sulfate (sodium salt) (5 kDa, Sigma-Aldrich, Co., St. Louis, MO) was introduced into the formulation to weaken the complexation of chitosan and DNA in order to limit excessive retention of DNA and thus ensure higher transgene expression [127].

CSpp were formulated at different ratios of nitrogen (N) atoms in chitosan able to be protonated to phosphate (P) groups in the pDNA backbone (N/P ratios) [77]. Chitosan solutions were prepared by dissolving the lyophilized purified chitosan in 1% (v/v) acetic acid solution, then adjusting to pH 5.5 - 5.7 using 1 N NaOH. Then 50 mM acetate buffer (pH 5.5) was added to the prepared solution to achieve a final chitosan concentration of 5 mg/ml. Dextran sulfate stock solution (1 mg/ml) was prepared in UltraPure™ DNase/RNase-Free distilled water (Invitrogen™, Grand Island, NY). Dextran sulfate:chitosan (1:10 (w/w)) was used in this study. Plasmid DNA (CpG(-) or CpG(+)) in UltraPure™ DNase/RNase-free distilled water (200 µg/ml for *in vitro* and 1000 µg/ml for *in vivo* experiments) was heated in a controlled temperature water bath to 50 – 55°C prior to mixing. All solutions were sterilized by filtering with a 0.22 µm syringe filter (Millex®-GS, Millipore Corporation, Billerica, MA). An equal volume (not more than 500 µl) of the desired concentration of cationic solution (chitosan) was pipetted into the anionic solution (pDNA) and then vortexed immediately for 20 – 30 seconds. The

polyplex suspensions were incubated at room temperature for 30 minutes before use. The final concentrations of pDNA after polyplex formation were 2.5 µg/50 µl (in vitro) and 12.5 µg/50 µl (in vivo). The conditions used to prepare CSpp were optimal for yielding stable and compact CSpp [127, 130]. All polyplexes were freshly prepared in all experiments.

As a positive control in the in vitro transfection experiments, branched PEI, MW 25 kDa (Sigma-Aldrich, Co., St. Louis, MO) was used to make polyplexes at a N/P ratio of 10 (Figure 2-2). These types of PEI/pDNA polyplexes (PEIpp) have previously displayed strong transfection efficiencies generating high luciferase activity in HEK293, COS7 and HeLa cell lines [131]. To prepare PEIpp, a stock solution (1 mg/ml) of PEI in UltraPure™ DNase/RNase-free distilled water was diluted to the desired concentration and mixed with pDNA in the same manner as CSpp.

Determination of size, polydispersity index and zeta potential of CSpp

Particle size, polydispersity index (PdI) and zeta potential of CSpp (at N/P ratios of 1, 5, 10, 20, 60 and 100) that were prepared at the concentration of 2.5 µg of pDNA per 50 µl total volume and PEIpp (at N/P ratio of 10) were measured using dynamic light scattering (DLS) via the Zetasizer Nano ZS (Malvern Instrument Ltd., Westborough, MA). Size and zeta potential measurements were performed on CSpp and PEIpp that were dispersed in acetate buffer solution, pH 5.46 and water, respectively at 25°C. The particle size and PdI were measured using 173° backscatter detection in disposable polystyrene cuvettes (DTS0012) with the total volume of the solution equal to 1 ml. Zeta potential was measured in a zeta potential folded capillary cell (DTS1060) with the total volume of 0.75 ml.

For the animal study, the particle size, PdI and zeta potential of CSpp at a N/P ratio of 10, prepared at the concentration of 12.5 µg of pDNA per 50 µl total volume, were measured as described above for CSpp (2.5 µg/50 µl).

Macroscopic imaging of CSpp

When CSpp were formed at a very high pDNA concentration, CSpp can form clumps and precipitates that are large enough to be visible to the naked eye. CSpp (at a N/P ratio of 10), freshly prepared at the concentrations of 2.5, 12.5, 25.0 and 50.0 µg of pDNA per 50 µl total volume, were imaged using Olympus Stereoscope DP (Olympus Scientific Solutions Americas Corp., Waltham, MA) without any staining.

Microscopic imaging of CSpp

The morphology of CSpp was observed using Transmission Electron Microscopy (TEM). Freshly prepared CSpp were diluted with sterile water that was filtered through a 0.22 µm filtration membrane. A drop of each of the diluted polyplexes was left on carbon coated Formvar in ethylene dichloride film (Electron Microscopy Sciences, Hatfield, PA) on a 400-mesh TEM copper grid for 2 minutes. Then, Whatman® filter paper was used to remove any excess liquid and air dried. Uranyl acetate (Electron Microscopy Sciences, Hatfield, PA) was used for the staining. Uranyl acetate (1% (w/v)) was prepared by dissolving 0.1 mg of uranyl acetate in 10 ml of distilled water, centrifuged at the 16100 x *g* and a clear supernatant was collected. The polyplexes were stained by adding 1 drop of clear 1% (w/v) uranyl acetate solution for 30 seconds. The excess liquid was also removed by Whatman® filter paper and air dried. TEM images were taken by JEOL JEM-1230 transmission electron microscope provided with Gatan UltraScan 1000 2k x 2k CCD camera. TEM beam current was used at an accelerating voltage of 120 kV. The TEM images were processed with ImageJ (Image Processing and Analysis in Java, Version 1.46b, http://rsbweb.nih.goc/ij/).

Investigation of the ability of chitosan to complex with pDNA

CpG(+) plasmid and the CSpp(CpG(+)) at N/P ratios of 1, 5, 10, 20, 60 and 100 were mixed with 2x BlueJuice™ gel loading buffer (Invitrogen™, Grand Island, NY). The

final solutions/suspensions which contained 1 µg pDNA were loaded into the wells of a 1.0% (w/v) agarose gel containing 0.5 µg/ml of ethidium bromide in 1X Tris-acetate-EDTA (TAE) buffer. Gels were exposed to a constant current of 100 mAmp for 2 hours. DNA migration was visualized with a UV transilluminator (Spectroline, Westbury, NY). TrackIt™ (1 Kb plus DNA ladder, Invitrogen™, Grand Island, NY) was used as a DNA ladder in this experiment.

Evaluating the cytotoxicity of CSpp in vitro

Cell lines and cell culture

Adenocarcinomic human alveolar basal epithelial cells (A549) were a generous gift from Peter S. Thorne's laboratory, University of Iowa. A549 cells were maintained in RPMI-1640 medium (Gibco®, Life technologies, Grand Island, NY). Human embryonic kidney 293 (HEK293) cells were purchased from the American Type Culture Collection (ATCC, Rockville, MD) and were maintained in Dulbecco's Modified Eagle Medium (DMEM) (Gibco®, Life technologies, Grand Island, NY). All of the media were supplemented with 10% fetal bovine serum (Atlanta Biologicals, Lawrenceville, GA), 10 mM HEPES (Gibco®, Life technologies, Grand Island, NY), 50 µg/ml gentamycin sulfate (Cellgro, Manassas, VA) , 1 mM sodium pyruvate (Gibco®, Life technologies, Grand Island, NY) and 1mM Glutamax™ (Gibco®, Life technologies, Grand Island, NY). Cells were incubated at 37°C and 5% CO_2. Cells were passaged before reaching 100% confluence.

Evaluation of the cytotoxicity of CSpp using the MTS assay

Twenty-four hours prior to treatment, A549 or HEK293 cells were seeded (1×10^4 cells/well in 200 µl of complete media) into a 96-well flat bottom polystyrene tissue culture plate (Celltreat® Tissue Culture Treated, Flat bottom, Celltreat Scientific Products, Shirley, MA). Treatments (CSpp at various N/P ratios, PEIpp and pDNA alone)

were added in a volume of 20 µl/well (every treatment contained pDNA equivalent to 1 µg), along with 80 µl of serum-free medium. Without aspiration, 100 µl of fresh, complete medium was added after 4 hours of incubation. After 48 hours, the treatment media was aspirated and replaced with 100 µl of fresh, complete media and 20 µl of the MTS tetrazolium compound or CellTiter 96® Aqueous One Solution reagent (Promega Corporation, Madison, WI). The plate was incubated at 37°C at 5% CO_2, incubated for 1 - 4 hours, and then the absorbance was recorded at 490 nm using a Spectra Max® plus 384 Microplate Spectrophotometer (Molecular Devices, Sunnyvale, CA). Percent relative cell viability values are expressed as the percentage of UV absorbance from wells containing treated cells compared to the control wells containing live cells treated with phosphate buffered saline (PBS) and multiplying the resultant value by a factor of 100. Background absorbance at 490 nm was corrected by subtracting the absorbance recorded for blank control wells, which contained only 100 µl of media and 20 µl of the MTS tetrazolium compound, from the absorbance obtained from the wells of interest.

To investigate the relationship between dose-, time- and cytotoxicity, A549 and HEK293 cells were seeded at the same manner as the above method. Cells were treated with CSpp(CpG(+)) in a volume between 20 – 120 µl per well (each treatment contains pDNA in the range from 1 – 36 µg per well), along with 80 µl of serum-free medium. An N/P ratio in all treatments is equal to 10. If treatments were exposed to cells longer than 4 hours, 100 µl of fresh complete medium was added to the well. Cells were exposed to treatments for 4, 12, 24 and 48 hours. MTS assay were conducted at the end according to the previous experiment.

Evaluation of the cytotoxicity of CSpp (apoptosis) using Caspase-3/7 assay

This experiment was conducted in parallel with the MTS assays. Twenty-four hours prior to treatment, HEK293 cells were seeded (1 x 10^4 cells/well in 200 µl of

complete media) into a 96-well plate. Treatments (CSpp and PEIpp at N/P ratio 10) were added along with serum-free medium. Without aspiration, 100 µl of fresh complete medium was added after 4 hours of incubation. Caspase-3-7 activity was measured according to the manufacturer's protocol (Promega Corporation). After 24 hours, the treatment was aspirated and replaced with 100 µl of fresh complete media and 100 µl of the Apo-ONE® Caspase-3/7 reagent (Promega Corporation). Apo-ONE® Caspase-3/7 reagent was prepared by diluting caspase substrate (100x) with Apo-ONE® homogeneous Caspase-3-7 buffer. The reagent was mixed with the media using a plate shaker for 30 seconds. The plate was incubated at room temperature for 4.5 hours and then the fluorescence in each well was recorded (ex/em = 485/530 nm) using a Spectra Max® plus 384 Microplate Spectrophotometer (Molecular Devices, Sunnyvale, CA). The blank value was the fluorescence obtained from wells that comprised media (100 µl) and Apo-ONE® Caspase-3/7 reagent (100 µl). Caspase-3/7 activity was determined from the fluorescence obtained from the assay wells minus the fluorescence of blank wells.

Evaluation of the intracellular superoxide levels when cells were treated with CSpp

A549 or HEK293 cells were plated in 60 mm^2 dishes (2 x 10^4 cells per dish in 4 ml of complete media) 24 hours prior to treatments. Cells were treated with different CSpp and PEIpp containing N/P 10 (20 µg of pDNA in 400 µl of CSpp suspension), chitosan solution, PEI solution or naked pDNA. The amount of chitosan and PEI added were adjusted to the amount used in CSpp and PEIpp groups. After 48 hours, cells were rinsed by PBS and harvested by trypsinizing the cultures. Cells were subsequently washed with 3 ml of PBS containing 5 mM pyruvate and collected by centrifuge at 230 x g for 5 minutes. Cells were incubated in a solution of PBS containing 5 mM pyruvate with 10 uM dihydroethidium (DHE) for 40 minutes at 37°C and 5% CO_2. The control tubes received 0.1% dimethyl sulfoxide (DMSO) at equal volume used in samples tubes and

the electron transport chain blocker Antimycin A (Ant A) was used as a positive control. Following the incubation, the cells were filtered through 35 micron mesh, transferred to flow tubes and placed on ice to stop the reaction. Samples were analyzed using a FACScan flow cytometer (Becton Dickinson Immunocytometry Systems, Inc., San Jose, CA) using an excitation wavelength of 488 nm and emission of 585 nm. The mean fluorescence intensity (MFI) of 10,000 cells was recorded for each sample and the mean of samples was calculated for each treatment group. The background fluorescence was subtracted from each sample to generate the net MFI. Each sample was normalized to the control group to yield the normalized MFI (NMFI).

Evaluating transfection efficiencies of CSpp *in vitro*

Cells (HEK293 and A549 cell lines) were seeded (8×10^4 cells/well in 500 µl of complete media) into a 24-well plate. After 24 hours, 500 µl of serum-free medium and 100 µL of the treatments (pDNA solution, the CSpp and PEIpp) were added. Each treatment contained 1 µg or 5 µg of pDNA. Additional complete medium (500 µl) was added at 4 hours after the treatment. The medium was then replenished every 24 hours. At 48 hours, the cells were treated with 200 µl of Reporter Lysis Buffer (Promega Corporation, Madison, WI) followed by two freeze-thaw cycles (frozen at -80°C for 20 minutes then thawed at room temperature for 30 minutes). Cell suspensions were then transferred to 1.5-ml microcentrifuge tubes and centrifuged at 16100 x g for 5 minutes using Eppendrof Microcentrifuge Model 5415 D (Eppendorf, Hauppauge, NY), after which the supernatants were collected. Luciferase expression was measured using a Luciferase Assay System according to the company protocol (Promega Corporation). Aliquots of supernatant (20 µl) were added to 100 µl of the luciferase assay reagent, vortexed briefly and luciferase activity was measured for 10 seconds using a Lumat LB 9507 luminometer (EG&G Berthold, Wildbad, Germany). Background was corrected by substracting the value obtained from each sample with an average of the values

collected from samples that contained only 20 µl of Reporter Lysis Buffer and 100 µl of the luciferase assay reagent.

The remaining supernatant was analyzed for total protein concentration using a Micro BCA™ Protein Assay Kit (Pierce Biotechnology Inc., Rockford, IL). Bovine serum albumin (BSA) (2 mg/ml, Pierce Biotechnology Inc., Rockford, IL) was used to create a standard curve (Figure 2-3A). BSA concentrations in the range between 1.95 – 62.5 µg/ml were within the linear response region (Figure 2-3B). The results are expressed as relative light units (RLU) per mg of total protein.

Evaluating transgene expression and inflammatory response induced by CSpp in mouse lungs

Animals

Mice (C57Bl/6, males, 6 weeks old) were purchased from The Jackson Laboratory (Bar Harbor, ME). Mice were kept in a vivarium in polypropylene, fiber-covered cages in HEPA-filtered Thoren caging units (Hazelton, PA, USA) in the Pulmonary Toxicology Facility at the University of Iowa. Animals were acclimatized in the vivarium for 10 days prior to the instillation exposures. Food (sterile Teklad 5% stock diet, Harlan, Madison, WI) and water (via an automated watering system) was provided ad libitum and a 12-hour light-dark cycle was maintained in the animal room. All animal protocols used in these studies were approved by the Institutional Animal Care and Use Committee and complied with NIH Guidelines.

Nasal instillation

For the first set of experiments, mice were exposed to CSpp by nasal instillation (dose 12.5 µg pDNA/50 µl) only once. The instilled volume of 50 µl per application was chosen because it is an optimum volume which gives high drug distribution in lungs [132]. The mice were anesthetized with isoflurane (3%) by inhalation using a precision Fortec

vaporizer (Cyprane, Keighley, UK) prior to instillation. There were two control groups in these studies: 1) mice without exposure (control); and 2) mice exposed to CpG(+) alone (CpG(+)). Mice were euthanized 24 hours after nasal instillation and bronchoalveolar lavage (BAL) fluid was collected and lungs were harvested as previously described [133]. This time point has previously been shown to be the time that mice have highest cytokine levels during acute inflammation responses [134]. Mice lungs were used to measure the level of transgene expression. BAL fluid was analyzed to determine the number of macrophages, neutrophils, lymphocytes and eosinophils as well as to determine cytokine concentrations.

For the second set of experiments, mice were treated in the same manner as the first set of experiments except they were exposed to CSpp by nasal instillation (dose 12.5 µg pDNA/50 µl) twice with a 1 hour interval between each dose. There were three control groups in these studies: 1) mice without exposure (control); 2) mice exposed to chitosan solution (CS) at the concentration used to prepared CSpp; and 3) mice exposed to CpG(+) alone (CpG(+)). Mice body weights were determined before and 24 hours after nasal instillation. Mice lungs were used to measure the level of transgene expression. BAL fluid was analyzed to determine the number of macrophages, neutrophils, lymphocytes and eosinophils, total protein concentrations, lactate dehydrogenase enzyme (LDH) activity and cytokine concentrations.

Measuring transgene expression in mouse lungs after nasal instillation of CSpp

The method used for tissue preparation was adapted from Mohammadi et al. [100], Manthorpe et al. [135] and Stammberger et al. [136]. Lungs from euthanized mice were washed with ice-cold PBS, weighed and homogenized using a Tissue Tearor (Biospec Products, Inc., Bartlesville, OK) in ice-cold Reporter Lysis Buffer (4 µl/mg of lung tissue) for 1 minute. Lysates were then passed through three freeze-thaw cycles (frozen at -

80°C for 20 minutes and thawed in a 37°C water bath for 5 minutes). Lysates were then centrifuged at 16100 x *g* for 5 minutes using Eppendrof Microcentrifuge Model 5415 D (Eppendorf, Hauppauge, NY), after which the supernatants were collected. Supernatants were analyzed for luciferase expression in the same manner as described in a previous section, "Evaluating transfection efficiencies of CSpp in vitro".

Evaluating pulmonary inflammatory responses

The lungs from each euthanized mouse (n = 6) were lavaged via the cannulated trachea three times, in situ, with approximately 1 ml/wash of sterile saline (0.9% (w/v) sodium chloride solution). Cells were collected from BAL fluid by centrifugation at 800 x g for 5 minutes at 4˚C. The cell pellets were resuspended in Hank's balanced salt solution, and the total white cells were counted using a hemocytometer. The remaining supernatants were stored at -80°C and used for measuring total protein, LDH activity and inflammatory cytokine/chemokine concentrations. Different cell types were counted after the BAL cells were placed on microscope slides, spun using Cytospin 4 (Thermo Shandon, Thermo Scientific, Waltham, MA) at 800 x *g* for 3 minutes, and stained using a HEMA 3® stain set (Fisher Scientific Company LLC, Midland, MI). A total of 400 cells (macrophages, neutrophils, lymphocytes and eosinophils) per mouse were counted.

The concentration of total protein in BAL fluid supernatants was determined using a Bradford protein assay (Bio-Rad Laboratories, Inc., Hercules, CA). The activity of lactate dehydrogenase enzyme (LDH) in BAL fluid supernatants was measured using a commercially available Cytotoxicity Detection Kit (LDH) (Roche Diagnostics, Mannheim, Germany). Inflammatory cytokine/chemokine (tumor necrosis factor [TNF]-α, interferon [IFN]-γ, interleukin [IL]-6, IL-12 (p40), keratinocyte-derived cytokine [KC], and macrophage inflammatory protein [MIP]-1α) levels in the BAL fluid were determined using a multiplexed fluorescent bead-based immunoassay (Bio-Rad Laboratories, Inc.). Values for each cytokine falling below the lower limit of detection (LLOD) or the nonzero

values, which cannot be measured but are known to be below the detection limit, were imputed with L / $\sqrt{2}$, where L was the limit of detection [137].

Statistical analysis

Data are expressed as mean ± SD. Statistical significance was determined using a one-way analysis of variance (ANOVA) with Bonferroni's Multiple Comparison Test compared to the control or a two-way analysis of variance (ANOVA) with Bonferroni's Multiple Comparison Test compared to the control. A p-value less than 0.05 was considered significant. Statistical analyses were performed using GraphPad Prism version 5.02 and 6.05 for Windows (Graphpad Software, Inc., San Diego, CA).

Results and discussions

Chitosan purification

Chitosan used in this study was derived from crustacean shells which usually have high contaminants from bacterial organisms [138]. Most chitosan products in the market have been used in food industry and water treatment where high purity grades are not necessary. However, when using chitosan for biomedical applications, such as in gene delivery, high purity is critical. According to recent studies from our laboratory, further treatments of chitosan by deproteinization (SDS) and demetallization (EDTA) agents, results in reduced protein contamination, or "purified chitosan" [127]. However, endotoxin content has never been reported in chitosan that was purified by this method. Endotoxins or lipopolysaccharides (LPS) are a major component of Gram-negative bacteria outer membranes. Since endotoxin contamination can induce lung inflammation and cause lung injury [139], it was crucial in this study to use endotoxin-free chitosan to prohibit any inflammatory responses caused by endotoxin in animal lungs.

Lyophilized purified chitosan was tested for endotoxin content using an LAL assay. Purified chitosan (1% w/v) in 1% (v/v) acetic acid tested negative (<LLOD, 0.024

endotoxin unit/ml (EU/ml)) for endotoxin while 1% (w/v) unpurified chitosan in 1% (v/v) acetic acid contained endotoxin 89.1 EU/ml (Table 2-1). The result obtained from insoluble purified chitosan (chitosan dispersed in LAL water) was consistent with the result obtained from soluble chitosan in acetic acid which was negative for endotoxin. It is possible that endotoxin was dissociated by SDS into small units [140, 141] and was removed by ultrafiltration (10 MWCO) [142].

Characterization of CSpp and PEIpp

CSpp sizes were reported as Z-average mean values which is the most stable parameter generated by the Zetasizer nano ZS [143]. Sizes of the CSpp prepared for the in vitro study (2.5 µg of pDNA/50 µl) were unimodal (Figure 2-4) and ranged between 200 to 400 nm in diameter for all N/P ratios tested. The sizes of the polyplexes at N/P ratios ranging from 1 to 20 were similar (~230 nm) for both CSpp(CpG(-)) (Figure 2-6A) and CSpp(CpG(+)) (Figure 2-6B) while polyplexes progressively increased in size at N/P 60 (250 - 300 nm) and N/P 100 (300 – 350 nm). In all samples tested, the PdI value was lower than 0.7, which indicated the suitability of measuring samples by the DLS technique [143]. From the low PdI value, both types of polyplexes had narrow size distributions (Figure 2-6C and Figure 2-6D). At N/P 1, because of an equally positive and negative charge, chitosan may not fully complex and condense pDNA. Some pDNA may be exposed to the surface of the polyplexes. Thus, the zeta potential values of both types of polyplex were negative (approximate -25 mV). However, when the concentration of chitosan increased (at N/P ratios of 5 to 100), all polyplexes tested were positively charged (25 – 35 mV) (Figure 2-6E and Figure 2-6F).

Since PEIpp(CpG(-)) and PEIpp(CpG(+)) will be used further in cytotoxicity and transfection experiments, size and zeta potentials of PEIpp prepared at the same pDNA concentration (2.5 µg of pDNA/50 µl) at N/P 10 were measured. PEIpp had small diameters of approximately 100 nm (Figure 2-7A). Zeta potentials of PEIpp(CpG(-)) and

PEIpp(CpG(+)) were equal to 45 mV and 42 mV, respectively (Figure 2- 7B). Zeta potentials obtained from PEIpp were slightly higher than zeta potentials obtained from CSpp (Figure 2-7E and Figure 2-7F).

Abbas et al. [127] showed that the particle size of CSpp increased when pDNA concentrations were increased above 2.5 µg/50 µl. In contrast, the pDNA concentrations below 2.5 µg of pDNA/50 µl (or 0.05 mg/ml) have no effect on the size of CSpp [127]. Hence, for the in vitro experiments, polyplexes were used at a concentration of 2.5 µg of pDNA/50 µl. However, for the in vivo experiments, the concentration was increased to 12.5 µg of pDNA/50 µl in order to overcome the limitation of small delivery volumes in mice. This increase in pDNA concentration resulted in an increase in polyplex size as well as a small amount of aggregation of the polyplexes and was consistent with findings from other groups [144, 145]. A bimodal distribution (Figure 2-5) was observed in particle size measurements for CSpp at N/P 10 with a pDNA concentration of 12.5 µg/50 µl (523.0 ± 3.8 nm, 94.6 ± 2.3 % by volume and 4888.0 ± 355.3 nm, 5.4 ± 2.3 % by volume).

Macroscopic images of CSpp

At a pDNA concentration of 12.5 µg/50 µl, although the particle size increased and some aggregations can be detected when measured by Zetasizer Nano ZS, this aggregation cannot be seen via Stereoscope (Figure 2-8A and Figure 2-8B). At this concentration, CSpp(CpG(-)) and CSpp(CpG(+)) could be administered to the animals via nasal instillation with pipettes. Concentrations of greater than 12.5 ug/50 µl pDNA; which are 25.0 µg/50 µl (Figure 2-8C and Figure 2-8D) and 50.0 µg/50 µl (Figure 2-8E and Figure 2-8F) resulted in substantial precipitation of the polyplexes rendering them unsuitable for pulmonary delivery.

Microscopic images of CSpp

CSpp morphology was studied by staining with uranyl acetate and observed under TEM. Figure 2-9 shows CSpp(CpG(+)) at a N/P ratio of 10 and is indicated by red arrows.

Ability of chitosan to complex with pDNA

Plasmid DNA complexed with chitosan did not migrate into an agarose gel (1% (w/v)) when an electric field was applied. The pDNA from CSpp remained in the loading wells at N/P ratios > 1 (Figure 2-10). This finding is consistent with the zeta potential data showing a negative charge for CSpp N/P = 1 and a positive charge for CSpp N/P ≥ 5 suggesting that at N/P ratios ≥ 5 chitosan binds to all free pDNA molecules, creating polyplexes.

These results may vary depending on the characteristics of the chitosan, since the binding strength between chitosan and DNA has been shown to be affected by the degree of deacetylation and the molecular weight of the chitosan. Chitosan with a high molecular weight and high degree of deacetylation binds to DNA more strongly than chitosan with a relatively low molecular weight and low degree of deacetylation [92, 105].

Evaluation of in vitro cytotoxicity

Cytotoxicity of CSpp

Cell viability assays involving A549, a human lung epithelial cell line, and HEK293, a human embryonic kidney cell line, commonly used in transfection studies, were used to test CSpp at N/P ratios of 1 - 100 using both types of pDNA (CpG(-) or CpG(+)). All treatments contained pDNA equal to 1 µg per well and the treatments were exposed to cells for 48 hours. All formulations of CSpp tested resulted in at least 85 – 90% cell viability of A549 (Figure 2-11A and 11B) and HEK293 (Figure 2-11C and 11D), with no significant differences when compared to PBS-treated control cells in both CSpp

prepared using CpG(-) and CpG(+). In contrast, PEIpp(CpG(-)) and PEIpp(CpG(+)) at N/P 10 showed significantly lower cell viabilities in both A549 (Figure 2-11A and 11B) and HEK293 (Figure 2-11C and 11D) (~25%, p-value < 0.001).

Since in vivo experiments require high doses of CSpp (12.5 µg/50 µl, once and twice administrations), it was necessary to investigate whether or not CSpp at these high doses would result in toxicity. A549 cells that were treated with CSpp(CpG(+)) at the pDNA amount between 1 – 36 µg per well for 48 hours (Figure 2-12A) showed no significant differences in cell viability compared to PBS-treated control cells. When HEK293 cells were used, some of the treatment groups showed statistically significant differences in cell viability when compared to the control group (Figure 2-12B). However, all groups tested showed relative cell viabilities higher than 70% after 48 hours exposure.

To study the relationship between time and cytotoxicity, HEK293 cells were treated with CSpp(CpG(+)) at pDNA amounts of 1 and 25 µg per well. PEIpp(CpG(+)) at pDNA amount of 1 µg per well were used as a positive control. Only cells that were treated with PEIpp(CpG(+)) for 12, 24 and 48 hours showed significantly reduction in cell viability (p-value < 0.001) when compared to PBS-treated group in a time-dependent manner. CSpp(CpG(+)) showed no significance difference in viability when compared to the control (PBS-treated) group even at high concentrations of pDNA (25 µg/well) (Figure 2-13).

Evaluation of the cytotoxicity of CSpp (apoptosis) using Caspase-3/7 assay

Caspases, a family of cysteine proteases, are involved in promoting apoptosis (programmed cell death). Among them, caspase-3 and caspase-7 are considered downstream effector caspases that lead to apoptosis. In this assay, non-fluorescent caspase-3/7 substrate (rhodamine 110, bis-(N-CBZ-L-aspartyl-L-glutamyl-L-valyl-L-

aspartic acid amide; Z-DEVD-R110) was used to react with caspase-3/7. The fluorescent product obtained (rhodamine) after enzyme cleavage (removing DEVD peptides by caspase-3/7) was measured [146]. HEK293 cells were exposed to CSpp(CpG(+)) and PEIpp(CpG(+)) for 28.5 hours. It appeared that only cells that were incubated with PEIpp(CpG(+)) at a pDNA amount of 1 µg/well showed high fluorescence levels indicating high caspase-3/7 activity. Caspase-3/7 activity in cells that were incubated with CSpp(CpG(+)) at pDNA amounts of 1 µg and 30 µg/well were not different from the control or untreated group (Figure 2-14). From this result, PEIpp(CpG(+)) at a pDNA amount of 1 µg/well can induce apoptosis in HEK293 cells.

Measurement of reactive oxygen species (ROS) generation by cells treated with CSpp

In order to determine if treatment of cells with the polyplexes affects intracellular reactive oxygen species (ROS) levels, superoxide levels were estimated using the oxidation sensitive fluorescent dye, dihydroethidium (DHE). DHE can be converted to 2-hydroxyethidium by superoxide, which then intercalates with nuclear DNA and becomes fluorescent (red) which can be detected by flow cytometry [147].

The results indicated that A549 cells treated with CSpp, PEIpp, chitosan solution (CS) or PEI solution showed significant increases (1.5 – 2.0–fold) in DHE oxidation relative to the control group (p-value < 0.001 and < 0.01) (Figure 2-15A). Treatment of HEK293 cells with the CSpp or the chitosan solution did not significantly affect the DHE oxidation levels compared to the control group. However, treatment with PEIpp, CpG(+) alone or PEI solution showed significant increases (1.5 – 3.0 –fold) in DHE oxidation (p-value < 0.001 and < 0.01) (Figure 2-15B). Both A549 and HEK293 cells treated with CSpp containing either CpG(+) or CpG(-) had lower DHE oxidation when compared with cells treated with PEIpp and PEI solution.

The results from both cell lines showed CSpp had a negligible impact on cell viability. CSpp did not increase caspase-3/7 activity when compared to untreated cells and cells treated with CSpp trended toward lower DHE oxidation when compared to cells treated with PEIpp.

Malich et al. studied the sensitivity and specificity of the MTS assay with human cell lines. They found that results from the in vitro cytotoxicity assay did not necessarily correlate well with in vivo results [148]. The in vitro models might not be capable of elucidating the inflammatory potency. Thus, the toxicity, oxidative stress levels and inflammatory response in an animal model needed to be assessed before CSpp delivery systems can be used for clinical applications.

In vitro transfection efficiencies of CSpp: presence versus absence of CpG sequences

The effect of the presence of CpG sequences within CSpp on transfection efficiencies was examined initially in vitro using A549 and HEK293 cell lines. A preliminary experiment in A549 cells was conducted to find an optimum pDNA amount to use per well to achieve high transfection efficiency as determined by luciferase expression. As shown in Figure 2-16, cells that were treated with CSpp(CpG(-)) at different N/P ratios showed the same trend in luciferase expression. N/P ratios of 10 and 20 yielded the highest luciferase expression among the four N/P ratios tested. Increasing the pDNA amount from 1 µg per well to 5 µg per well resulted in an increase in luciferase expression for all N/P ratios tested. Thus, from this experiment, 5 µg of pDNA was chosen for comparing transfection efficiencies in two types of cell lines, A549 and HEK293, when treated independently with two types of CSpp (CSpp(CpG(-)) and CSpp(CpG(+)) at six different N/P ratios (1, 5, 10, 20, 60 and 100).

The transfection efficiency of CSpp(CpG(-)) at a N/P ratio of 10 and 20 was significantly higher than the control groups for A549 as shown in Figure 2-17A. In

contrast, relatively low transgene expression was observed when CSpp(CpG(+)) were used to transfect A549 cells (Figure 2-17B). In the HEK293 cell line, the luciferase expression pattern was similar for both CSpp(CpG(-)) and CSpp(CpG(+)) (Figure 2-17C and Figure 2-17D). It has been reported that A549 cells express the Toll-like receptor 9 (TLR-9), which recognizes unmethylated CpG sequences in pDNA [149] and it has also been reported that CpG-oligodeoxynucleotides can suppress A549 cell proliferation via TLR-9 signaling [150]. We speculate that this may have had a detrimental effect on CSpp(CpG(+))-mediated transfection of A549 cells . Finally, A549 cells showed higher luciferase expression than HEK293 cells when treated with CSpp(CpG(-)). Mao *et al*., in studies investigating transfection efficiencies of CSpp in cell lines of different lineages reported differences in luciferase expression levels indicating that the transfection efficiency when using CSpp may be dependent on cell type [130].

In vivo transfection efficiencies in mouse lungs: effect of presence versus absence of CpG sequences in CSpp

When mice were administered three different treatments; CSpp(CpG(-)), CSpp(CpG(+))at a N/P ratio of 10 (12.5 µg of pDNA/50 µl) and CpG(+) at the same concentration used to prepare CSpp, luciferase expression in all groups tested was low (Figure 2-18). There was no significant difference in luciferase expression in any of the groups tested. Among these groups, the highest luciferase expression was obtained from mice lungs that were treated with soluble CpG(+) (mean: 4296 RLU/mg of total protein, median: 867). CSpp(CpG(-)) caused luciferase expression (mean: 2053 RLU/mg of total protein, median: 221) at levels higher than mice treated with CSpp(CpG(+)) (mean: 196 RLU/mg of total protein, median: 191) (Figure 2-18).

When administration dose(s) were increased from once (12.5 µg of pDNA/50 µl) to twice, the luciferase expression values in mice lungs that were treated with CSpp(CpG(-)) greatly increased (11 times higher than single administration) (Figure 2-

22). The supernatant obtained from homogenized lungs of mice treated with CSpp(CpG(-)) (at an N/P ratio of 10) demonstrated significantly ($p < 0.01$) higher luciferase expression (mean: 23846 RLU/mg of total protein, median: 23043) than mice treated with CSpp(CpG(+)) (mean: 1969 RLU/mg of total protein, median: 777) (Figure 2-22). In addition, only the group in which mice were treated with CSpp(CpG(-)) expressed significantly higher luciferase than the controls ($p < 0.01$). These results are consistent with our in vitro data using A549 cells. A possible explanation for our in vivo transgene expression results is that CpG sequences stimulate inflammatory responses that deleteriously affect transfection. We subsequently performed experiments to investigate this possibility.

Inflammatory responses measured in BAL fluids

The inflammatory response to CSpp was investigated by harvesting and analyzing BAL fluids from variously treated mice. Acute inflammatory responses were assessed by enumeration of white blood cell types (macrophages, neutrophils, lymphocytes and eosinophils) 24 hours subsequent to nasal instillation of CSpp formulations. In the first in vivo experiment (single dose administration), CSpp(CpG(-)) caused an insignificant 4-fold increase in the total number of white blood cells in the BAL fluid compared to the control treatment, while CSpp(CpG(+)) caused a 2-fold increase over controls (Figure 2-19A). The majority of white blood cells found in BAL fluids from mice that were treated with CSpp(CpG(-)) and CSpp(CpG(+)) were macrophages and neutrophils which indicates a classical inflammatory response. Only small numbers of lymphocytes were detected in all groups and there were no eosinophils detected in any of the samples (Figure 2-19B). Six different types of cytokines/chemokines in BAL fluids (TNF-α (Figure 2-19A), IL-6 (Figure 2-19B), IL-12 (Figure 2-19C), KC (Figure 2-19D), MIP-1α (Figure 2-19E) and INF-α) were measured. All groups showed low cytokine concentrations and the cytokine levels were not significantly different from the control

group. The levels of INF-α were below the lower limit of detection (0.95 pg/ml) in all samples analyzed (data not shown). Mouse body weights were recorded. There was no significant difference between body weight before, and 24 hours after, administration of complexes or controls in all groups tested (Figure 2-21).

In the second in vivo experiment (double dose administration), the number of white blood cells obtained from each treatment group increased. CSpp(CpG(-)) caused a significant 9-fold increase in the total number of white blood cells in the BAL fluid compared to the control treatment, while CSpp(CpG(+)) caused a 7-fold increase (albeit not statistically significant) over controls (Figure 2-23A). The majority of these infiltrating white cells proved to be neutrophils (Figure 2-23B). Concentrations of total protein in BAL fluid (an indicator of the increased permeability of the alveolar capillary membrane), was significantly higher (compared to control) in mice treated with CSpp(CpG(+)). Total protein concentration was also enhanced (but not significantly) in mice receiving CSpp(CpG(-)) (Figure 2-24A). Another parameter that was assessed was that of the activity of the cytoplasmic cellular enzyme, LDH. Activity of LDH, which denotes cell membrane damage, [151] was not significantly different in BAL fluid from mice treated with either CSpp(CpG(-)) or CSpp(CpG(+)) (Figure 2-24B). There were no statistically significant differences for both total protein levels and LDH activity between mice treated with CSpp(CpG(-)) and with CSpp(CpG(+)). However, LDH activities for both types of CSpp were higher than the control ($p < 0.001$). Finally, levels of cytokines (IL-6, IL-12, KC and MIP-1α) were consistently significantly higher in the BAL fluids from mice treated with CSpp(CpG(+)) compared to CSpp(CpG(-)) treated mice (Figure 2-25). Of particular distinction were IL-12 and KC levels. TNF-α levels were also higher in the mice receiving CSpp(CpG(+)), however, not significantly. These observed increases in inflammatory cytokines could be due to the presence of CpG since it is well established that triggering TLR-9 can result in a MyD88-dependent, NF-kB-mediated upregulation of inflammatory cytokines, including IL-12 [152]. We also tested for IFN-α, however, levels were below the

lowest limit of detection (0.95 pg/ml) in all samples analyzed (data not shown). Mice body weights were recorded. There was no significant difference between body weights before and 24 hours after administration in all group tested (Figure 2-26).

The results gathered from the BAL fluids showed that both CSpp(CpG(-)) and CSpp(CpG(+)) induced inflammation, as determined by an increased influx of neutrophils as well as increases in total protein, LDH activity, and inflammatory cytokines. Mice treated with chitosan solution alone trended towards increased cytokine levels in their BAL fluid compared to untreated mice. These levels were further enhanced for all cytokines tested when chitosan was complexed with CpG(+) pDNA while CSpp(CpG(-)) treatment resulted in only marginally higher levels (TNF-α, IL-6, MP-1α). Thus, in terms of cytokine levels, chitosan polyplexes made from plasmids devoid of CpG sequences induced lower inflammatory responses than polyplexes harboring plasmids that contained CpG sequences.

In this study, there was a limitation regarding the use of CSpp. These polyplexes can only be prepared at low pDNA concentrations (12.5 µg pDNA/50 µl or 250 µg pDNA/ml). While this has no impact on in vitro experiments, it was a major barrier in mice nasal instillation experiments. In the future, it may be possible to solve this problem by inline mixing the chitosan and pDNA solutions, followed by ultracentrifugation to concentrate the CSpp and adding sucrose, which acts as an aggregation inhibitor [145, 153].

Conclusions

The mixing of plasmid DNA with chitosan resulted in polyplexes with the potential for use in pulmonary gene delivery systems. In this study, we formulated CSpp with 2 different plasmids (CpG(-) and CpG(+)) at N/P ratios of 1, 5, 10, 20, 60 and 100. CSpp showed higher transfection efficiency both in vitro (using A549 cells) and in vivo (mouse nasal instillation) when the dose was increased. However, the inflammatory response also increased. We found that CSpp(CpG(-)) generated superior transfection efficiencies

both in vitro and in vivo when compared with CSpp(CpG(+)). In addition, CSpp(CpG(-)) generated lower levels of proinflammatory cytokines (TNF-α, IL-6, IL-12, KC and MIP-1α) in BAL fluids. Our findings suggest that N/P ratios, dose and plasmid CpG sequence content of CSpp are important factors to consider in achieving optimal gene expression with minimal toxicity and inflammation.

Table 2-1 Endotoxin test of purified and unpurified chitosan using a modification of the kinetic chromogenic Limulus Amebocyte Lysate (LAL) assay. Limit of detection (LLOD) is equal to 0.024 EU/ml, (n = 1).

Description	Endotoxin concentration (EU/ml)
Purified chitosan, 1% w/w in 1% v/v acetic acid	< LLOD
Unpurified chitosan, 1% w/w in 1% v/v acetic acid	89.1
Purified chitosan, 10 mg/ml in LAL water	< LLOD
Unpurified chitosan, 10 mg/ml in LAL water	29.4

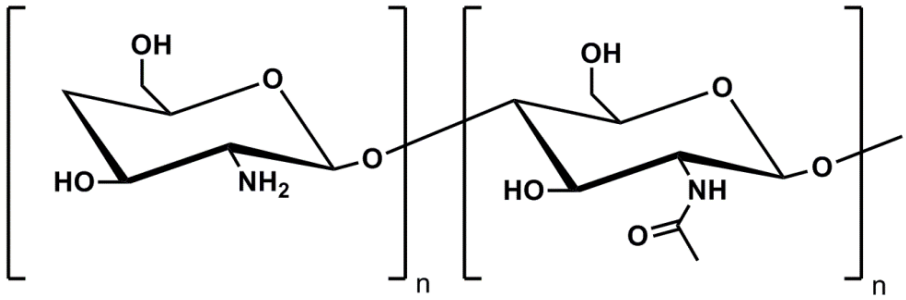

Figure 2-1 Chitosan structure composed of randomly distributed β-(1-4)-linked D-glucosamine (deacetylated unit, left) and N-acetyl-D-glucosamine (acetylated unit, right).

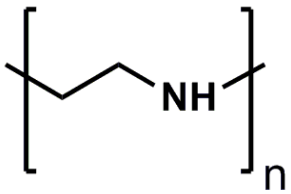

Figure 2-2 Polyethylenimine (PEI) structure composed of a repeating unit of the amine group and two aliphatic hydrocarbons.

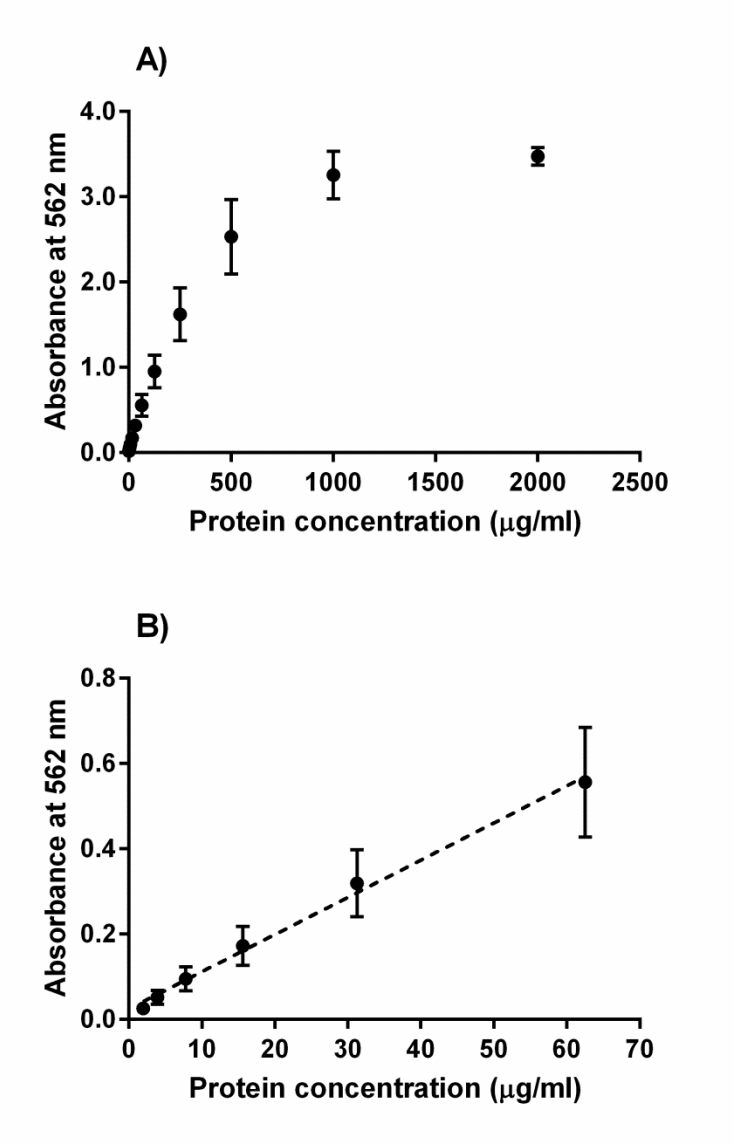

Figure 2-3 Absorbance obtained from bovine serum albumin standard using Micro BCA™ Protein Assay Kit (Pierce Biotechnology Inc., Rockford, IL) in the range of 0 – 200 µg/ml (A). Linear relationship between protein concentration and absorbance was in the range of 1.95 – 62.50 µg/ml, y = 0.008721x + 0.02449 (B). Data are expressed as mean ± SD (n = 12-13).

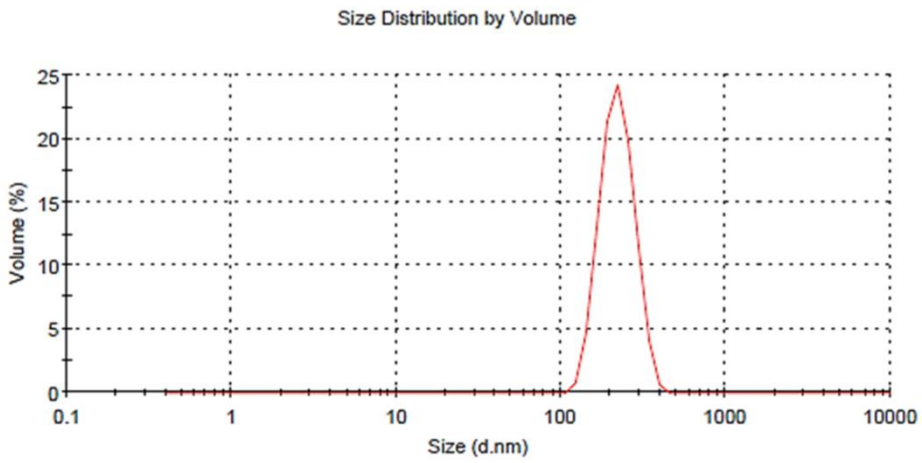

Figure 2-4 Size distribution (diameter) of CSpp prepared for the in vitro study at the concentration of pDNA equal to 2.5 µg/50 µl measured by Zetasizer Nano ZS. Size distribution was expressed by volume. The distribution was unimodal.

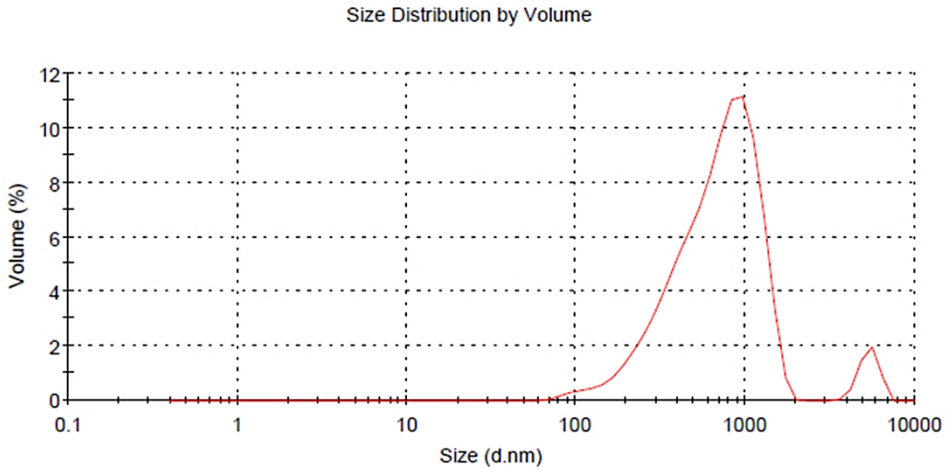

Figure 2-5 Size distribution (diameter) of CSpp prepared for the in vivo study at the concentration of pDNA equal to 12.5 µg/50 µl measured by Zetasizer Nano ZS. Size distribution was expressed by volume. The distribution was bimodal.

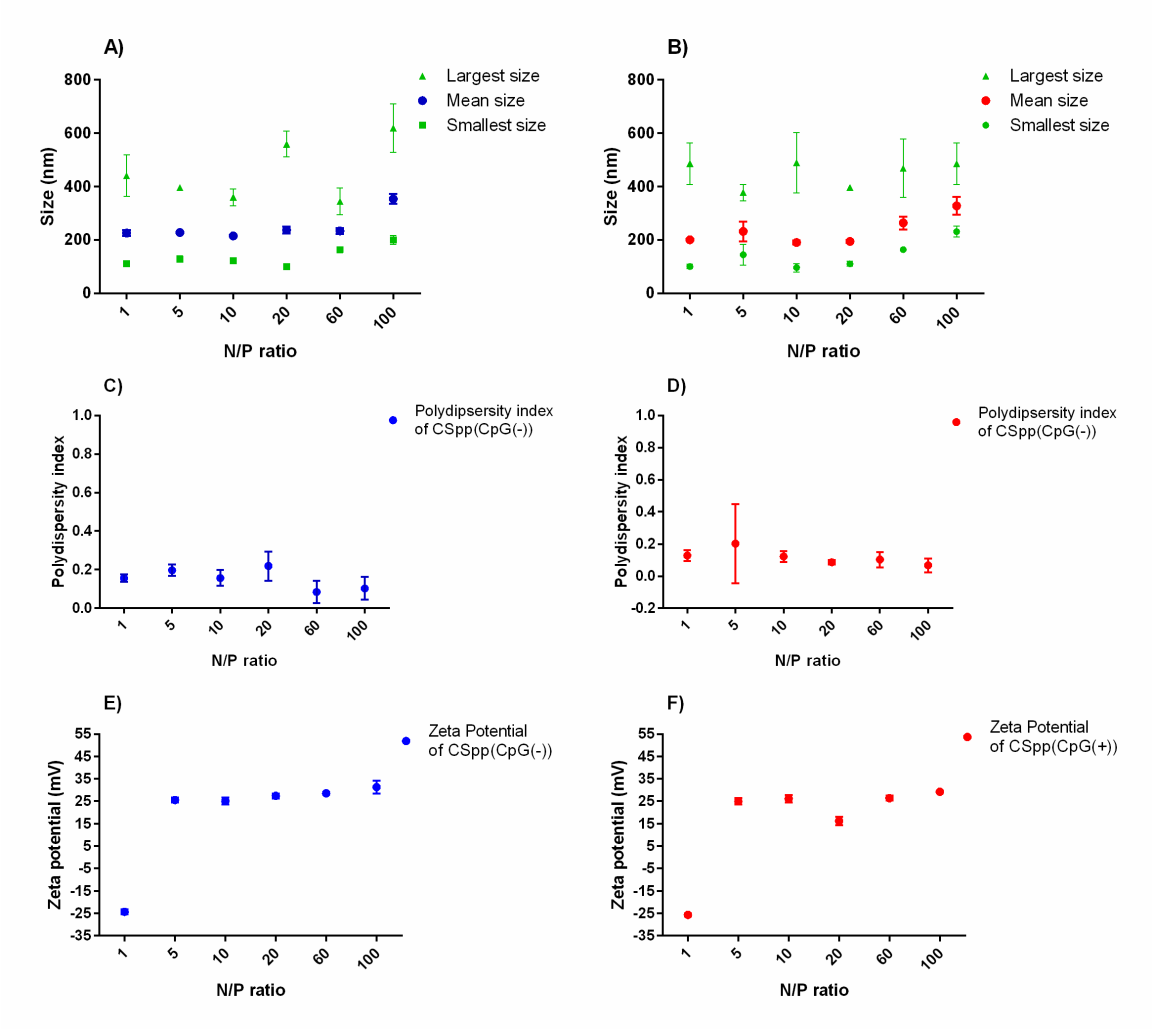

Figure 2-6 Particle sizes of CSpp(CpG(-)) (A) and CSpp(CpG(+)) (B), polydispersity index of CSpp(CpG(-)) (C) and CSpp(CpG(+)) (D) and zeta potentials of CSpp(CpG(-)) (E) and CSpp(CpG(+)) (F) at N/P ratios ranging from 1-100. Results obtained from CSpp(CpG(-)) and CSpp(CpG(+)) were shown in blue (●) and red (●), respectively. In Figure A and B, green color represents the smallest (■) and largest (▲) particle size detected. All measurements were made in acetate buffer, pH 5.46, at 25°C using a Zetasizer nano ZS. Data are expressed as mean ± SD (n = 3).

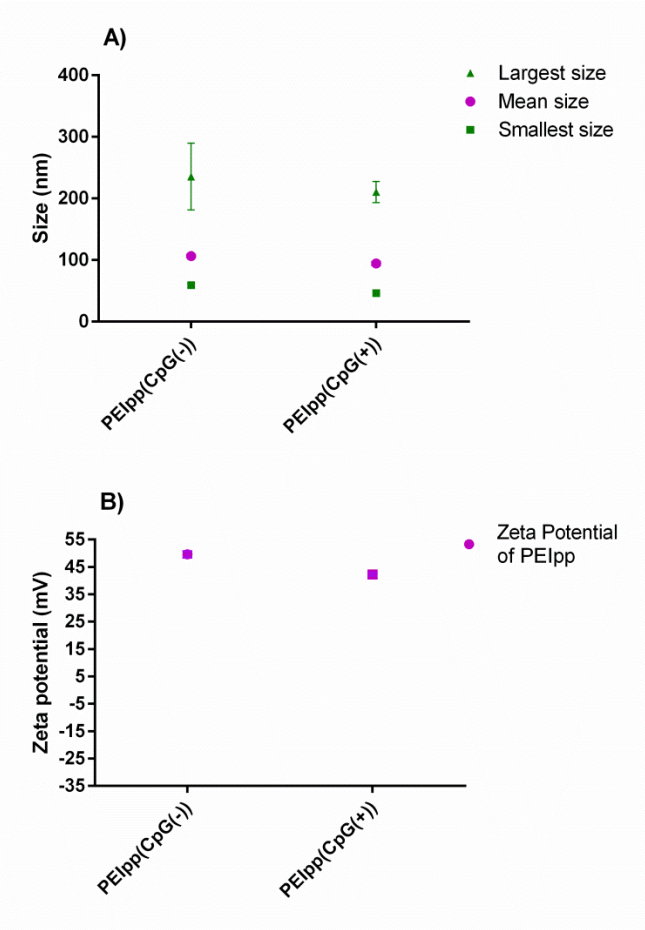

Figure 2-7 Particle sizes (A), and zeta potentials of PEIpp(CpG(-)) and PEIpp(CpG(+)) (B) at N/P 10 in water, at 25°C and measured by Zetasizer nano ZS. Results obtained from PEIpp(CpG(-)) and PEIpp(CpG(+)) were shown in pink (●).In Figure A, green color represents the smallest (■) and largest (▲) particle size detected. Data are expressed as mean ± SD (n = 3).

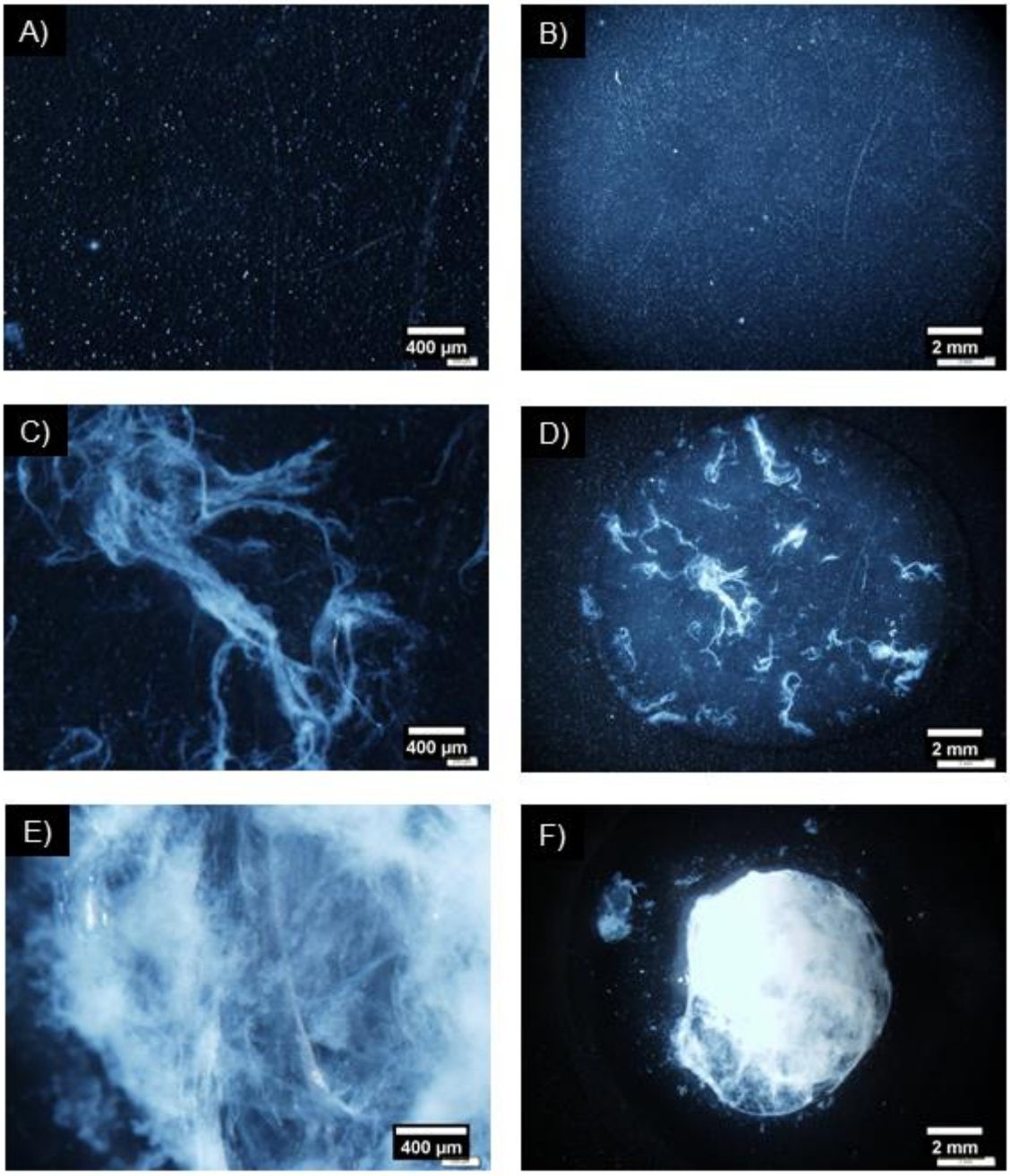

Figure 2-8 CSpp suspensions on slides at a pDNA concentration of 12.5 µg/50 µl (A & B) showing no precipitation. Aggregates of CSpp at pDNA concentrations of 25.0 µg/50 µl (C & D) and 50.0 µg/50 µl (E & F) occurred when high pDNA concentrations were used to prepare the polyplexes. Scale bars in Figure 2-3 (A, C & E) represent 400 µm. Scale bars in Figure 2-3 (B, D & F) represent 2 mm. All images were taken using an Olympus Stereoscope DP (Olympus Scientific Solutions Americas Corp., Waltham, MA).

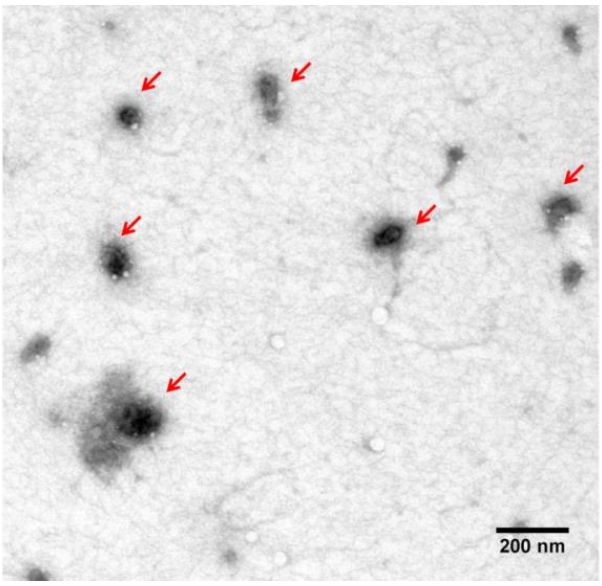

Figure 2-9 Transmission electron micrograph (TEM) of CSpp(CpG(+)) at N/P 10 (indicated by arrows) that were taken via JEOL JEM-1230 transmission electron microscope. Scale bar represents 200 nm.

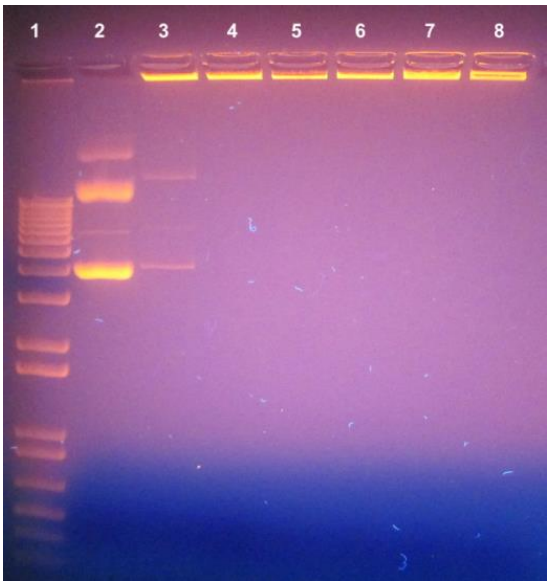

Figure 2-10 Gel retardation assay in 1% agarose gel containing ethidium bromide: lane 1, DNA ladder; lane 2, naked CpG(+) pDNA; lanes 3 – 8, CSpp(CpG(+) with N/P ratios of 1, 5, 10, 20, 60 and 100, respectively.

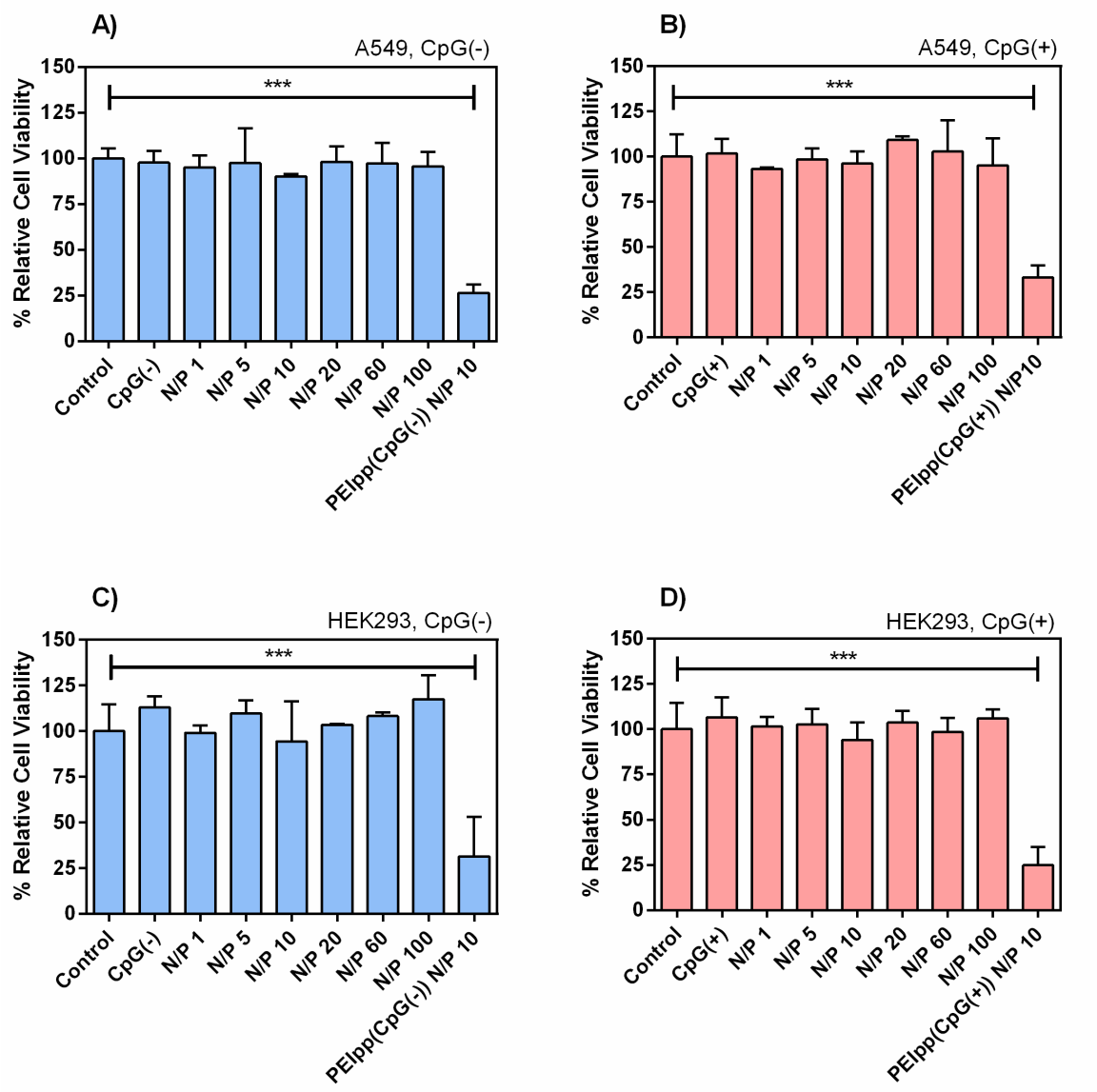

Figure 2-11 Cell viability of A549 (A, B) and HEK293 (C, D) cell lines treated with CSpp(CpG(-)) (A, C) and CSpp(CpG(+)) (B, D) were determined by MTS assays. Cells were treated with CSpp with N/P ratios ranging from 1 – 100. CpG(-) represents soluble CpG-free plasmid DNA while CpG(+) represents soluble CpG-containing plasmid DNA. PEIpp(CpG(-)) or PEIpp(CpG(+)) were PEI complexes with pDNA at N/P 10. Control = cells treated with PBS. The cells were seeded into a 96-well plate at a density of 1 x 10^4 cells per well one day prior to treatment and then exposed to the indicated treatments for 48 hours. Each treatment contained 1 µg of pDNA per well. Data are expressed as mean ± SD (n=3). Percent relative cell viability was compared to cells treated with PBS. One-way ANOVA with Bonferroni's multiple comparison test was used. *** $p < 0.001$. Results obtained from CSpp(CpG(-)) and CSpp(CpG(+)) were shown in blue and pink, respectively.

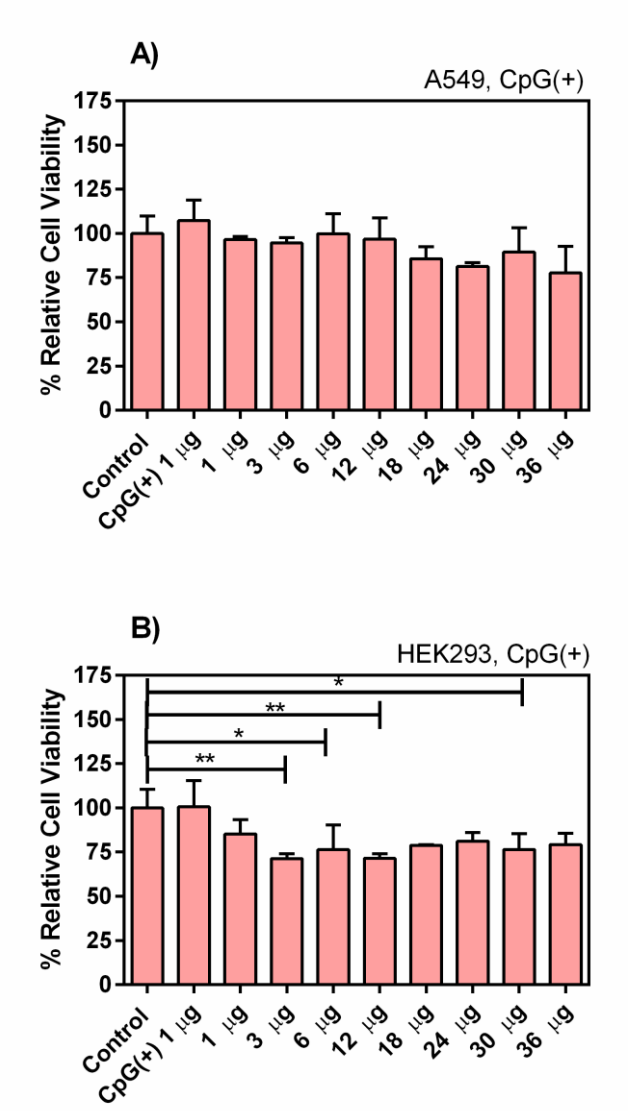

Figure 2-12 Cell viability of A549 (A) and HEK293 (B) cell lines treated with CSpp(CpG(+)) were determined by MTS assays. In all groups, except control and CpG(+) 1 ug, cells were treated with CSpp(CpG(+)) at a N/P ratio of 10 at pDNA amounts of 1 – 36 µg per well. CpG(+) represents soluble CpG-containing plasmid DNA. Control = cells treated with PBS. The cells were seeded into a 96-well plate at a density of 1 x 10^4 cells per well one day prior the experiment and exposed to the treatments for 48 hours. Data are expressed as mean ± SD (n=3). Percent relative cell viability was compared to cells treated with PBS. One-way ANOVA with Bonferroni's multiple comparisons test compared to the control group was used. ** $p < 0.01$, * $p < 0.05$.

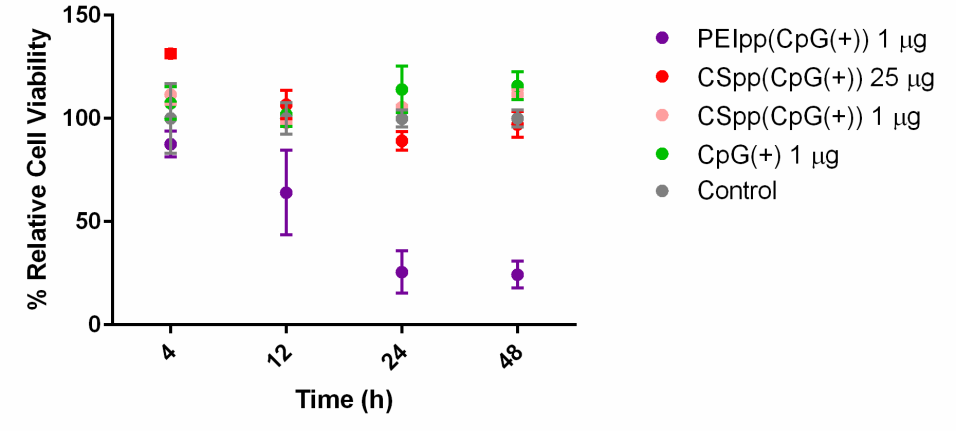

Figure 2-13 Cell viabilities of HEK293 cell line treated with different amounts of CSpp(CpG(+)) were determined by MTS assays. Cells were treated with CSpp(CpG(+)) at pDNA amounts of 1 μg (represents in pink) and 5 μg (represents in red) per well. CpG(+) represents soluble CpG-containing plasmid DNA (shown in green). Control = cells treated with PBS (grey). PEIpp(CpG(+)) was used as a positive control with pDNA amount of 1 μg per well (purple). The cells were seeded into a 96-well plate at a density of 1 x 10^4 cells per well one day prior to exposure to the treatments for 4, 12, 24 and 48 hours. Data are expressed as mean ± SD (n=3). Percent relative cell viability was compared to cells treated with PBS. Two-way ANOVA with Bonferroni's multiple comparisons test was used. Only PEIpp(CpG(+)) treated cells showed significantly reduced cell viabilities when compared to the control (*p*-value < 0.001) at 12, 24 and 48 hours of treatment.

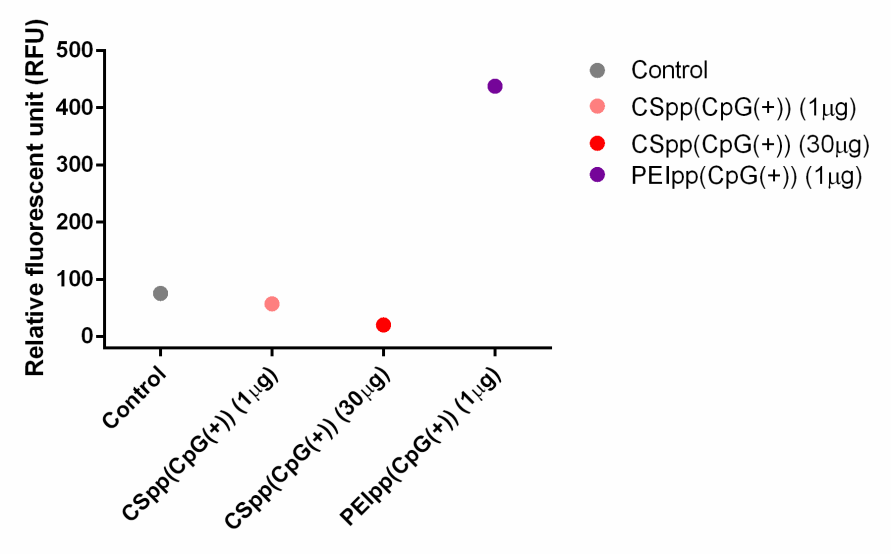

Figure 2-14 Caspase-3/7 activity of HEK293 cell line treated with CSpp(CpG(+)) and PEIpp(CpG(+)) were determined by the Apo-ONE® Homogeneous Caspase-3/7 Assay (see methods). Cells were treated with CSpp(CpG(+)) at pDNA amounts of 1 µg (shown in pink) and 30 µg (shown in red) per well. Control = cells treated with PBS (grey). PEIpp(CpG(+)) was used as a positive control with pDNA amount of 1 µg per well (purple). Data are expressed as mean (n = 2).

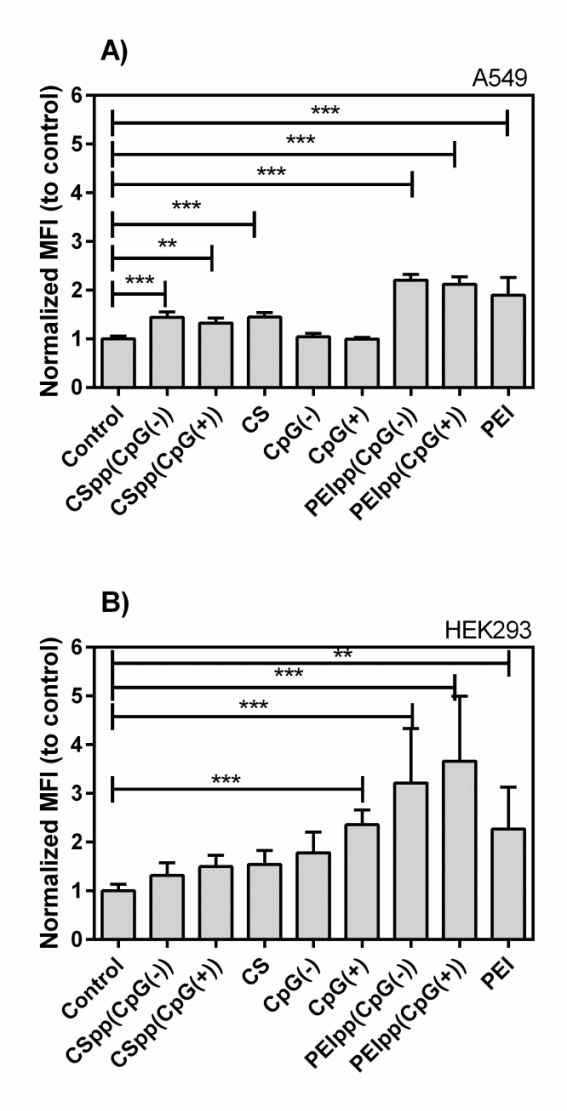

Figure 2-15 DHE oxidation levels indicated as normalized mean fluorescence intensity (Normalized MFI) showing estimates of relative intracellular superoxide levels in A549 cells (A) and HEK293 cells (B) treated with indicated polyplexes. Cells were treated with CSpp(CpG(-)) or CSpp(CpG(+)) at a N/P ratio of 10. CS is chitosan solution without pDNA. PEIpp(CpG(-)) or PEIpp(CpG(+)) were PEI complexes with pDNA at N/P 10. PEI = PEI solution without pDNA. Control = cells treated with PBS. Data are expressed as mean ± SD (n = 6 - 9). One-way ANOVA with Bonferroni's multiple comparisons test was used. *** $p < 0.001$, ** $p < 0.01$. Antimycin A which was used as a positive control for the experiment showed the normalized MFI equal to a 4.7-fold increase in A549 cells and a 4.0-fold increase in HEK293 cells.

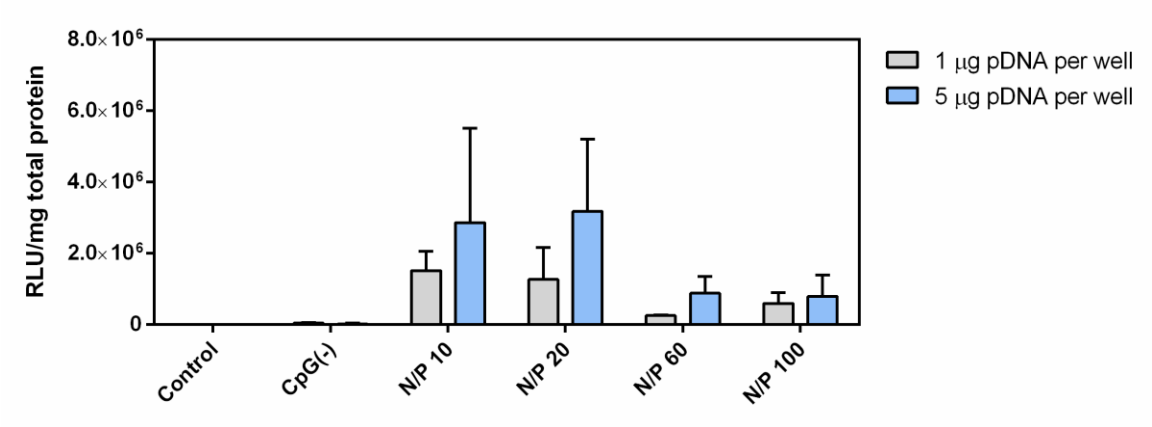

Figure 2-16 Transfection efficiency of A549 cells treated with CSpp(CpG(-)) at two different pDNA concentrations (1 µg (grey) and 5 µg (blue) pDNA per well). Varying N/P ratios are indicated. Control = cells treated with PBS. Data are expressed as mean ± SD (n = 3 - 7). Two-way ANOVA with Bonferroni's multiple comparisons test was used. There was no significant difference when A549 cells treated with CSpp(CpG(-)) containing 1 µg pDNA/well and 5 µg pDNA/well were compared.

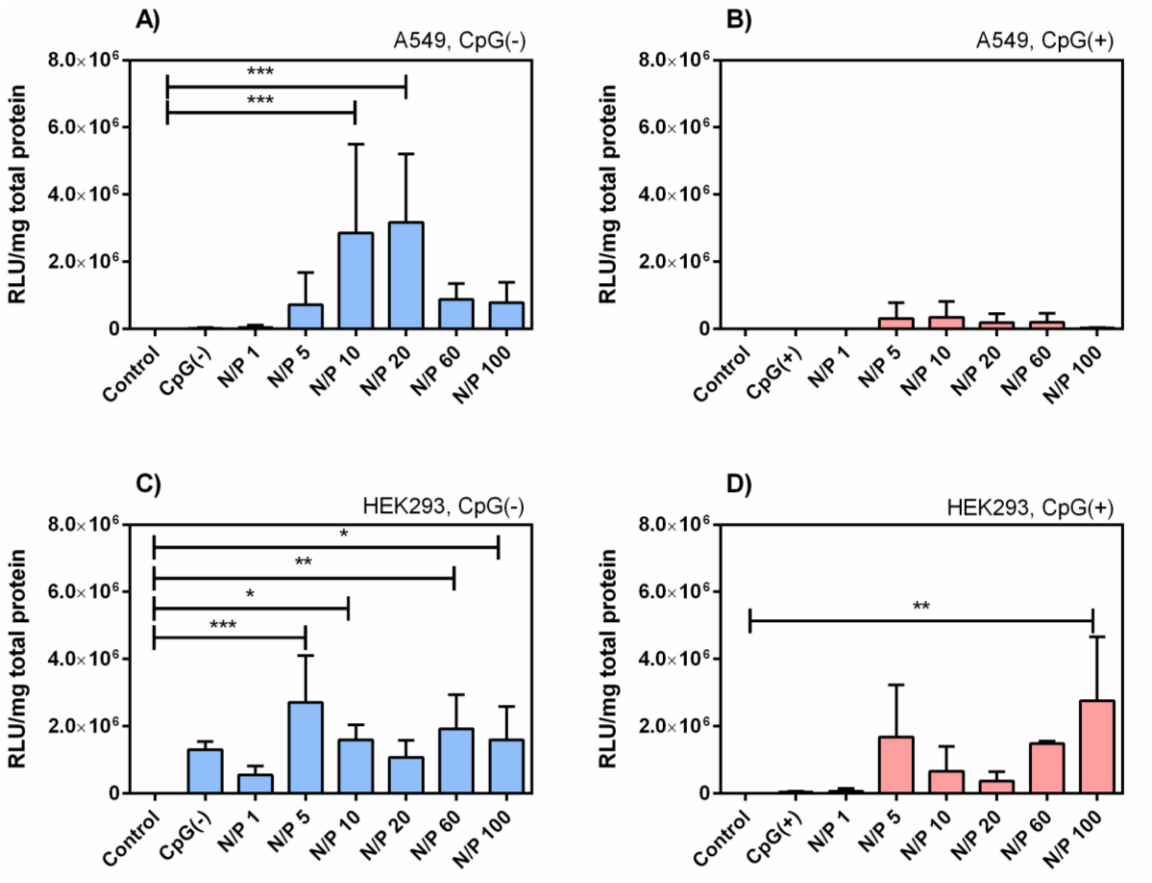

Figure 2-17 Transfection efficiency of A549 (A, B) and HEK293 (C, D) cells treated with CSpp(CpG(-)) (A, C) or CSpp(CpG(+)) (B, D). Varying N/P ratios are indicated. Control = cells treated with PBS. Each treatment contained 5 µg pDNA/well. Data are expressed as mean ± SD (n = 3 - 7). One-way ANOVA with Bonferroni's multiple comparisons test was used. * $p < 0.05$, ** $p < 0.01$, *** $p < 0.001$. PEIpp N/P 10 was used as a positive control for transfection (not shown in graphs). The luciferase expression of PEIpp-transfected A549 cells was equal to $2.32 \times 10^{10} \pm 7.45 \times 10^{9}$ RLU/mg (total protein) (for PEIpp(CpG(-)) and $2.54 \times 10^{10} \pm 1.62 \times 10^{10}$ RLU/mg (for PEIpp(CpG(+)). The luciferase expression in HEK293 cells was $5.38 \times 10^{10} \pm 3.96 \times 10^{9}$ RLU/mg (for PEIpp(CpG(-)) and $4.23 \times 10^{10} \pm 2.92 \times 10^{10}$ RLU/mg (for PEIpp(CpG(+)).

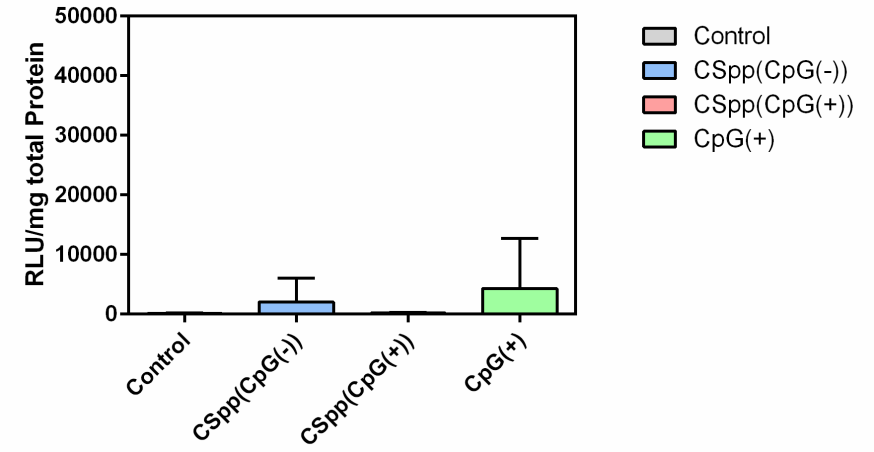

Figure 2-18 Luciferase expression in mouse lungs 24 hours after nasal instillation of indicated CSpp formulations. Control = no treatment (grey); CpG(+) = CpG(+) solution (green). Each treatment, aside from control, contained 12.5 µg of pDNA (12.5 µg pDNA/50 µl, 1x nasal instillation). One-way ANOVA with Bonferroni's multiple comparisons test was used. Data are expressed as mean ± SD (n = 4-5). There was no significant difference in luciferase expression when each treatment was compared to the control or CSpp(CpG(-)) was compared to CSpp(CpG(+)).

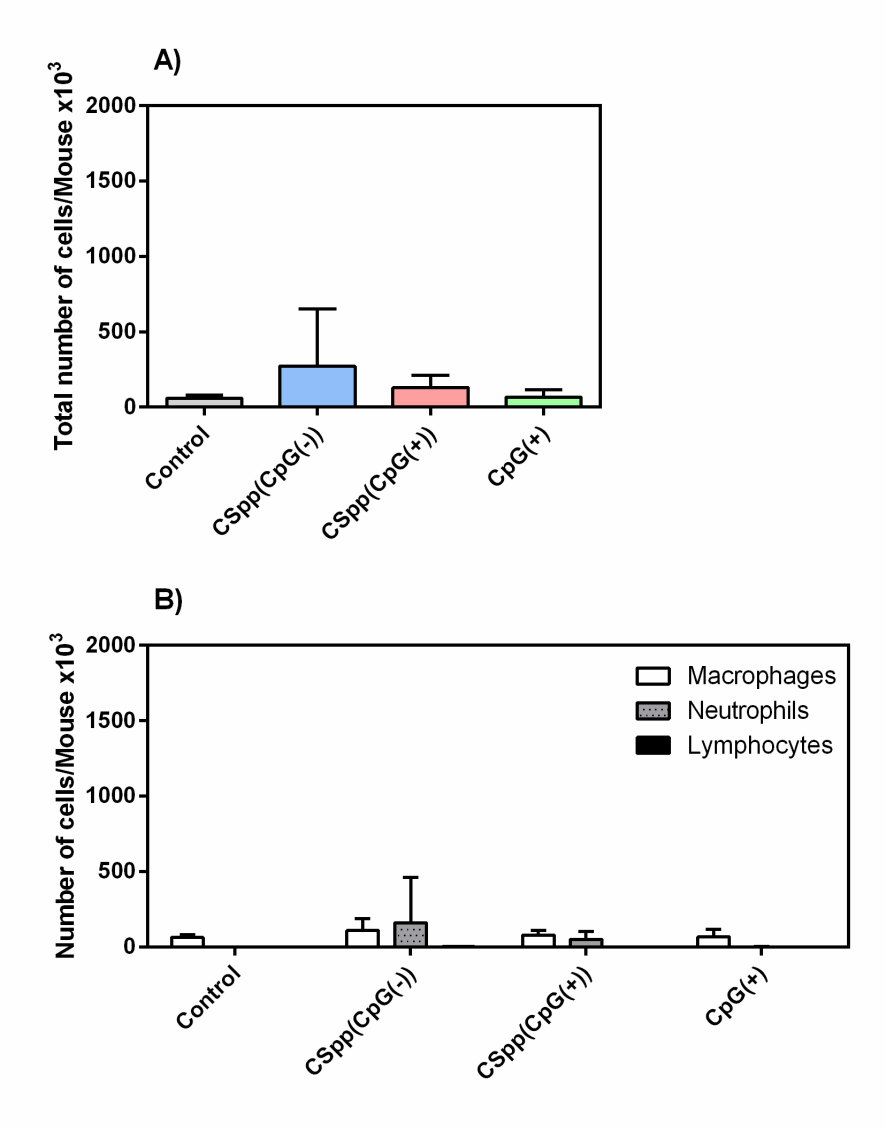

Figure 2-19 BAL cell counts: total number of cells (A) and the number of macrophages, neutrophils and lymphocytes (B) in the BAL fluid of mice 24 hours after nasal instillation of indicated CSpp formulations. Control = no treatment (grey); CpG(+) = CpG(+) solution (green). Each treatment (aside from control) contained 12.5 µg of pDNA (12.5 µg pDNA/50 µl, 1x nasal instillation). Data are expressed as mean ± SD (n = 4-5). One-way ANOVA with Bonferroni's multiple comparisons test was used. There was no significant difference in cell numbers when each treatment was compared to the control or CSpp(CpG(-)) was compared to CSpp(CpG(+)).

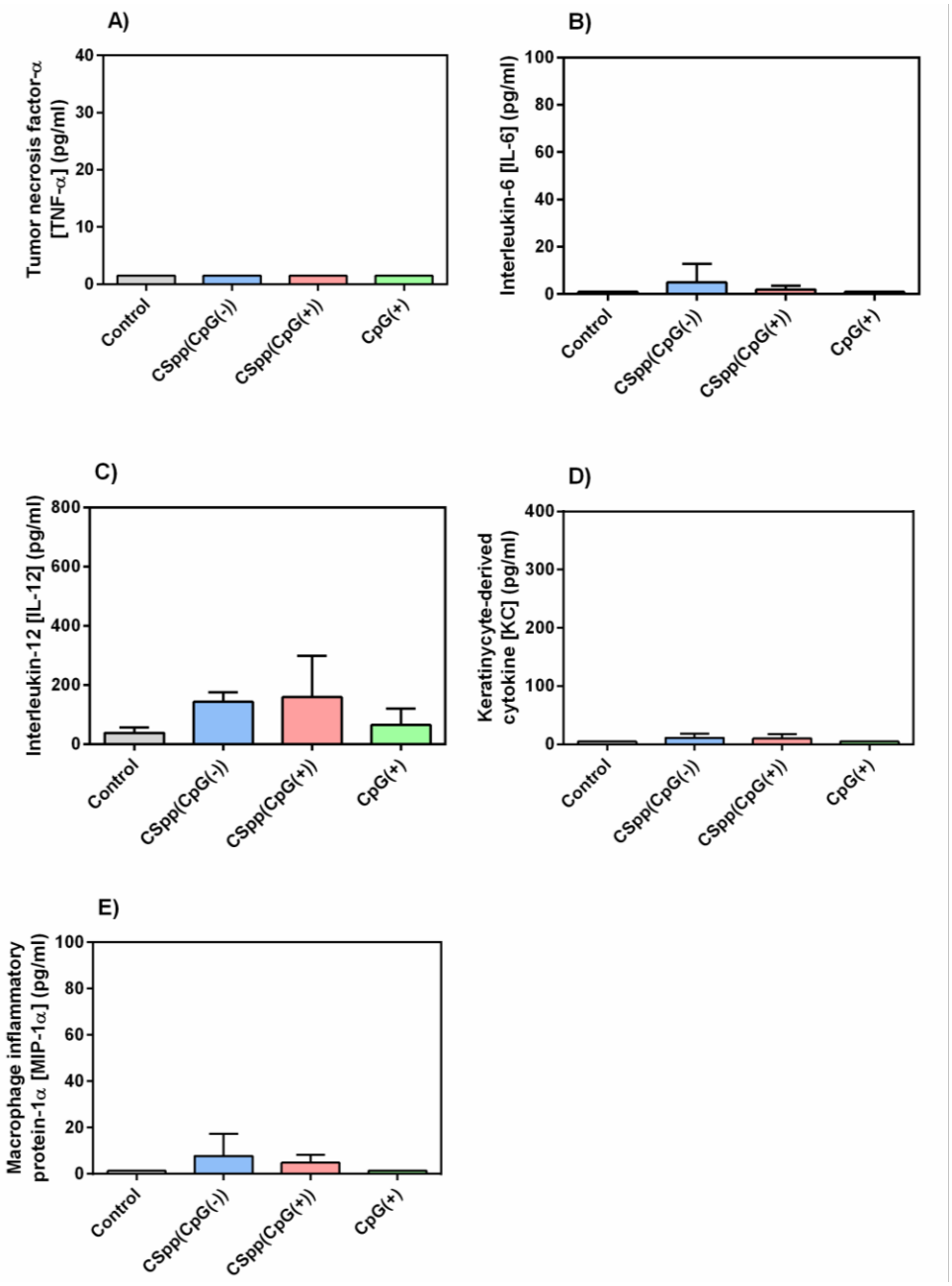

Figure 2-20 The concentration of proinflammatory cytokines/chemokines detected in BAL fluid of mice 24 hours subsequent to nasal instillation of indicated CSpp formulations. Control = no treatment (grey); CpG(+) = CpG(+) solution (green). LLOD for: TNF-α = 1.50 pg/ml (A), IL-6 = 0.96 pg/ml (B), IL-12 = 6.38 pg/ml (C), KC = 4.95 pg/ml (D) and MIP-1α = 1.3 pg/ml (E). Each treatment aside from control contained12.5 µg of pDNA (12.5 µg pDNA/50 ul, 1x nasal instillation). Data are expressed as mean ± SD (n = 4-5). One-way ANOVA with Bonferroni's multiple comparisons test was used. There was no significant difference in cytokine/chemokine levels when each treatment was compared to the control or CSpp(CpG(-)) was compared to CSpp(CpG(+)).

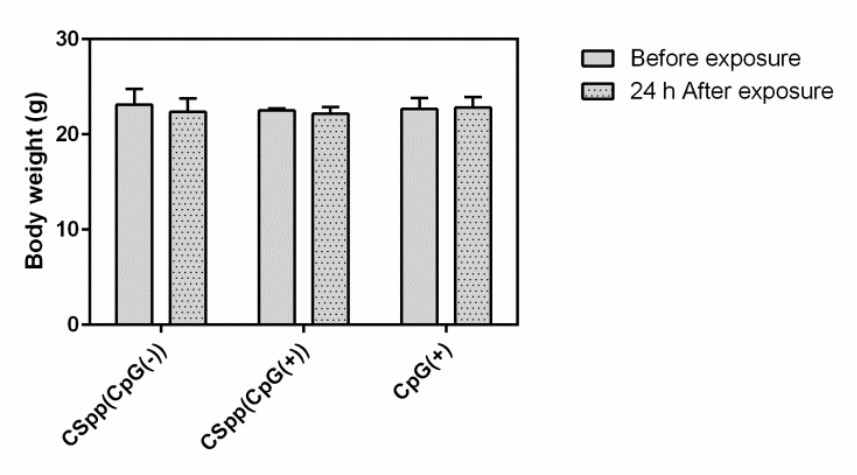

Figure 2-21 Mouse body weights before, and 24 hours after, exposure to CSpp(CpG(-)) and CSpp(CpG(+)). CpG(+) = naked CpG(+) pDNA solution. Each treatment aside from control and CS, contained 12.5 µg of pDNA (12.5 µg pDNA/50 µg, 1x nasal instillations). Data are expressed as mean ± SD (n = 5). Two-way ANOVA with Bonferroni's multiple comparisons test was used. There was no significant difference in mouse body weights before and after 24 hour exposures.

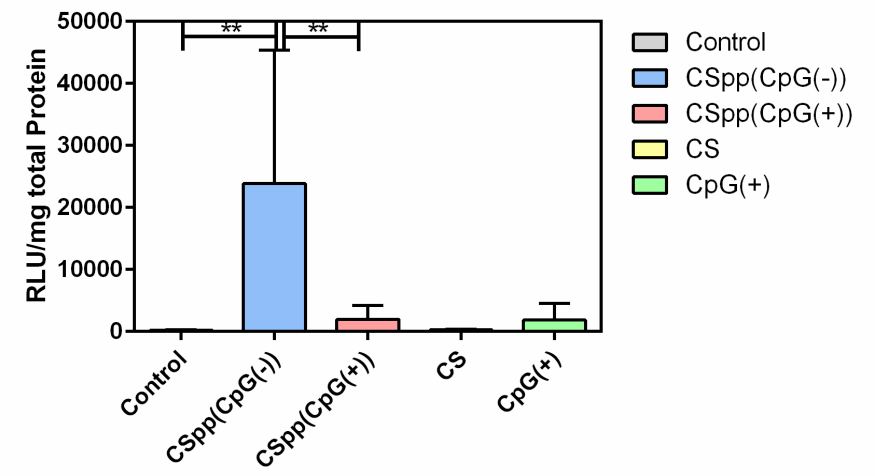

Figure 2-22 Luciferase expression in mouse lungs after nasal instillation of indicated CSpp formulations. CS = chitosan solution (yellow); control = no treatment (grey); CpG(+) = CpG(+) solution (green). Each treatment, aside from control and CS, contained 25 µg of pDNA (12.5 µg pDNA/50 µl, 2x nasal instillations). One-way ANOVA with Bonferroni's multiple comparisons test was used. Data are expressed as mean ± SD (n = 6). ** $p < 0.01$.

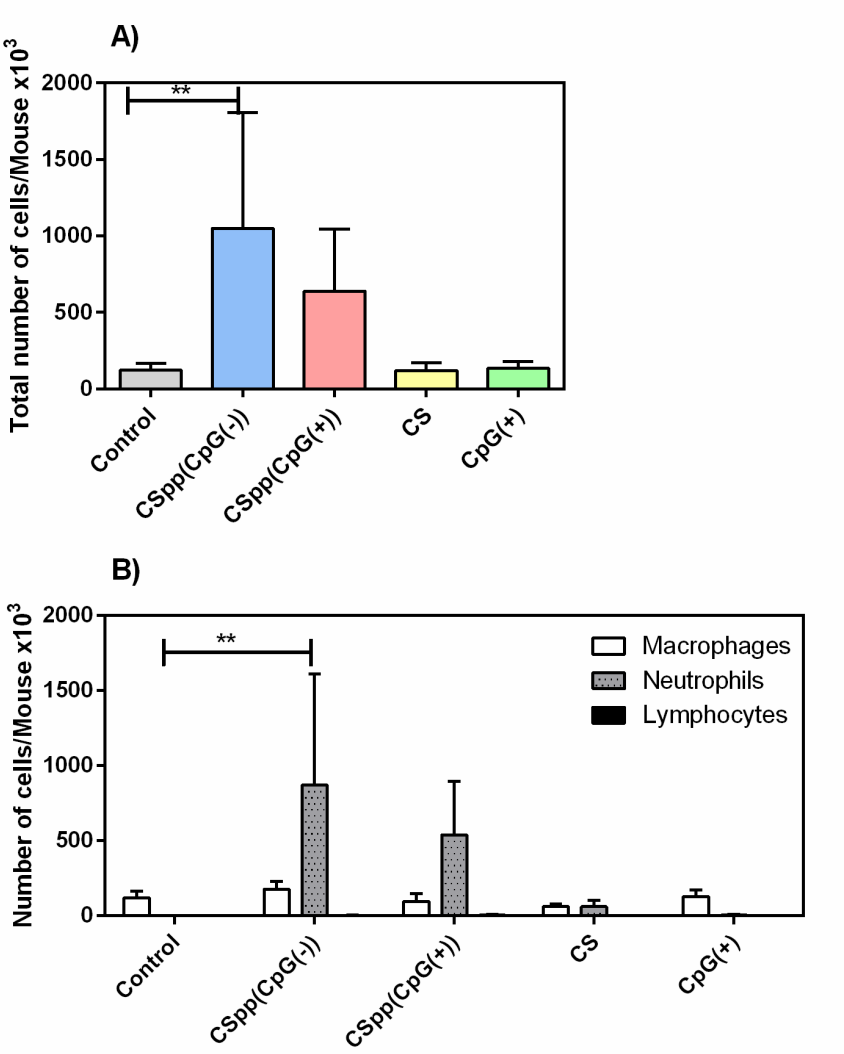

Figure 2-23 BAL cell counts: total number of cells (A) and the number of macrophages, neutrophils and lymphocytes (B) in the BAL fluid of mice after nasal instillation of indicated CSpp formulations. CS = chitosan solution (CS, yellow), CpG(+) = naked CpG(+) pDNA solution (green). Control = no treatment (grey). Each treatment (aside from control and CS) contained 25 µg of pDNA (12.5 µg pDNA/50 µg, 2x nasal instillations). Data are expressed as mean ± SD (n = 6). One-way ANOVA with Bonferroni's multiple comparisons test was used. ** $p < 0.01$.

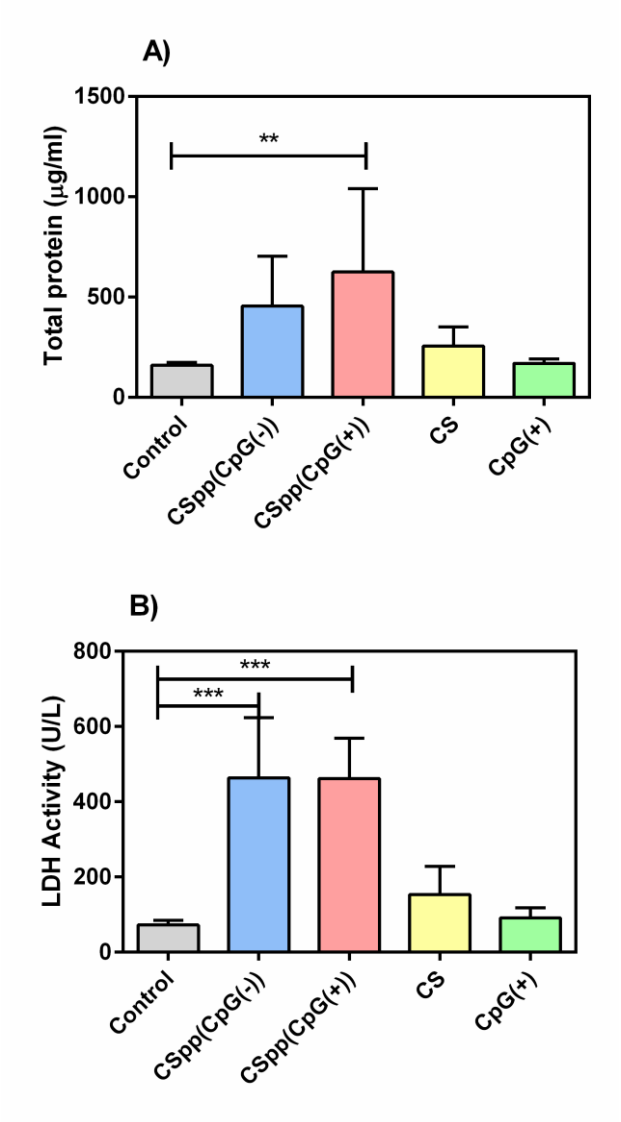

Figure 2-24 Total protein and LDH activity levels: the concentration of total protein (A) and LDH activity (B) in BAL fluids of mice 24 hours subsequent to nasal instillation of indicated CSpp formulations. CS = chitosan solution (CS, yellow), CpG(+) = naked CpG(+) pDNA solution (green). Control = no treatment (grey). Each treatment aside from control and CS, contained 25 µg of pDNA (12.5 µg pDNA/50 µg, 2x nasal instillations). Data are expressed as mean ± SD (n = 6). One-way ANOVA with Bonferroni's multiple comparisons test was used. *** $p < 0.001$, ** $p < 0.01$.

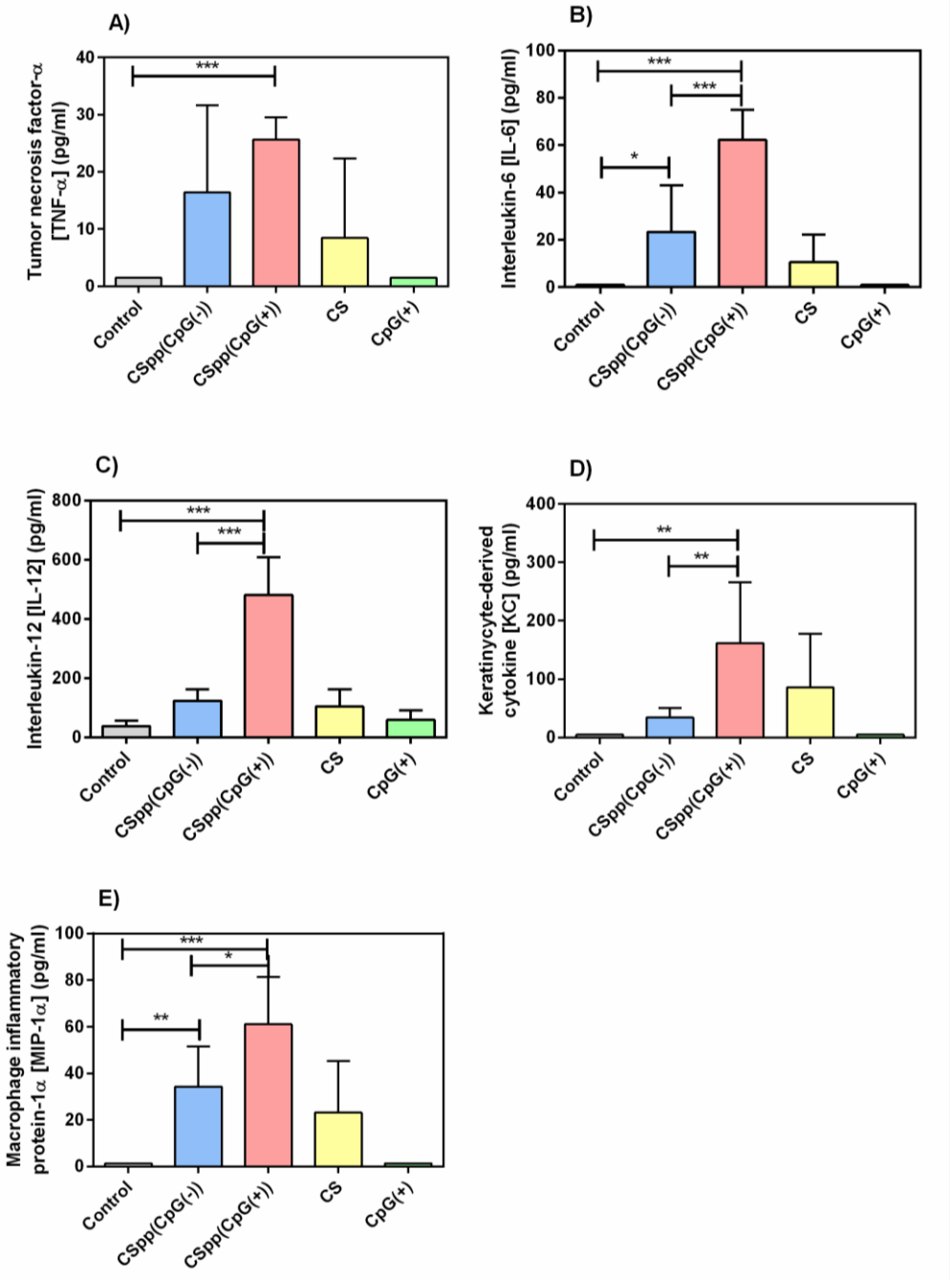

Figure 2-25 Concentrations of proinflammatory cytokines/chemokines detected in BAL fluid of mice 24 hours subsequent to nasal instillation of indicated CSpp formulations. CS = chitosan solution (yellow); control = untreated (grey); CpG(+) = naked CpG(+) pDNA solution (green). LLOD for: TNF-α = 1.50 pg/ml (A), IL-6 = 0.96 pg/ml (B), IL-12 = 6.38 pg/ml (C), KC = 4.95 pg/ml (D) and MIP-1α = 1.3 pg/ml (E). Each treatment aside from control and CS contained 25 µg of pDNA (12.5 µg pDNA/50 ug, 2x nasal instillations). Data are expressed as mean ± SD (n = 6). One-way ANOVA with Bonferroni's multiple comparisons test was used. *** $p < 0.001$, ** $p < 0.01$, * $p < 0.05$.

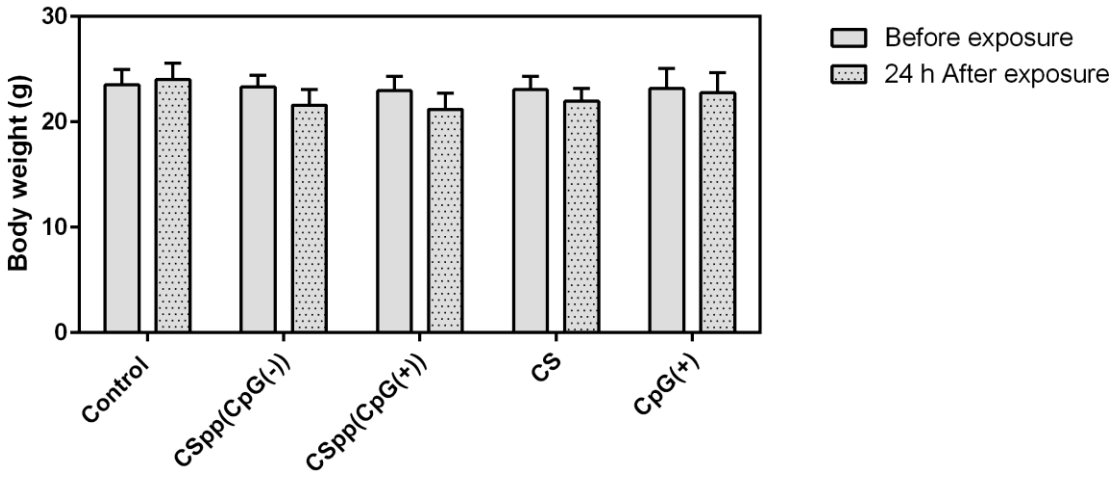

Figure 2-26 Mouse body weights before exposure and 24 hours after exposure to CSpp(CpG(-)) and CSpp(CpG(+)). CS = chitosan solution (CS), CpG(+) = naked CpG(+) pDNA solution. Control = no treatment. Each treatment aside from control and CS, contained 25 µg of pDNA (12.5 µg pDNA/50 µg, 2x nasal instillations). Data are expressed as mean ± SD (n = 6). Two-way ANOVA with Bonferroni's multiple comparisons test was used. There was no significant difference in mouse body weights before, and 24 hours after, the exposures.

CHAPTER 3 POLY(GALACTARAMIDOAMINE) IS AN EFFICIENT CATIONIC POLYMERIC NON-VIRAL VECTOR WITH LOW CYTOTOXICITY FOR TRANSFECTING HUMAN EMBRYONIC KIDNEY (HEK293) AND MURINE MACROPHAGE (RAW64.7) CELLS

Introduction

Cationic polymers have shown strong potential for delivery of plasmid DNA (pDNA) to cells. Cationic polymers condense pDNA into polyplexes that can be efficiently internalized by cells as well as conferring protection against enzymatic degradation [131, 154-156]. The most commonly used synthetic cationic polymer in non-viral gene delivery, poly(ethyleneimine) (PEI), promotes high transfection efficiencies of a broad range of cell lines, however, PEI is also associated with high toxicity [157, 158]. Chitosan, a natural polysaccharide, is relatively non-toxic, however, when used in gene delivery it yields low transfection efficiencies when compared with PEI [64, 159-161]. Poly(glycoamidoamine)s are a new class of cationic polymer that have shown promise as a transfection reagent with reduced toxicity relative to PEI [162, 163]. The synthesis of poly(glycoamidoamine)s was based upon PEI and chitosan structures. The class of poly(glycoamidoamine) comprise 16 polyamides. Since it has been reported that high molecular weight cationic polymers exhibit high cytotoxicity, all 16 polymers in the poly(glycoamidoamine)s family were synthesized to have low molecular weight with similar degrees of polymerization (number average molecular weight/molecular weight of monomer unit) [77]. Stable polyplexes can form when negatively charged pDNA is mixed with poly(glycoamidoamine)s, which possess positively charged amine groups [78]. These polyamides have been tested for their DNA encapsulation ability, transfection efficiency (luciferase expression) and cytotoxicity. Among all 16 polyamides, a co-polymer of dimethyl-*meso*-galactarate and pentaethylenehexamine or poly(galactaramidoamine) (PGAA) that is synthesized by AABB step growth polymerization showed the best results

(Figure 3-1) [77, 164, 165]. PGAA has a molecular weight equal to 4.6 kDa with the degree of polymerization equal to 11 – 14 [77, 162]. PGAA contains an oligoamine, providing a cationic charge to bind with pDNA electrostatically. PGAA also contains a carbohydrate moiety which reduces the positive charge density of amine groups in the polymer structure to be lower than PEI but still higher than chitosan, thereby decreasing the overall toxicity and increasing transfection efficiency [78]. The overall strength of the electrostatic binding interaction is dependent on the ratio of the moles of amine groups to the moles of phosphate groups. This amine to phosphate ratio is referred to as the N/P ratio. Mixing of PGAA with pDNA results in PGAA polyplexes (PGAApp) which have shown robust transfection efficiencies in HeLa, BHK-21 and HepG2 cell lines. PGAA can form polyplexes with DNA at N/P ratios as low as 5 [164, 165]. One of the building blocks of PGAA is ethylenimine and as such, increasing the N/P ratio increases the ethylenimine content and would therefore be expected to increase toxicity. In general, optimal transgene expression is the result of a careful balance between the toxicity and transfection efficiency of the polymer. Optimizing the N/P ratio at which PGAApp cause maximum transfection is therefore necessary prior to using these polyplexes in subsequent studies. The optimal N/P ratio also has the potential to vary from one cell line to another [131].

A specific aim for this study was to evaluate PGAA as a transfection reagent. PGAA were used at N/P ratios of 40, 60 and 80 in human embryonic kidney cells (HEK293 cells). This is a rapidly dividing cell line which is highly susceptible to transfection [166]. Given that transfection efficiencies can vary from cell line to cell line, we also evaluated transfection efficiency and cytotoxicity of PGAApp using RAW264.7 cells. This cell line, derived from mouse macrophages is notoriously difficult to transfect [167].

Materials and methods

Plasmid amplification and purification

Plasmid encoding for the firefly luciferase (VR1255, 6413 bps) was transformed into *Escherichia coli* (*E. coli*) DH5α-competent cells. The plasmid were amplified by first streaking E.coli contained plasmid of interested in Lennox L Agar (875 mg in 25 ml of nanopure water, RPI Research Products International Corp, Mt. Prospect, IL) and incubated overnight at 37°C. A single colony was added into Lennox L Broth medium (Lennox L Broth powder 10 g in 0.5 L of nanopure water, RPI Research Products International Corp, Mt. Prospect, IL). Both Lennox L Agar and Lennox L Broth contain 100 µg/ml of kanamycin monosulfate (RPI Research Products International Corp, Mt. Prospect, IL) for pDNA selection.

All plasmids were purified using a GenElute™ HP Endotoxin-Free Plasmid Maxiprep Kit (Sigma-Aldrich Co., St. Louis, MO), according to the manufacturer's protocol. pDNA concentrations were determined using a NanoDrop 2000 spectrophotometer (Thermo Fisher Scientific Inc., Waltham, MA). An absorbance ratio of 260 nm to 280 nm and 260 nm to 230 nm was used to access the quality of extracted pDNA. The 260/280 ratio approximately 1.8 with the 260/230 ratio approximately 2.0 – 2.2 was considered free of contaminants [129 168].

PGAApp preparation

PGAA (Glycofect™) was obtained from Techulon Inc (Blacksburg, VA). PGAA was dissolved in UltraPure™ DNase/RNase-Free distilled water (Invitrogen™, Grand Island, NY). Plasmid DNA at a concentration of 200 µg/ml was pre-heated to 50–55°C prior to mixing to improve dissolution. PGAA solutions were then diluted with UltraPure™ DNase/RNase-Free distilled water to reach the desired amine to phosphate (N/P) ratio. Equal volumes of pDNA solution (350 µl) were added to PGAA solutions (350 µl) which were then vortexed for 20–30 seconds and incubated at room temperature for 30

minutes to form polyplexes. All polyplexes in this study were freshly prepared prior to use.

Determination of size, polydispersity index and zeta potential of PGAApp

Particle size and polydispersity index (PdI) of PGAApp at N/P ratios of 40, 60 and 80 were measured using the Zetasizer Nano ZS (Malvern Instruments Inc., Westborough, MA). Size and zeta potential measurements were performed on polyplexes that were dispersed in nanopure water at 25°C. The particle size and PdI were measured at 173° backscatter detection in disposable polystyrene cuvettes (DTS0012) with the total volume of the solution equal to 1 ml.

Cell lines and cell culture

Human embryonic kidney 293 (HEK293) cells and murine macrophage cells (RAW264.7) were purchased from the American Type Culture Collection (ATCC, Rockville, MD). HEK293 cells were maintained in Dulbecco's Modified Eagle Medium (DMEM) (Gibco®, Life technologies, Grand Island, NY). RAW264.7 cells were maintained in RPMI-1640 medium (Gibco®, Life technologies, Grand Island, NY). All of the media were supplemented with 10% fetal bovine serum (Atlanta Biologicals, Lawrenceville, GA), 10 mM HEPES (Gibco®, Life technologies, Grand Island, NY), 50 µg/ml gentamycin sulfate (Cellgro, Manassas, VA) , 1 mM sodium pyruvate (Gibco®, Life technologies, Grand Island, NY) and 1 mM Glutamax™ (Gibco®, Life technologies, Grand Island, NY). Cells were incubated at 37°C and 5% CO_2. Cells were passaged before reaching 100% confluence. Both types of cells were detached from culture flasks using trypsinization via trypsin-EDTA (0.25%) with phenol red (Gibco®, Life technologies, Grand Island, NY). However, RAW264.7 cells need additional vigorous rinsing with media to encourage cell detachment.

In vitro gene transfection

Cells (HEK293 and RAW264.7 cell lines) were seeded in 48-well plates at a density of 8×10^4 cells/well in a volume of 500 µl twenty-four hours prior to transfection. PGAApp prepared at three different N/P ratios (40, 60 and 80), each containing 1 µg of pDNA/well in 100 µl total volume, were added to the cells in serum-free media (500 µl). Cells transfected with naked pDNA at an equal amount of pDNA (1 µg per well) were used as a negative control. Four hours after cells were exposed to PGAApp, media containing the polyplexes was removed and replaced with complete media (1 ml/well) and incubated for a further 48 hours. Complete media was replenished every 24 hours. After 48 hours, cells were isolated and treated with 200 µl of Reporter Lysis Buffer (Promega, Madison, WI) followed by two freeze-thaw cycles to ensure complete lysis. Cell debris was centrifuged 16100 x *g* for 5 minutes using an Eppendorf Microcentrifuge Model 5415 D (Eppendorf, Hauppauge, NY), after which the supernatants were collected to measure luciferase expression using the Luciferase Assay System (Promega, Madison, WI). Supernatants were added to the luciferase assay reagent at a ratio of supernatant:luciferase assay reagent of 1:5 and vortexed briefly. Luminescence was measured for 10 seconds using the Lumat LB 9507 luminometer (EG&G Berthold, Bad Wildbad, Germany) and expressed in relative light units (RLU) with respect to control. Supernatants were analyzed for the amount of total protein content using the Micro BCA™ Protein Assay Kit (Pierce Biotechnology Inc., Rockford, IL). Bovine Serum Albumin standard (2 mg/ml, Pierce Biotechnology Inc., Rockford, IL) was used to create a standard curve. Luciferase activity was expressed as relative light units (RLU)/mg protein in cell lysates.

In vitro cytotoxicity assay

Cells were seeded in 96-well plates at a density of 1×10^4 cells/well. Twenty-four hours later, cells were incubated in serum-free media with 1 µg of pDNA complexed to

PGAA at various N/P ratios. After 4 hours of incubation, 100 µl of complete media was added to each well. After 24 hours of exposure to treatments, media was replaced with complete media. After 48 hours, the media in each well was replaced with 100 µl of fresh complete media and 20 µl of the MTS tetrazolium compound or CellTiter 96® Aqueous One Solution reagent (Promega Corporation, Madison, WI). The plate was incubated at 37°C, 5% CO_2 for 1 - 4 hours and the absorbance was recorded at 490 nm using a Spectra Max® plus Microplate Spectrophotometer (Molecular Devices, Sunnyvale, California). Percent relative cell viability values were calculated by dividing the UV absorbance value from wells containing treated cells by the value obtained from untreated wells and multiplying the resultant value by a factor of 100.

Statistical analysis

Data are expressed as mean ± SD. Statistical significance was determined using Kruskal-Wallis with Dunn's multiple comparison test compared to the control. A *p*-value less than 0.05 was considered significant. Statistical analyses were performed using GraphPad Prism version 5.02 for Windows (GraphPad Software, San Diego, CA, www.graphpad.com).

Results and discussions

Plasmid amplification and purification

After purification with the GenElute™ HP Endotoxin-Free Plasmid Maxiprep Kit, the yield of VR1255 pDNA was equal to 1.66 g per 500 ml Lennox L Broth. Since pDNA was used for transfection, purity was critical. The 260/280 ratio is used to evaluate the presence of contaminating protein in the pDNA [168]. Another ratio that is used to evaluate the purity of pDNA is 260/230. If this ratio is lower than 2.0, it is an indication of contaminants that exhibit an absorbance near 230 nm, such as ethylenediaminetetraacetic acid (EDTA) and guanidine hydrochloride which were used in

nucleic acid purification from cell extracts [168, 169]. On average the 260/280 and 260/230 ratios were equal to 1.83 and 2.09, respectively, which corresponded to DNA with high purity.

Size and polydispersity index (PdI) of PGAApp

The average size of polyplexes as tabulated in Table 1 shows that changing the N/P ratio from 40 to 60 resulted in an increase in nanoparticle diameter from 396.8 to 487.4 nm. Polyplexes prepared at an N/P ratio of 80 displayed an average size of 458.8 nm. In addition, small and consistent values of PdI suggest that particle aggregation did not vary greatly as the N/P ratio at which the polyplexes were prepared changed.

In vitro gene transfection

The transfection efficiency of PGAApp was evaluated by measuring luciferase expression. Figure 3-2 shows RLU values obtained from each treatment group normalized against total protein in each sample. PGAApp generated significantly stronger transgene expression when compared to naked pDNA in both HEK293 (Figure 3-2A) and RAW264.7 (Figure 3-2B) cell lines. Using polyplexes prepared at increasing N/P ratios results in decreased expression of luciferase. The maximum expression of luciferase was obtained with polyplexes prepared at an N/P ratio of 40. This level of expression was significantly different from all other treatment groups in both cell lines.

In vitro cytotoxicity assay

After 48 hours of incubation, the viability of cells was found to decrease as the N/P ratio of the polyplexes increased. PGAApp prepared at an N/P ratio of 40 were less cytotoxic than PEI-pDNA polyplexes (PEIpp) prepared at an N/P ratio of 20 in both types of cell lines (Figure 3-3).

PGAA is a cationic polymer that consists of carbohydrate groups and four oligoethyleneamines linked together by amide bonds [162]. PGAA polymers are

degradable and hydrolyze under physiological conditions and this degradation may enhance the release of pDNA from polyplexes [79]. Previous studies evaluating the optimal construct of PGAA for transfection have shown that the quantity and position of the hydroxyl groups can have a significant impact on transfection efficiency and that galactarate polymers with four ethylenimine units generated the strongest transgene expression [77, 170]. Complexing PGAA with pDNA results in polyplexes that have a net positive charge similar to polyplexes made from PEI that are capable of binding to the net negative charge on the surface of cells that are typically coated with sulfated glycosaminoglycans. Internalization of the PGAApp is reported to take place through endocytosis with 80% of PGAApp internalization blocked when cells were exposed to filipin III (a macrolide antibiotic which inhibits caveolae-mediated endocytosis[171]) [172]. Since PGAApp contain positively-charged amines, they were expected to escape the endosomes through the “proton sponge” effect. However, intracellular delivery of pDNA from PGAApp after cellular uptake is, as yet, undetermined [170].

Optimizing the transfection efficiency using cationic polymers complexed with pDNA can be achieved by evaluating varying N/P ratios at which the polyplexes are prepared [131, 154, 155]. In this study, we showed that PGAApp prepared at an N/P ratio of 40 gave the maximum expression of luciferase in both HEK293 and RAW264.7 cells among all N/P ratios tested. In addition, we show that PGAApp prepared at an N/P ratio of 40 have the lowest cytotoxicity relative to polyplexes prepared at N/P ratios of 60 and 80. PGAApp were also found to have cytotoxicity that was lower than PEIpp prepared at an N/P ratio of 20. Although it should be acknowledged that this difference in cytotoxicity might be reduced if PEIpp were utilized at lower N/P ratios.

We discontinued the study due to the limited amount of PGAA. From this study, the lowest N/P ratio tested (PGAApp at N/P 40) showed the highest luciferase expression. In future studies, the PGAApp formed at lower N/P ratios should be

characterized and tested for luciferase expression and cytotoxicity since lower N/P ratios should cause lower cytotoxicity which could result in higher transfection efficiency.

Conclusions

This study provides independent verification of the strong potential of PGAA as a non-viral vector and shows that PGAA (Glycofect™) has strong potential for transfecting murine macrophage-like (RAW264.7) cells and human embryonic kidney (HEK293) cells with low cytotoxicity.

Table 3-1 Particle size and polydispersity index (PdI) of PGAApp prepared at different N/P ratios

N/P ratio	Particle size (diameter)	Polydispersity index
40	397	0.427
60	487	0.424
80	459	0.426

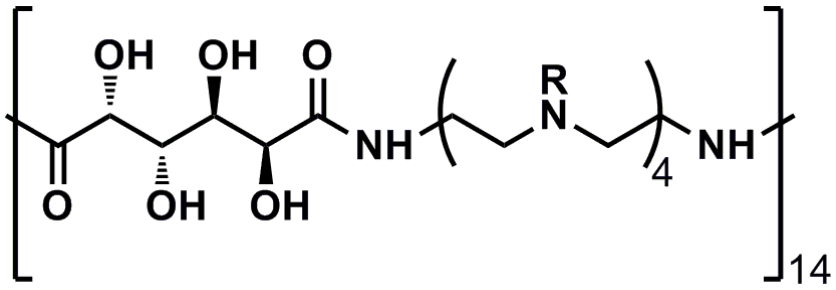

Figure 3-1 Poly(galactaramidoamine) (PGAA) structure.

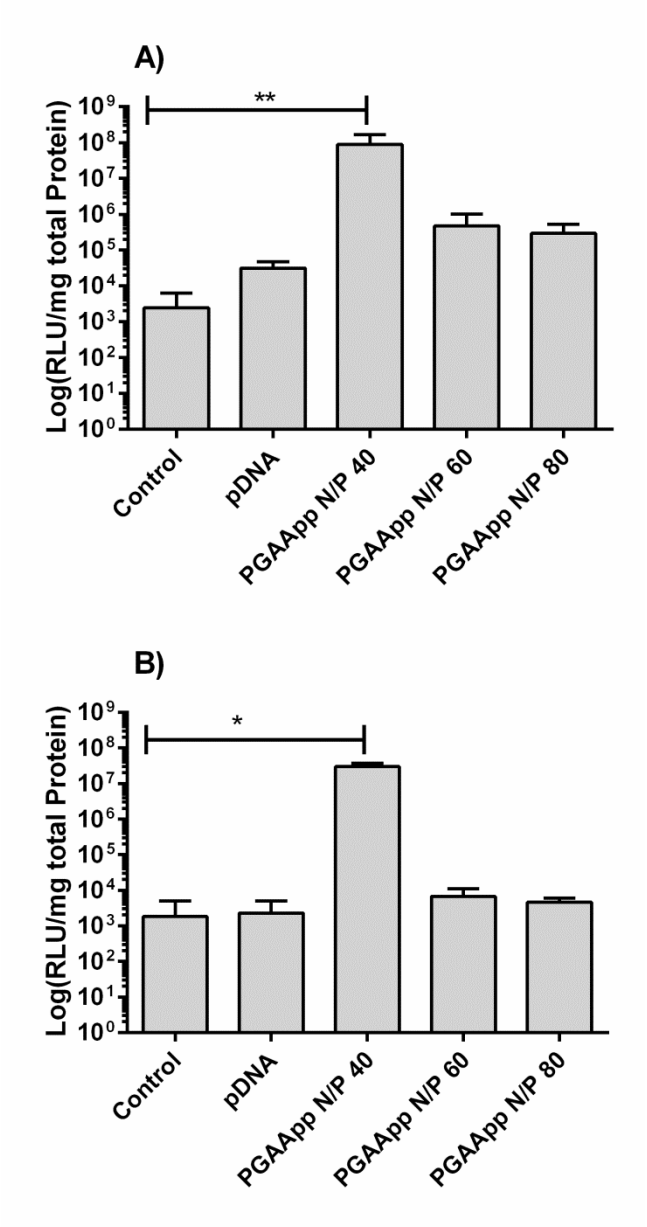

Figure 3-2 Luciferase expression of HEK293 (A) and RAW264.7 (B) cells that have been treated as indicated. Transfection experiments were carried out by incubating cells with PGAApp, where indicated, for 4 hours (see methods section for further details). Control = cells treated with PBS. Each treatment involving pDNA contained 1 µg pDNA/well. Data are expressed as mean ± SD (n = 3). Kruskal-Wallis with Dunn's multiple comparison test compared to the control was used. * $p < 0.05$, ** $p < 0.01$.

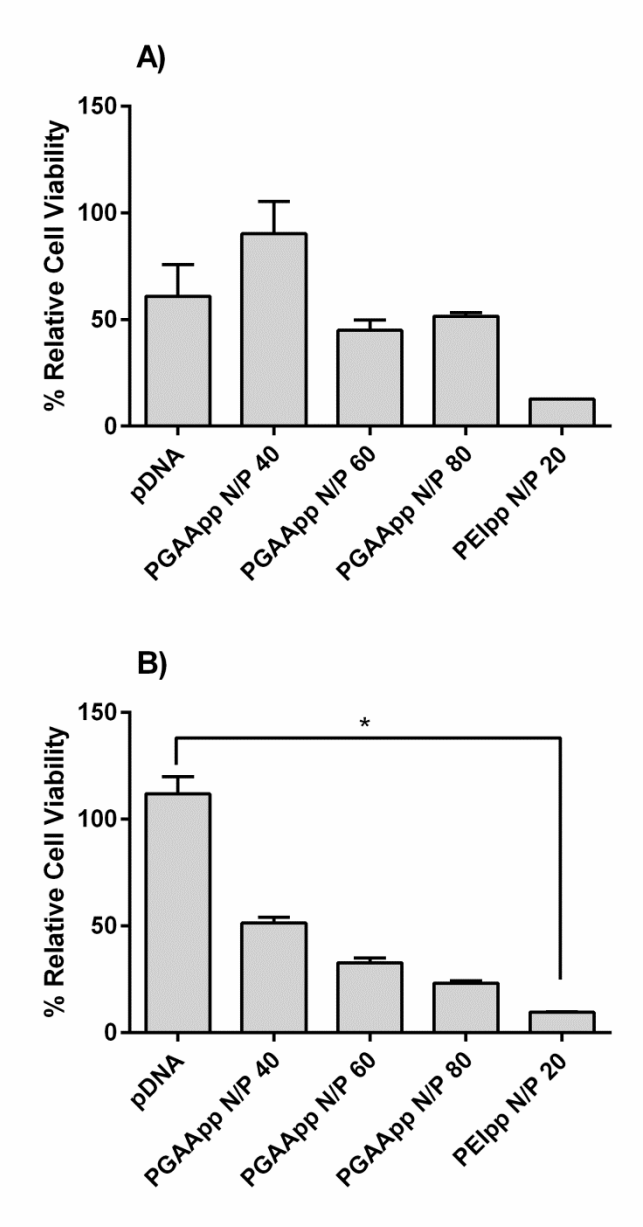

Figure 3-3 Cytotoxicity of PGAApp in HEK293 (A) and RAW264.7 (B) was determined by MTS assay (see methods). The cells were seeded into a 96-well plate at a density of 1 x 10^4 cells per well one day prior the experiment and exposed to the indicated treatments (1 µg pDNA per well) for 48 hours. pDNA = cells that were treated with pDNA (VR1255) solution at the concentration of 1 µg/well. Data are expressed as mean ± SD (n = 2). Kruskal-Wallis with Dunn's multiple comparison test compared to pDNA was used. * $p < 0.05$.

CHAPTER 4 CORRELATING INTRACELLULAR NON-VIRAL POLYPLEX LOCALIZATION WITH TRANSFECTION EFFICIENCY USING HIGH-CONTENT SCREENING

Introduction

High-content screening (HCS) is a combination of high-throughput techniques and multicolor fluorescent cellular imaging enabling simultaneous quantitative measurements of multiple parameters in a single cell level from one experiment. HCS can study both live and fixed cells. In live cell assays, HCS can collect kinetic information from each individual cell within a well. HCS can follow and quantify dynamic behavior such as chemotaxis. Fixed cell assays allow the experiment to be easily controlled and conducted in larger scale automation with a wide variety of fluorescent probes and antibodies. HCS collects a large amount of differential subcellular spatio-temporal information, providing unbiased, statistically significant data, making it an excellent candidate for the intracellular tracking of submicron materials, such as DNA vectors [173, 174]. In general, cellular studies using fluorescence microscopes are conducted on a small-scale which usually refers to 10 – 100 cells per sample [175]. These small-scale experiments nevertheless require extensive human labor to collect and analyze the data. HCS makes it possible to perform cell-based studies on a large-scale where one can collect and analyze data from more than 10^6 cells per sample [175].

Although, to date, HCS has been mainly focused on primary screening for candidate drug molecules [174, 176, 177], it also has the potential to be of value in the gene delivery field. HCS can be used to assess the effect of non-viral gene vectors on cells in vitro where multiple parameters (such as cytotoxicity, transfection efficiency, cell permeability) can be rapidly and simultaneously measured [178].

Gene delivery/therapy is the process where genetic materials are transferred into cells with the ultimate goal of curing or abating diseases thereby improving patients'

clinical status [179]. Gene delivery vehicles that transport DNA/RNA into cells can be divided into two categories, viral and non-viral vectors. Viral vectors usually result in much higher transfection efficiencies when compared to non-viral vectors. However, their toxicity and immunogenicity issues are sometimes problematic and consequently need to be addressed or avoided [180]. Non-viral gene delivery has gained substantial interest as a therapeutic tool because of its safety profile, ability to deliver large gene sizes, ease of preparation and its potential to be modified for cell- or tissue-targeting [180-182]. These traits are generally considered strong advantages over current viral-based gene delivery systems. However, low transfection efficiencies are still a major concern for non-viral based gene delivery [180, 183-186]. To achieve high transfection efficiencies, the DNA encoding the gene of interest needs to be effectively taken up by cells and then transported to the nucleus [187, 188]. To design a highly efficient gene vector, it is important to gain an insight into the mechanics and kinetics of uptake and intracellular trafficking pathways of gene vectors, DNA and polyplexes. Thus, the factors contributing to suboptimal transgene expression may be identified and potentially averted through subsequent modifications [48].

Manifold efforts have been made to study intracellular trafficking processes and numerically quantify gene carriers within the cell and its subcellular compartments. For example, the importance of various uptake and trafficking pathways such as endocytosis and macropinocytosis has been assessed using conditions to specifically inhibit crucial steps in these pathways [48]. The internalization kinetics of single particles can be tracked using wide-field fluorescence microscopy in combination with custom-built software for single-particle tracking [189]. Confocal microscopy and two-photon fluorescence correlation spectroscopy have also been used to track polyplexes [190-192]. Among these studies, only Akita et al. have both quantified and localized the transfecting materials (using confocal image-assisted three-dimensionally-integrated quantification)[191]. The study was conducted by analyzing approximately 30 - 50 randomly selected cells [191]. Although it is

possible to observe the uptake and cellular trafficking of polyplexes by the aforementioned novel methodologies, they are limited by the number of cells that can be analyzed manually, thereby placing limitations on attaining statistically significant outcomes.

This study entails a report on an application for HCS that involved evaluating the transfection efficiency and cytotoxicity of a cationic polymer, polyethylenimine (PEI) [158, 188, 193]. Since PEI was first used for gene delivery purposes in 1995, it has become one of the most effective non-viral gene vectors [49, 61, 158, 194]. PEI was chosen as a model polymer because of its well characterized properties. This study also shows, for the first time, a relationship between successfully transfected cells and the number of PEI or polyplexes or polyplex clusters inside the cytoplasm. Thus it is demonstrated here that HCS has the potential to be a powerful tool for analyzing uptake and intracellular trafficking of non-viral gene delivery vectors along with measuring other parameters, such as cytotoxicity and transfection efficiency (GFP expression), simultaneously.

Materials and methods

Cell lines and cell culture

Human Embryonic Kidney cells (HEK293) were purchased from American Type Culture Collection (ATCC, Rockville, MD). Cells were maintained in Dulbecco's modified Eagle's medium (DMEM) (Gibco®, Life technologies, Grand Island, NY) supplemented with 10% fetal bovine serum (Atlanta Biologicals, Lawrenceville, GA), 1 mM Glutamax™ (Gibco), 1 mM sodium pyruvate (Gibco), 10 mM HEPES (Gibco) and 50 µg/ml gentamycin sulfate (Cellgro, Manassas, VA). Cells were maintained at 37°C and 5% CO_2. Cells were passaged before reaching 100% confluence.

Amplification and purification of pDNA

A 4.7 kb plasmid encoding enhanced green fluorescent protein (GFP), pEGFP-N1, was a generous gift from Satheesh Elangovan, College of Dentistry, University of Iowa. This pDNA was transformed into *Escherichia coli* DH5α and amplified in Lennox L broth (Research Products International Corp., Mount Prospec, IL) media and purified using a GenElute^{TM} HP Endotoxin-Free Plasmid Maxiprep Kit (Sigma-Aldrich, St. Louis, MO), according to the manufacturer's protocol. pDNA concentration in endotoxin-free water (Sigma-Aldrich) was determined using a NanoDrop 2000 spectrophotometer (Thermo Fisher Scientific Inc., Waltham, MA).

Preparation of PEI polyplexes (PEIpp)

To be able to track the polyplexes, fluorescently tagged branched polyethylenimine (PEI) was chosen. Rhodamine tagged branched PEI (rhPEI, MW 25 kDa with a labeling ratio, $Mol_{monomer}/Mol_{dye}$, of 180/1) was purchased from Surflay Nanotech GmbH (Schwarzschildstr, Berlin, Germany). Branched PEI (bPEI, MW 25 kDa: Sigma-Aldrich) was used as a positive control for transfection.

rhPEI polyplexes (rhPEIpp) were formed based on the ionic interaction between positively charged rhPEI and negatively charged pDNA. rhPEIpp can be formed at varying ratios of amine groups in PEI to phosphate groups in pDNA (N/P ratios). In this study an N/P ratio of 10 was used. The rhPEI (9.96 mg/mL) and pDNA (200 µg/ml) solutions were prepared in UltraPure DNase/RNase-Free distilled water (Invitrogen, Grand Island, NY). All solutions were sterilized using 0.22 µm syringe filters (Millex®-GV, merck Millipore Ltd., Carrigtwohill, Germany). An equal volume of 125 - 250 µL of rhPEI solution (cationic) was pipetted into an equal volume of pDNA solution (anionic), vortexed for 20 s and then incubated at room temperature for 30 min before use. The rhPEIpp were prepared fresh. The final concentration of pDNA after the rhPEIpp were formed was 50 µg/ml. In the same manner, bPEIpp were prepared with a bPEI starting

concentration of 1.0 mg/ml (Table 4-1). bPEIpp were fixed at N/P ratio of 10 which is known to give best transfection efficiencies [195, 196]. The final concentration of pDNA after bPEIpp were formed was also equal to 50 µg/ml.

Transfection and sample preparations for HCS

Black 96-well plates (cell carrier with transparent bottom, Perkin Elmer Inc., Waltham, MA) were sterilized using ultraviolet light prior to use. A solution of 0.01% poly-l-lysine (MW 150,000 – 300,000, Sigma-Aldrich) was used to coat the surface of the wells of the microplates. Poly-l-lysine solution was added into each well at a volume of 50 µl. Plates were rocked gently to ensure an even coating. After 10 min of incubation, poly-l-lysine was removed. Wells were rinsed with 100 µl of UltraPure DNase/RNase-Free distilled water and allowed to dry in a sterile environment (class II biosafety cabinet with laminar flow) overnight.

HEK293 cells at a density of 5000 or 7500 cells per well were plated in a total volume of 100 µl of fully supplemented media. After 24 h, the media was gently aspirated and replaced with 100 µl of serum-free media containing bPEIpp or rhPEIpp at N/P 10 with pDNA amounts of 0.5 or 1 µg per well (10 and 20 µl, respectively). An untreated group was used as a negative control. All treatments were added according to the pictured 96-well plate map (Figure 4-1). After cells were exposed to PEIpp for 4 h, the media was gently aspirated and the cells were gently rinsed once with 100 µl of warm PBS and then 100 µl of fully supplemented media was added to each well. Twenty hours later media was removed and cells were gently rinsed once with PBS before being fixed with 4% formaldehyde (Alfa Aesar, Ward Hill, MA) in PBS for 30 min. Cells were then rinsed with PBS prior to incubating with 1 µg/ml of Hoechst dye to stain the nucleus for at least 15 min prior to imaging.

Imaging using HCS and image analysis

The aforementioned microplates containing fixed and stained cells were loaded onto a High Content Screening Operetta® system (HCS, Perkin Elmer Inc. Waltham, MA). This system comprises an inverted epifluorescence microscope that uses a xenon arc lamp excitation source with interchangeable excitation and emission filters [173, 197]. Three fluorescent channels for GFP (ex. at 460 – 490 nm, em. at 500 – 550 nm), Hoechst (ex. at 360 - 400 nm, em.at 410 - 480 nm) and rhodamine (ex.at 520 – 550 nm, and em. at 560 - 630 nm), were utilized, with 18 fields/well and with each field comprising 1 stack of 8 images taken over a vertical span of 4 µm with 0.5 µm intervals (Figure 4-2 to Figure 4-4).

Images were acquired on an Operetta System using a 20x high NA objective lens. The images collected were analyzed by the accompanying Harmony® Image Analysis software (Perkin Elmer Inc., Waltham, MA) (Figure 4-2). The analysis of each field was performed, where each field was one stack (8 images per stack), and included: 1) defining the nuclei of cells, as determined by the intensity of staining and morphology of the nuclei using the Hoechst Channel and Method B (proprietary algorithm, Perkin Elmer Inc.). The nuclear areas of these cells were then identified as "true nuclei". Based on the following features (Figure 4-5): possessing areas smaller than 280 μm^2; having Hoechst intensities (a mean value derived from the total pixel intensity values for each nucleus) larger than 2000; and having contrasts larger than 0.30. The contrast is the readout of intensity after normalization of the highest and lowest intensity to 1 and 0, respectively. 2) Defining cells using the GFP channel and Method B. By using the same method used for the calculation of intensity and morphology of the nuclei, the areas of the cells, or "true cells", were defined as follows: possessing areas smaller than 1040 μm^2; having GFP intensities (mean) larger than 0 (for both GFP(+) and GFP(-) cells); and having contrasts larger than 0.25. 3) Defining GFP(+) and GFP(-) cytosols using the GFP channel, true nuclei and Method E (proprietary algorithm, Perkin Elmer Inc.).

Designating cytosols as GFP(+) meant that they had to have areas larger than 180 μm^2 (calculated by subtracting the areas of the true nuclei from the areas of true cells) and GFP intensities larger than 120 (Figure 4-5A). The GFP(-) cytosols were assigned similarly except that they had to possess GFP intensities smaller than 120 (Figure 4-5B). 4) Locating the PEIpp, or "micronuclei" (as defined by Harmony® Image Analysis software), using the rhodamine channel, the cytosolic region or nuclear region, and Method B. The PEIpp in the GFP(+) or GFP(-) cytosolic region were further defined by their particle area being smaller or equal to 80 μm^2. In general, polyplexes made from branched PEI and pDNA at a N/P ratio of 10 are approximately 100 nm in diameter with a positive charge when measured in water at room temperature by dynamic light scattering [198]. However, we cannot determine the accurate size of polyplexes which are smaller than half of the wavelength of the excitation source (*1/2λ:* 260 – 275 nm) due to the light diffraction limit in our optical system. Thus, in the context of the HCS analysis here, PEI polyplexes or PEIpp may be referring to single PEI polyplex particles or a cluster of PEI polyplexes. In the analysis, the true nuclei values were used to define viable cell numbers per well, and the percentage of GFP(+) cells of the total cell population (both GFP(+) and GFP(-) cells) was used to define the transfection efficiency.

Manual counting of GFP(+) cells

Manual counting of GFP(+) and GFP(-) cells from the same set of images was performed using Paint (Microsoft Windows version 6.1 Build 7601: Service Pack 1, Microsoft Corporation, WA). Images from HEK293 cells treated with rhPEIpp (0.5 µg and 1.0 µg pDNA/well) were used. In each well, at least 900 cells were counted.

Cytotoxicity of PEIpp using MTS assay

Cytotoxicity of PEIpp was determined using an MTS assay. HEK293 cells were plated into wells of a poly-l-lysine coated 96-well plate at two different seeding densities, 5000 and 7500 cells per well. Twenty-four hours later, media was aspirated and

replaced with PEIpp N/P 10 (containing either 0.5 or 1 µg of pDNA) in serum free media. Cells were exposed to treatments for 4 h, rinsed gently with warm PBS and then complete DMEM media was added. After 24 h, media was aspirated and cells were rinsed gently with PBS before being replaced with 100 µL of fresh media plus 20 µL of MTS tetrazolium compound (CellTiter 96® AQueous One Solution, Promega Corporation, Madison, WI). The plate was incubated at 37°C and 5% CO_2 for 4 h and then the absorbance of the solution in each well was recorded at 490 nm using a Spectra Max plus 384 Microplate Spectrophotometer (Molecular Devices, Sunnyvale, CA). Background of 490 nm absorbance was corrected by subtracting absorbance obtained from the experimental well with absorbance obtained from 100 µL of media and 20 µL of MTS tetrazolium compound which was equal to 0.2848. Percent relative cell viability values were determined by dividing the absorbance obtained from wells containing treated cells by the absorbance obtained from untreated cells with the same seeding cell density (5000 or 7500 cells per well) and multiplying the resultant value by a factor of 100.

Statistical analysis

Data are expressed as mean ± SEM. To analyze GFP expression in cells with 0.5 µg and 1.0 µg of pDNA in PEIpp, one-way ANOVA with Tukey's multiple comparisons test was performed. To analyze the number of PEIpp in cytoplasm, two-way ANOVA with Bonferroni's multiple comparisons test was used. To analyze cell numbers, two-way ANOVA with Dunnett's multiple comparisons test was performed. All statistical analyses were conducted using GraphPad Prism 6 for Windows (GraphPad Software, Inc., San Diego, CA, www.graphpad.com). The *p*-values of less than 0.05 were considered significant.

Results and Discussion

HCS can rapidly determine transfection efficiencies

As a proof of concept, transfection of HEK293 cells with PEIpp was performed in these studies. PEI is a well-known cationic polymer that has been used as a gene vector since 1995 [49]. The HEK293 cell line was chosen because it is widely used in transient gene expression systems [42, 166]. As described in the methods section, HEK293 cells were exposed to PEIpp complexes (containing pEGFPN-1) and subsequently (24 hours later) imaged using HCS. In order to determine transfection efficiency, the fluorescence intensity obtained from each cell was determined. By contrasting untreated cells (negative controls) and GFP transfected cells, a threshold (mean intensity of the cell) was set at 120 so that there were less than 0.08% GFP(+) cells per well for the untreated samples, whilst in the treated samples, cells with a mean intensity larger than 120 were considered successfully transfected. The ratio of GFP(+) cells to total cells was used to define the transfection efficiency. Figure 4-6A and 4C shows images generated from HCS from HEK293 cells that were treated with bPEIpp (0.5 µg pDNA/well) and untreated, respectively. In Figure 4-6B, an analyzed image shows GFP(+) cells from the same image (Figure 4-6A) as green and cells expressing undetectable levels of GFP (GFP(-)) as red. Figure 4-6D shows untreated cells with no GFP expression (all cells were labeled in red).

It was determined that rhPEIpp had transfection efficiencies of 4.0% and 8.9% with 0.5 µg and 1.0 µg of pDNA per well, respectively. Under the same conditions, bPEIpp showed higher transfection efficiencies of 7.5% and 10.7% with 0.5 µg and 1.0 µg of pDNA per well, respectively (Figure 4-7A). Increasing the amount of pDNA per well from 0.5 µg to 1.0 µg increased the transfection efficiency in cells that were treated with either rhPEIpp or bPEIpp. Since there were two cell seeding densities (5000 and 7500 cells per well), the number of GFP(+) cells in the 7500 cells/well seeding density group

(Figure 4-7D) was higher than the group with 5000 cells/well seeding densities (Figure 4-7B). Nevertheless, the percent GFP(+) cells in both groups were quite similar (Figure 4-7A and Figure 4-7C).

To confirm results obtained with HCS, manual counting of GFP(+) and GFP(-) cells (at least 900 cells per well) from the same set of images was performed (Figure 4-8). Using two-way ANOVA with Bonferroni's multiple comparisons test, there was no significant difference when percent GFP(+) cells derived from either method was compared. In Figure 4-8, manual counting showed that rhPEIpp had transfection efficiencies of 5.2% and 8.0% with 0.5 µg and 1.0 µg of pDNA per well, respectively. This manual counting is a validation for using HCS as a reliable tool to measure transfection efficiencies when the transgene product is inherently detectable or rendered detectable through fluorescence. To provide statistically significant data, large sample sizes are needed. As the sample size (cell number) increases, the time and labor used to manually gather the data proportionally increases. The results from HCS were automatically obtained from images that consisted of between 1000 – 8000 cells per well. Thus, HCS provides an opportunity to reduce bias and analyze a larger data set compared to manual counting which requires tedious labor and inordinately longer times, particularly when multiple parameters are being acquired.

Cell enumeration using HCS as an indicator of cytotoxicity

In addition to measuring the transfection efficiency, HCS can also count the cells simultaneously for cytotoxicity evaluation. Using Hoechst dye stained nuclei as a marker for cells, it was possible to program the HCS software to identify and enumerate the number of cells in each well (Figure 4-9). It is clear that an image obtained from a well with 5000 cells/well seeding density (Figure 4-9A) indicated a lower number of cells when compared to an image obtained from a well with 7500 cells/well seeding density

(Figure 4-9B). However, it will be excessively time consuming to manually count all the cells in each well. HCS, on the other hand, can perform this function rapidly.

An algorithm in the HCS software was set to exclude dying (or dead) cells containing fragmented nuclei from the analysis. Only cells containing intact nuclei were enumerated as shown in Figure 4-9C. To validate the reliability of HCS in measuring the cytotoxicity of PEIpp, an MTS assay was run in parallel. The MTS assay is a well-known colorimetric assay for measuring cell cytotoxicity [199]. The results obtained from this assay were expressed as percentage relative cell viability compared to the untreated cells (Figure 4-8B).

Viable cell numbers per well obtained from HCS (Figure 4-10A) were compared to results obtained from the MTS assay (Figure 4-10B) and were found to be comparable (Figure 4-10). Using two-way ANOVA with Bonferroni's multiple comparisons test, there was no significant difference when results obtained from HCS and MTS were compared. Wells containing cells that were treated with higher amounts of rhPEIpp (1.0 µg pDNA per well) possessed lower cell numbers, as determined by HCS, compared to wells treated with rhPEIpp containing 0.5 ug pDNA. The findings were corroborated by the results from the MTS assay performed in parallel. Moreover, HCS provided, in contrast to the MTS assay, absolute viable cell numbers per well.

Thus, HCS, along with being capable of accurately measuring transfection efficiency (shown above), can simultaneously be used to measure cytotoxicity of non-viral gene delivery systems.

GFP(+) cells possessed a higher number of PEIpp in the cytoplasm than GFP(-) cells

Using HCS, the cytoplasmic area of each cell (or region of interest) was identified using endogenous autofluorescence at excitation and emission ranges similar to GFP (Figure 4-3 and 11B). The cytoplasmic region was programmed to be delineated from

the nuclear region by differential fluorescence detection using Hoechst stain. The location of rhPEIpp was detected and enumerated in the cytoplasm and the nucleus in both GFP(+) and GFP(-) cells (Figure 4-11C). For the first time, a relationship was observed between successfully transfected cells and the number of rhPEIpp within the cell. Whilst no rhPEIpp were detected in the nuclei of either GFP(+) or GFP(-) cells, approximately 4-5 complexes/cell were detected in the cytoplasm of GFP(+) cells that were treated with rhPEIpp delivering 0.5 or 1.0 ug pDNA per well. This was found to be significantly (p-value < 0.0001) higher than the number of rhPEIpp found in the cytoplasm of GFP(-) cells (less than 1 complex/cell, on average). Although cells that were treated with rhPEIpp (1.0 µg pDNA/well) showed a significantly higher transfection efficiency than cells that were treated with rhPEIpp (0.5 µg pDNA/well) (Figure 4-7B), there was no significant difference in the number of rhPEIpp per cell when 0.5 µg versus 1 µg of pDNA was compared in the GFP(+) populations (Figure 4-12). Since rhPEIpp toxicity increases with the dose of rhPEIpp, it is possible that cells that contained more than 4 – 5 rhPEIpp could not survive long enough to be detected at the time of data acquisition (24 hours post-transfection). It is possible that 4 - 5 polyplexes in the cytoplasm is an optimal amount for the successful transfection of healthy cells.

In this study, PEIpp were not detected inside the nuclei of HEK293 cells at 24 hours post-transfection. This result suggests that pDNA may disassociate from the PEIpp in the cytoplasm prior to reaching the nucleus, where it is then available for transcription. Support for this idea comes from Remy-Kristensen et al. [200] who studied the role of fluorescently (FITC) labelled bPEIpp endocytosis in mouse fibroblasts (L929) using confocal microscopy. Ninety minutes post-transfection, labeled bPEIpp could not be detected inside the transfected L929 nucleus but instead were found on the outer nuclear membrane surface. In addition, Itaka et al. [195] studied intracellular distribution of bPEIpp using confocal microscopy with fluorescence resonance energy transfer (FRET) in human embryonic kidney (293T) cells. Twenty-four hours after transfection, bPEIpp

were distributed in the cytoplasm but there was no evidence of bPEIpp in the nuclei. In contrast, Godbey et al. [190] studied PEIpp in EA.hy 926 cells (derived from a fusion of human lung carcinoma, A549, and human umbilical vein endothelial cells) using confocal microscopy. PEIpp were localized in nuclei 3.5 - 4.5 hours post-transfection. However, to the best of our knowledge this latter finding has not been reproduced in other cell types and may reflect an idiosyncratic trait that pertains to this particular cell line.

Conclusion

The purpose of this study was to demonstrate the potential of using HCS as a tool to study non-viral gene vector-mediated transfection. Specifically, regarding PEIpp, there is much interest in enhancing the transfection efficiency of these polyplexes whilst simultaneously reducing their cytotoxicity. Thus, studies of mechanism of transfection by these polyplexes are believed to be important [201, 202]. Since HCS is an image based system, it is feasible to track non-viral vectors and pDNAs by labeling them with fluorescent tags. Because of its automation, HCS has the potential to be used to elucidate optimal conditions achieving maximal transgene expression with minimum toxicity for a variety of gene vectors using various cell types under a wide range of conditions [203, 204]. Conventional modes of analysis (manual counting and MTS assays) were used to validate the HCS used here. Although in this study, fixed cells were used for simplicity, HCS also has the ability to study polyplexes using live cell imaging and thus collect meaningful data at different time points which could be used to elucidate the steps of intracellular trafficking of non-viral based gene carriers.

The capacity of HCS to make quantitative multi-parametric measurements of cells and cell populations through rapid automated fluorescence image capturing has been of great value in drug discovery. HCS, however, also has great promise in the gene delivery field, where not only information about transfection efficiencies and cytotoxicities of various non-viral gene vectors can be accrued, but also, as shown here,

the tracking of vectors (such as rhPEIpp) inside cells can be simultaneously achievable. This provides a strong rationale for using HCS in the future as a screening system for tens or hundreds of novel transfection reagents simultaneously, so long as transgenes expressing fluorescent proteins are used for determining transfection efficiencies, and fluorescently tagged vectors are used for establishing the mechanism(s) of transfection through subcellular tracking.

Table 4-1 An example of the volume of each substances used to prepared polyplexes.

	Cationic solution (250 µl total volume)		Anionic solution (250 µl total volume)	
	PEI solution (µl)	Water (µl)	pEGFP solution (µl)	Water (µl)
rhPEIpp	6*	244	125***	125
bPEIpp	33**	217	125***	125

*The concentration of rhPEI is equal to 9.96 mg/ml.
**The concentration of bPEI is equal to 1.0 mg/ml.
***The concentration of pEGFP is equal to 200 µg/ml.

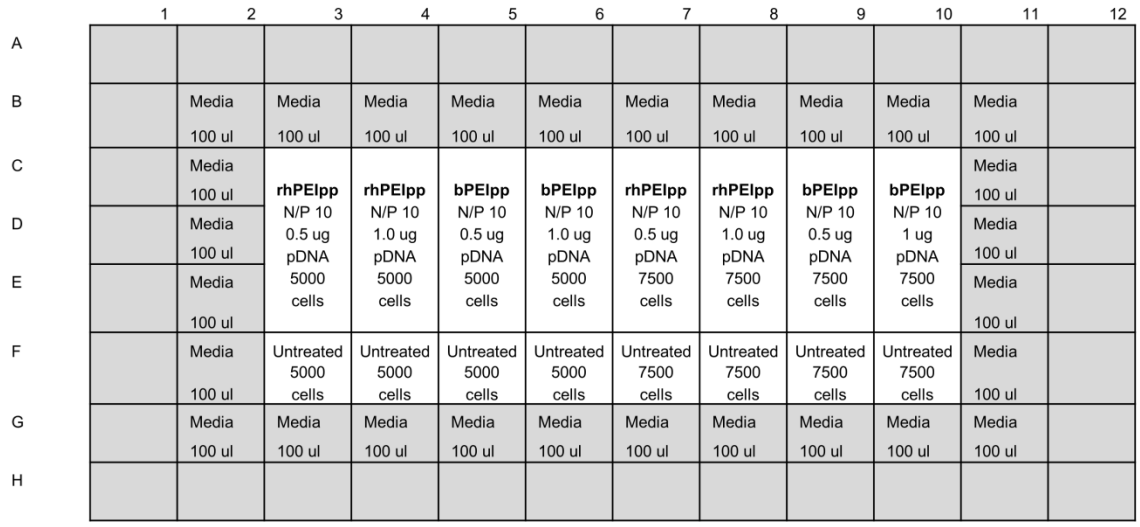

Figure 4-1 96-well plate map showing cell seeding and treatment plan. HEK293 cells (5000 or 7500 cells per well) were treated indicated polyplexes (rhPEIpp and bPEIpp) at the pDNA amount of 0.5 and 1.0 µg/well for 4 hours. Media (100 µl) was added into surrounded wells to reduce evaporation. Wells located at the outermost perimeter of the 96-well plate were left empty because the HCS camera cannot fully capture these wells.

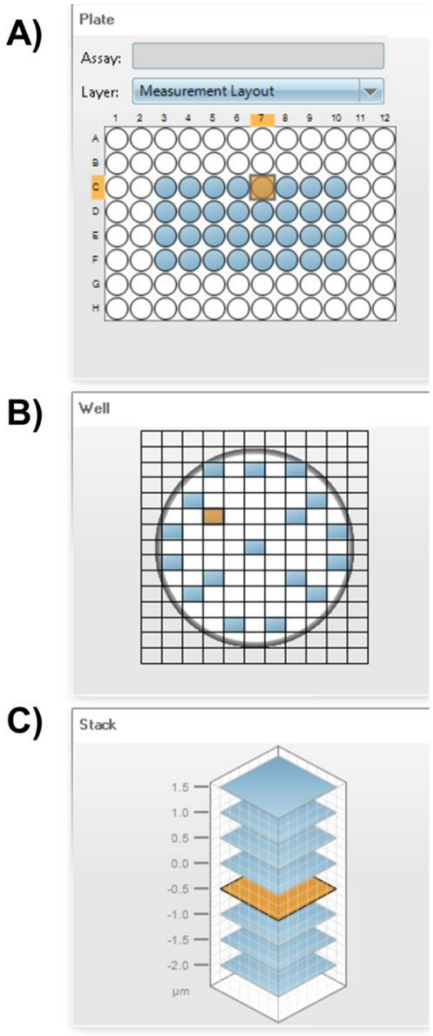

Figure 4-2 Caption of part of the Harmony® Image Analysis software (Perkin Elmer Inc., Waltham, MA)[1] showed 96-well plate map (A), fields of interest in each well (B) and stacks in each field showing interval length of 0.5 µm in vertical between each image (C). The wells of interest and the fields of interest within each well are shown in blue. Yellow (overlaying a blue well/field) represents the spot of interest which in this case is cells image at the stack -0.5 µm, from the upper left corner in well C7.

[1] This image was published with the permission from Jacob G. Tesdorpf, PhD, Director Cellular Imaging & Detection, Life Sciences & Technology, Perkin Elmer, Hamburg, Germany.

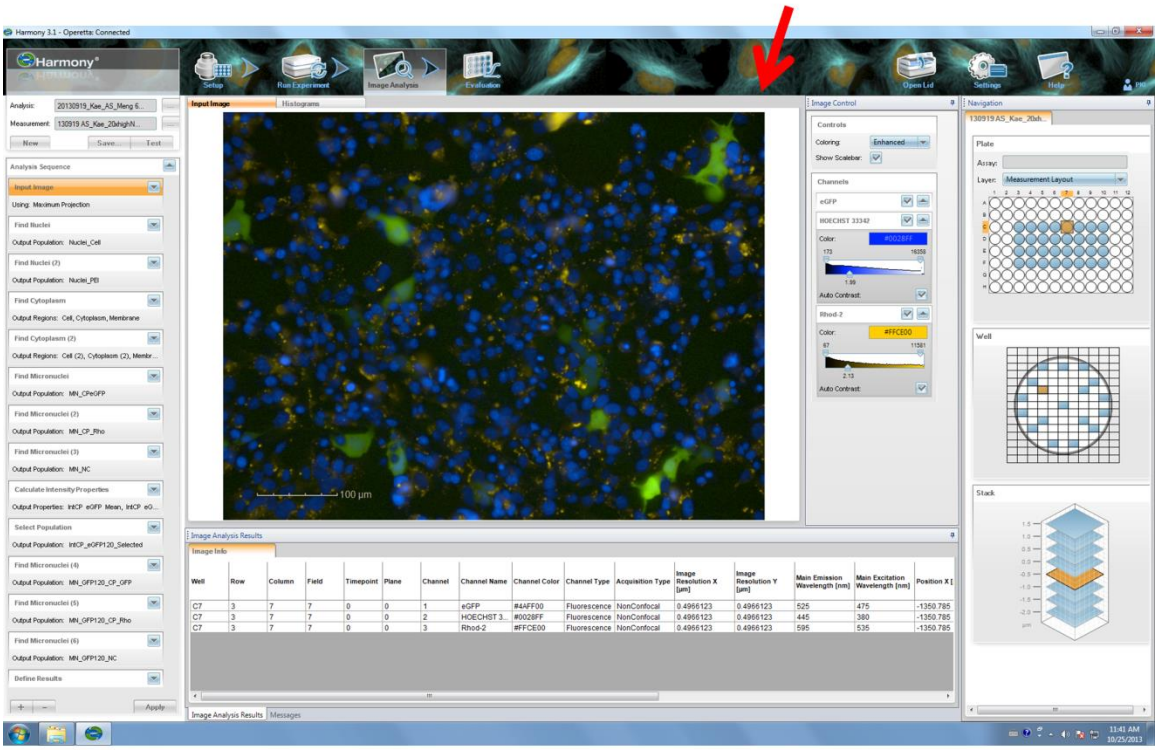

Figure 4-3 Caption of the Harmony® Image Analysis software (Perkin Elmer Inc., Waltham, MA)[2] Image in the middle (red arrow) represents cells obtained from the stack position -0.5 µm, the upper left corner in well C7 (more explanation in Figure 4-2.

[2] This image was published with the permission from Jacob G. Tesdorpf, PhD, Director Cellular Imaging & Detection, Life Sciences & Technology, Perkin Elmer, Hamburg, Germany.

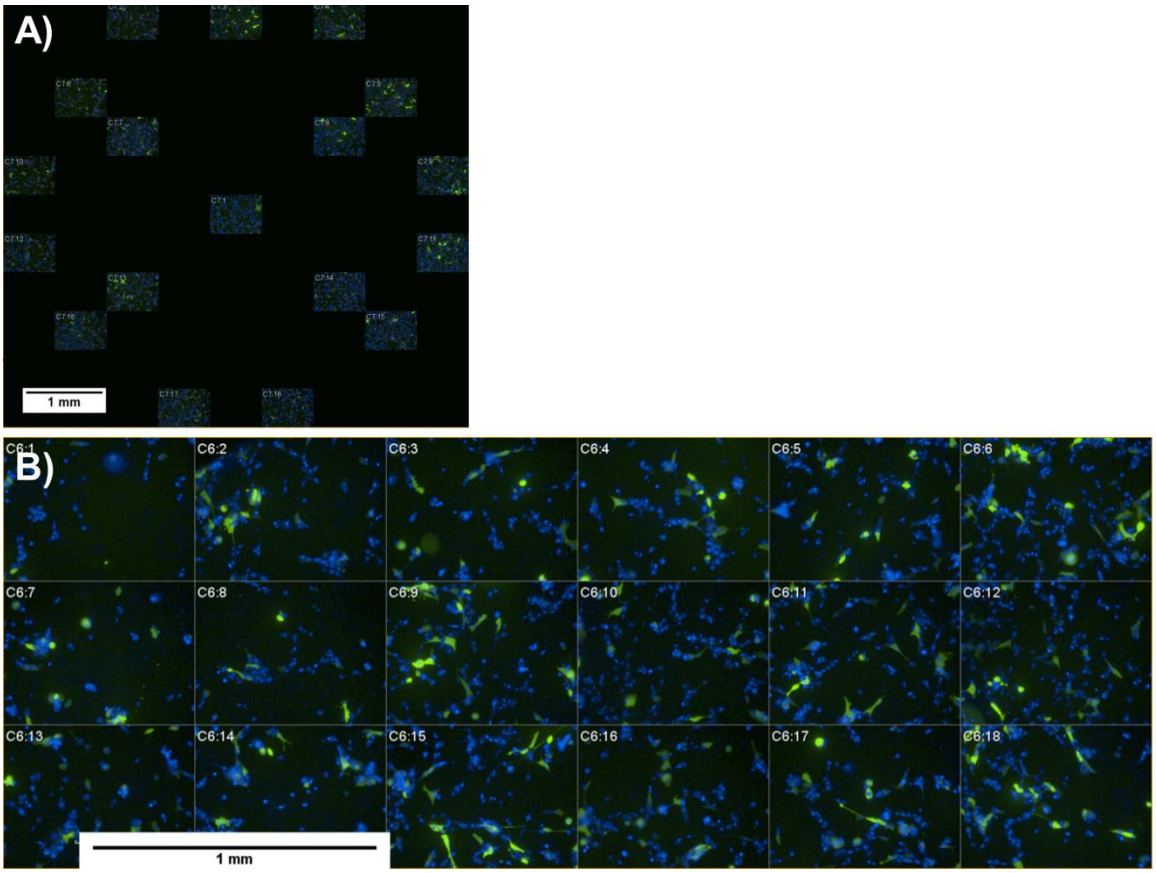

Figure 4-4 A) The 18-fields realistic view obtained from 1 well in 96-well plate and (B) the 18-fields (from one well) packed view. Scale bars in both images represent 1 mm.

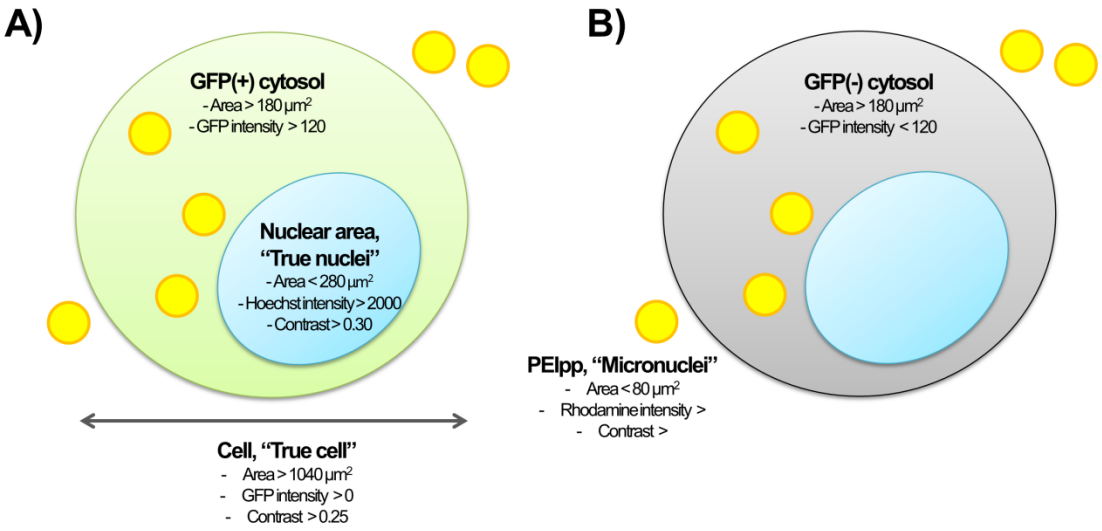

Figure 4-5 Cartoons representing cells and parameters used in the image analysis by the Harmony® Image Analysis software (Perkin Elmer Inc., Waltham, MA). GFP(+) cells are cells that have GFP intensities in the cytosol larger than 120 (A). GFP(-) cells are cells that have GFP intensities in the cytosol smaller than 120 (B). Nucleus (blue), GFP(+) cytosol (green), GFP(-) cytosol (grey), PEIpp (yellow).

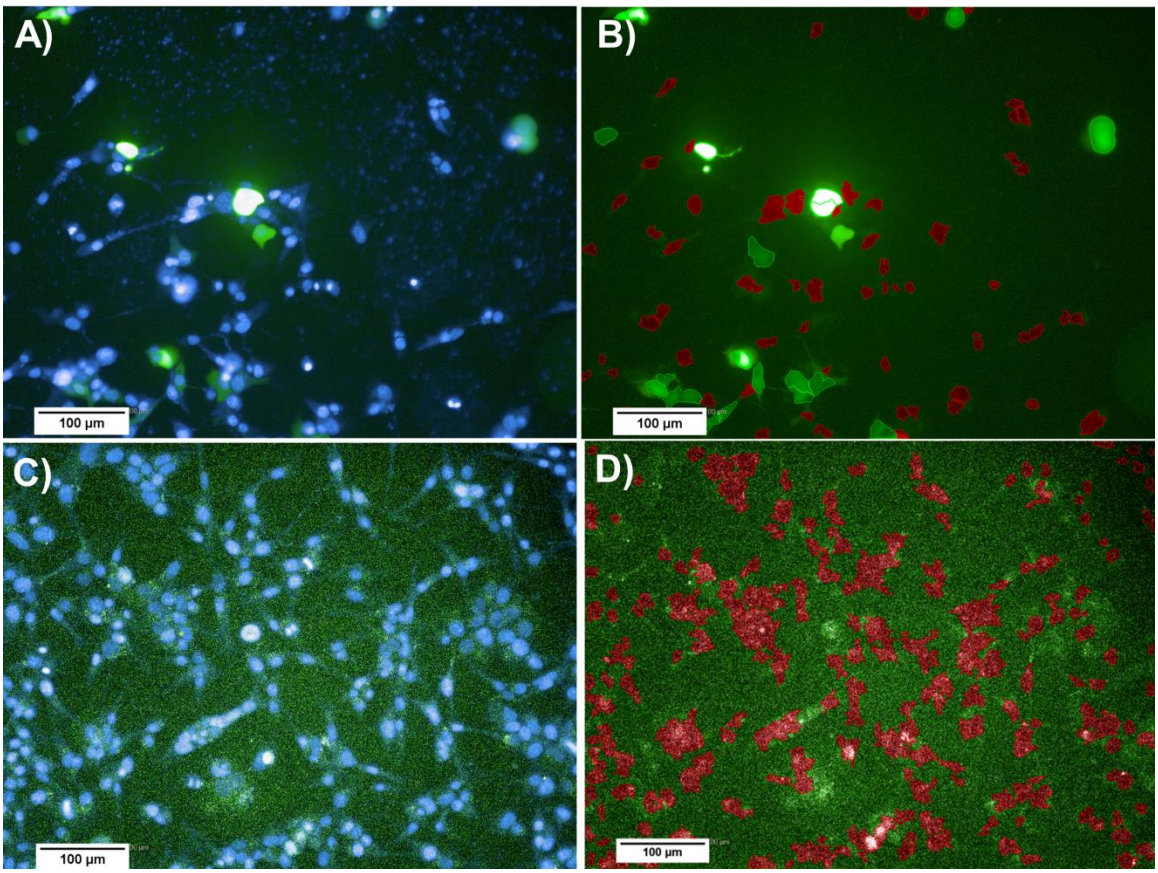

Figure 4-6 Images obtained from cells that had been treated with bPEIpp (0.5 µg/well) (A) and untreated cells (C). (B) and (D) are the same respective images as ((A) and (C)) showing GFP(+) (green) and GFP(-) (red) cells after analysis by HCS. Designation of GFP(+) versus GFP(-) was based on cell fluorescence intensity above and below a set threshold, respectively (see methods section for details). All scale bars represent 100 µm.

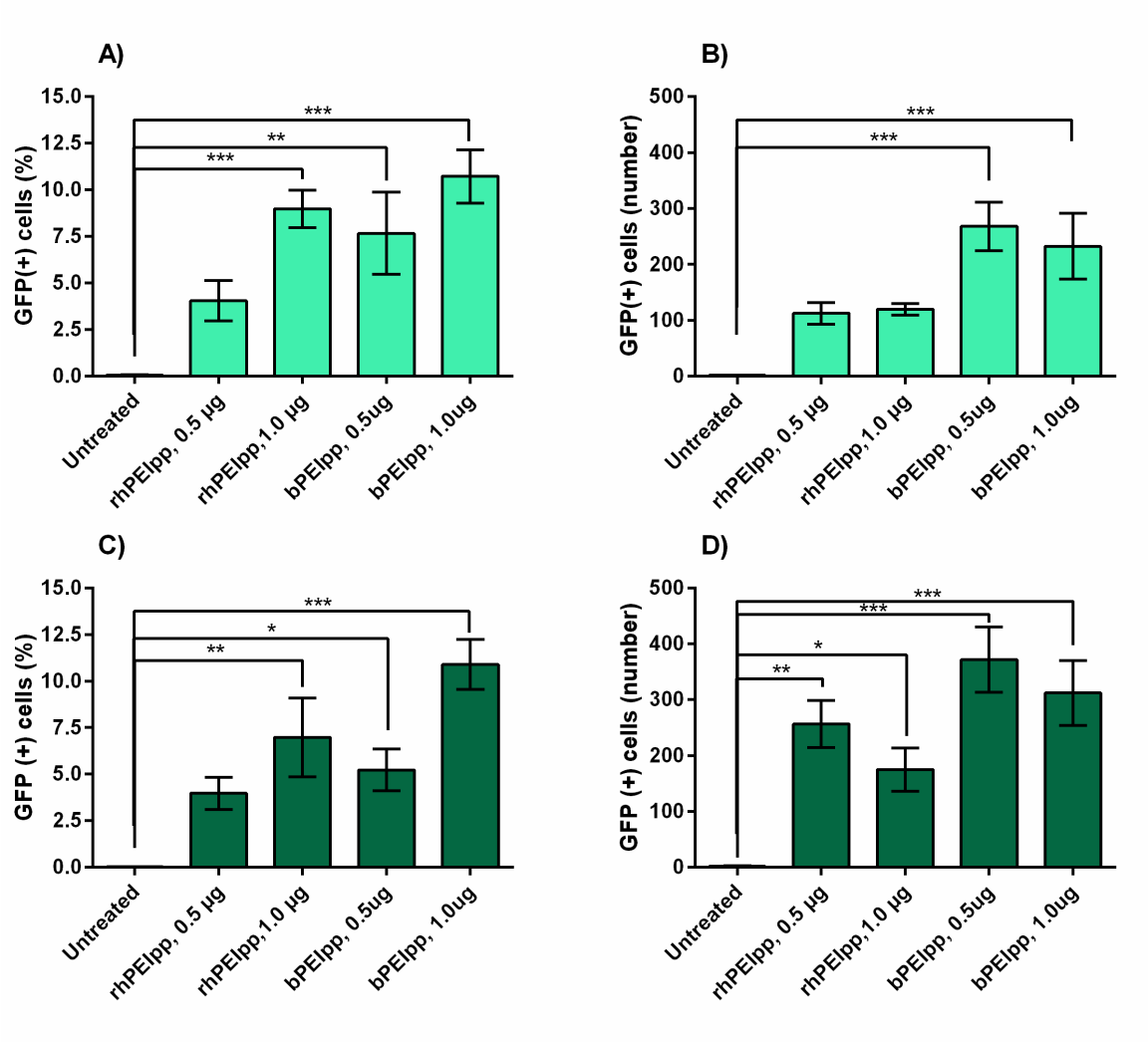

Figure 4-7 *Percentage GFP(+) cells* in HEK293 cultures treated as indicated and plated at (A) 5000 and (C) 7500 cells per well, respectively, **as determined using HCS**. *Number of GFP(+) cells* in HEK293 cultures treated as indicated and plated at (B) 5000 and (D) 7500 cells per well, respectively. Data are presented as mean ± SEM (n = 3 - 4). One-way ANOVA with Dunnett's multiple comparisons test was performed to assess statistically significant differences between treated and untreated groups. *** $p < 0.001$, ** $p < 0.01$,* $p < 0.05$. 0.5 µg and 1.0 µg represent the amount of pDNA in each well.

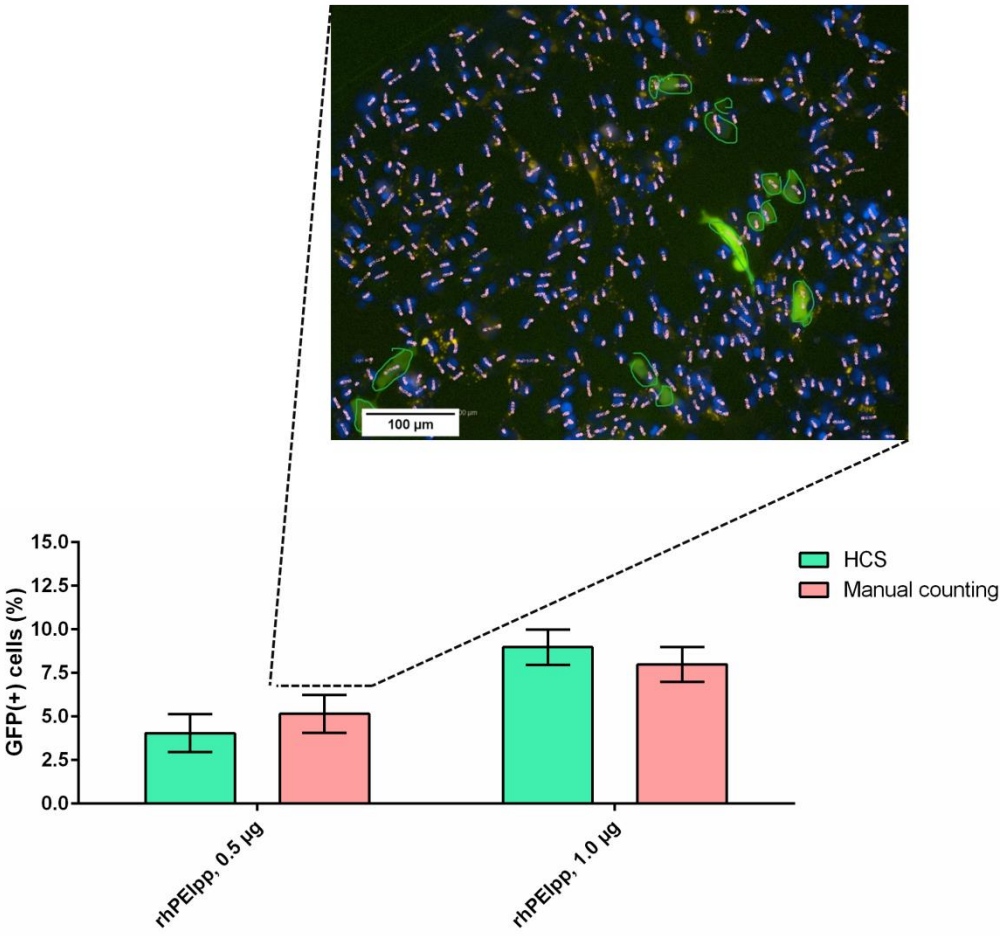

Figure 4-8 Percent GFP(+) cells identified **using manual counting versus HCS**, in HEK293 cell cultures that were treated with rhPEIpp at the indicated pDNA amount. Data are presented as mean ± SEM (n = 3). Two-way ANOVA with Bonferroni's multiple comparisons test was used. There is no significant difference when percent GFP(+) values obtained from HCS versus manual counting were compared. In the inset showed an image that was used for manual counting. Nuclei were marked and counted using a pink brush. GFP(+) cells were marked and counted using a green brush. Scale bar represents 100 µm.

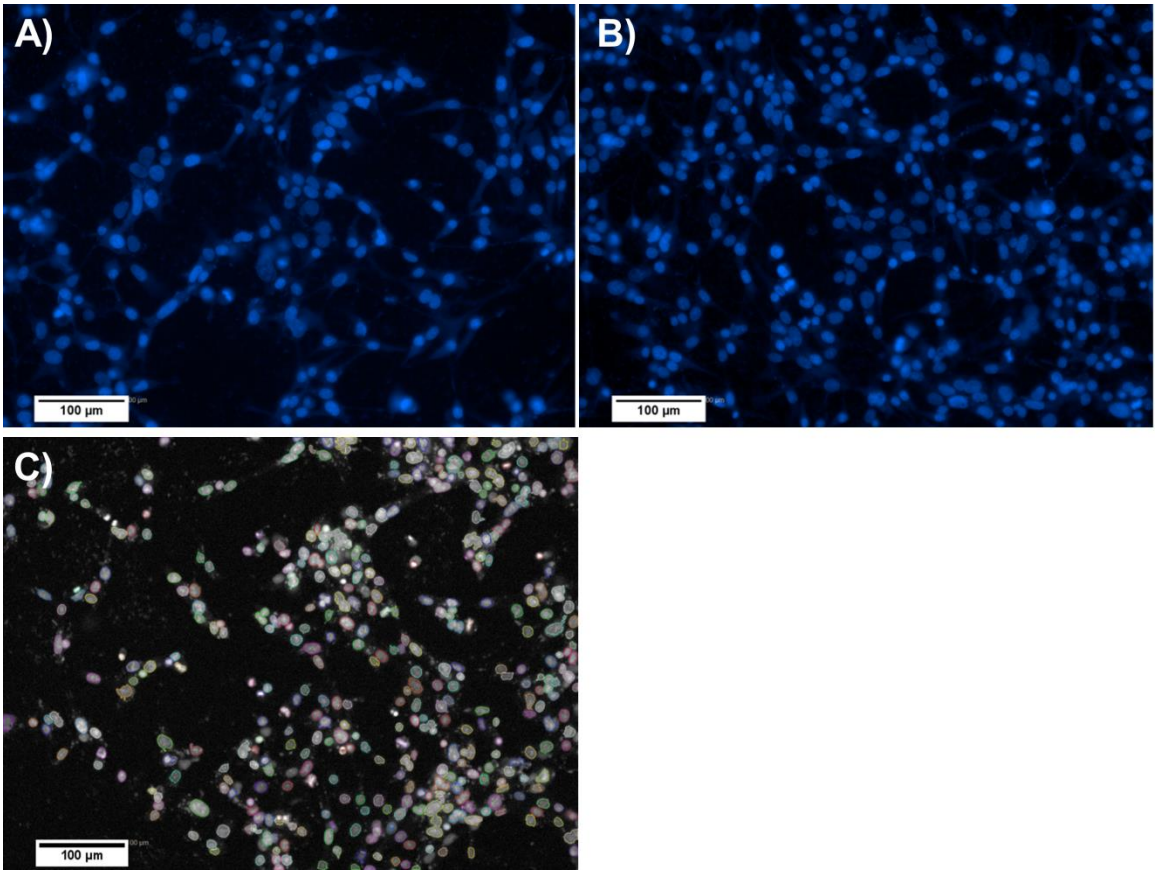

Figure 4-9 Nuclei stained by Hoechst dye were used to determine cell number, using HCS, from wells seeded with (A) 5000 cells and (B) 7500 cells. (C) The nuclei were counted as shown using different colored cell perimeters. These different colors allowed adjacent nuclei to be distinguished. Scale bars in all images represent 100 µm.

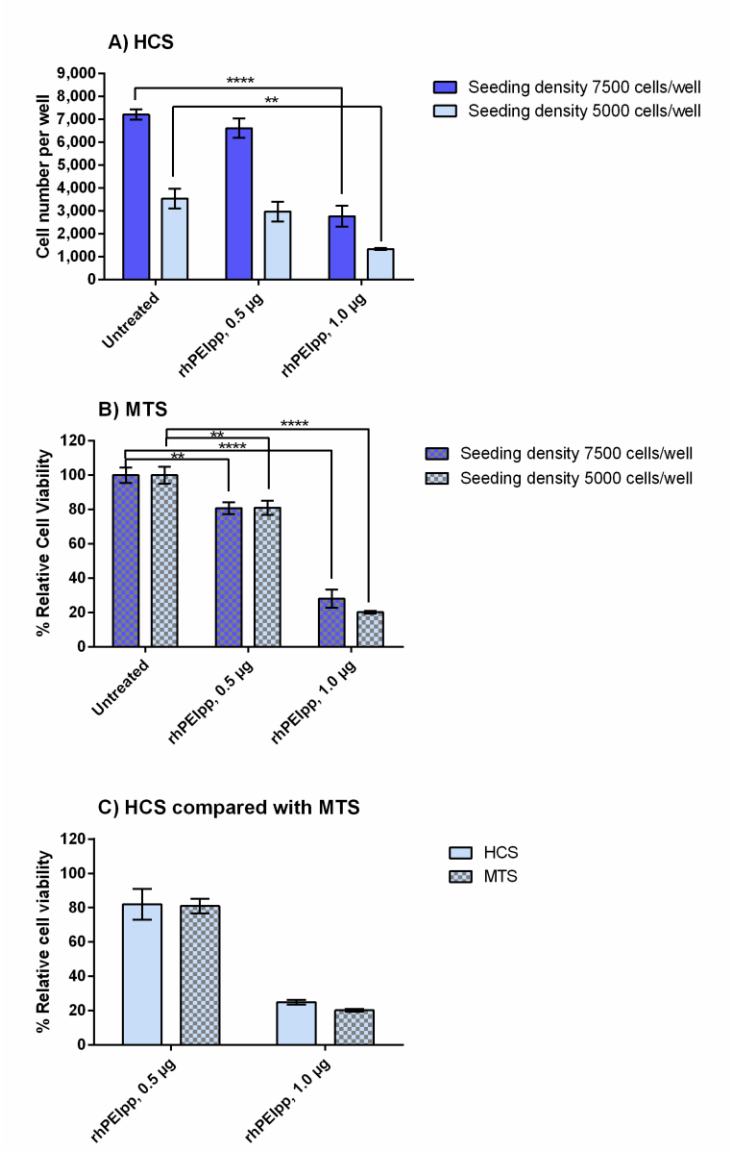

Figure 4-10 Cell viability of HEK293 cells treated with rhPEIpp (containing indicated amount of pDNA), as measured by (A) HCS, which determined the number of cells per well, and (B) MTS assay, which determined percentage relative cell viability. Percentage relative cell viability values were determined as described in the methods section. Two-way ANOVA with Dunnette's multiple comparisons to the untreated group was used. 0.5 µg and 1.0 µg represent the amount of pDNA in each well. (C) Representative result comparing both methods (HCS and MTS). Two-way ANOVA with Dunnette's multiple comparisons to the untreated group was used for (A) and (B). Two-way ANOVA with Bonferroni's multiple comparison test was performed for (C) where no significant difference was found when comparing the percent relative cell viabilities, obtained from each method, of HEK293 cells treated with rhPEIpp. Data are presented as mean ± SEM (n = 3–4:A, n = 5:B). **** $p < 0.0001$, ** $p < 0.01$.

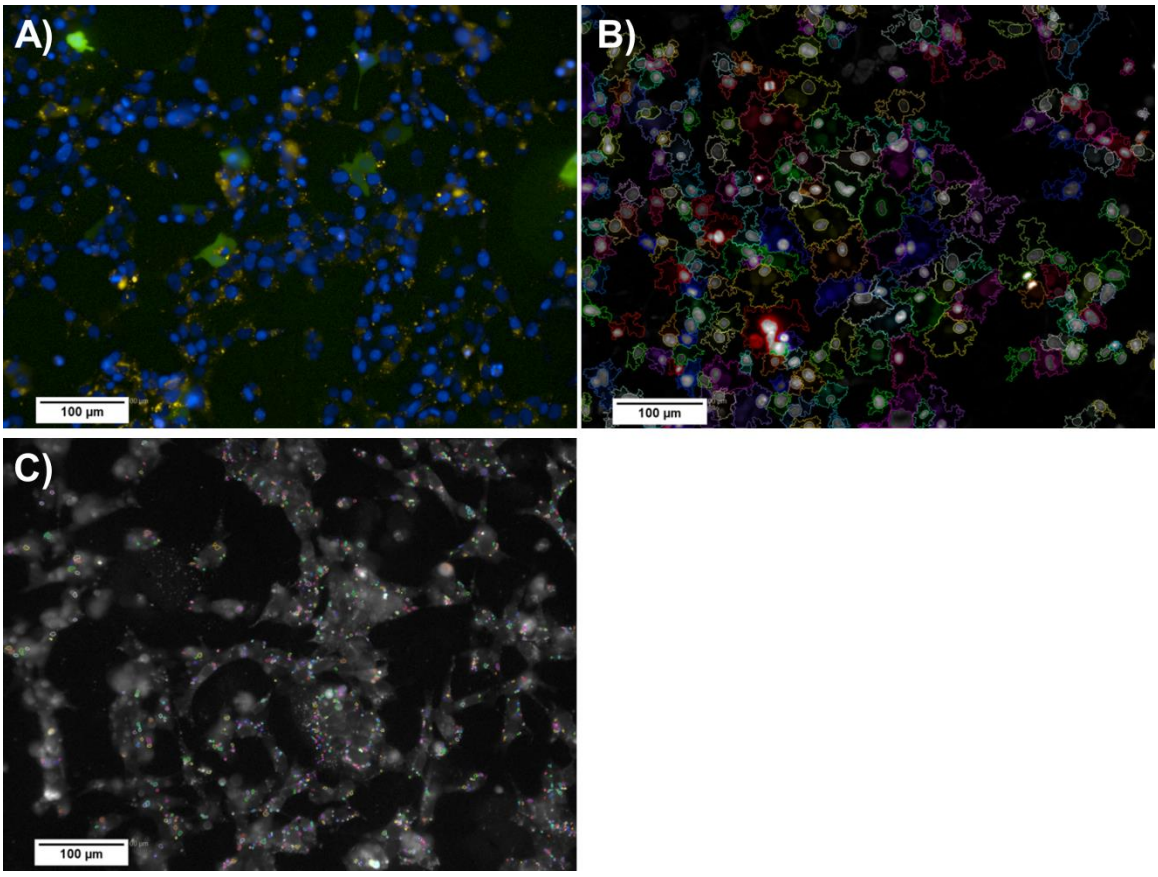

Figure 4-11 Images showing: (A) GFP expression (green) in HEK293 cells (nuclei are blue) with PEIpp (yellow); (B) the cytoplasmic region as determined through computer programmed software designed to delineate, through differential fluorescence detection, the nucleus (stained with Hoechst stain) from the cytoplasm (detected through expression of endogenous GFP); (C) the presence of PEIpp (indicated here as multicolored dots) in the cytoplasm. Scale bars in all images represent 100 µm.

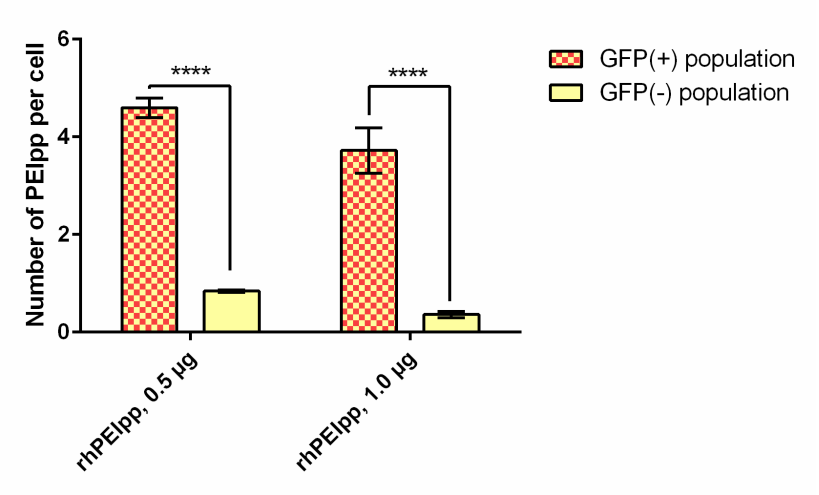

Figure 4-12 Number of PEIpp in cytoplasmic region of GFP(+) and GFP(-) cell populations, as calculated using HCS. Data are presented as mean ± SEM (n = 3). **** $p < 0.0001$. 0.5 µg and 1.0 µg represent the amount of pDNA in each well.

CHAPTER 5 CONCLUSION AND FUTURE DIRECTIONS

In Chapter 2, we formulated chitosan/pDNA polyplexes or CSpp in the size range of 200 – 400 nm in diameter with amine to phosphate (N/P) ratios that ranged from 1 to 100. We compared two types of pDNA within CSpp: pDNA that was free of CpG sequences (CpG(-)) and pDNA that contained CpG sequences (CpG(+)). Both forms of CSpp showed low cytotoxicity when incubated with A549 and HEK293 cells in vitro as seen by MTS assay (cell proliferation), caspase-3/7 assay (apoptosis) and superoxide levels detection (intracellular ROS). CSpp(CpG(-)) generated higher luciferase expression in both in vitro, for A549 cells, and in vivo (C57BL/6, murine model), when compared with CSpp(CpG(+)), indicating enhanced transfection efficiency. In addition, CSpp(CpG(-)) elicited milder inflammatory responses in mice twenty-four hours subsequent to nasal instillation, as determined by proinflammatory cytokine levels within the bronchoalveolar lavage fluid (Figure 5-1). Our findings suggest that to achieve optimal gene expression with minimal cytotoxicity, inflammatory responses and oxidative stress, we must not only consider the traits of the delivery vehicle, such as the cationic polymer used here, but also the chemical nature of the pDNA. CpG sequences in the pDNA of the polyplexes need to be taken into account. These findings will inform the preclinical safety assessments of CSpp in pulmonary gene delivery systems.

After this study was completed, in 2015, Lindberg et al. [205] also investigated the relationship between CpG sequence in pDNA and transfection efficiency of non-viral vectors. Lindberg et al. tested the lipoplexes made from the cationic lipid with plasmids composed of/free of CpG sequence in vivo. The lipoplexes were administered to Swiss mice intravenously [205]. It was found that lipoplexes composed of CpG-free pDNA gave higher and more stained transgene expression than those lipoplexes composed of CpG-pDNA. The result confirms our finding that plasmid free of CpG increases transgene expression. This theory holds true in the systems made from different non-viral vectors

(cationic polymer and cationic lipid), different plasmids, different mice strains and different routes of administration.

In Chapter 3, the new cationic co-polymer, poly(galactaramidoamine) or PGAA was tested for its transfection efficiency and cytotoxicity in vitro. PGAA electrostatically complexes with pDNA form small sized particles. We showed that PGAA/pDNA polyplexes or PGAApp generated high transfection efficiencies in HEK293 and RAW264.7 cells. PGAApp mediated transfection was a function of the N/P ratio. The maximum luciferase expression was obtained using PGAApp made at an N/P ratio of 40. This was consistent in both cell lines. Cytotoxicity of PGAApp increased as the N/P ratios increased.

In the future, to fully optimize transfection efficiency and cytotoxicity of PGAApp, more experiments are necessary. N/P 60 was chosen as recommended by the company (Techulon ^{TM}, Blacksburg, VA). We expanded the N/P ratios tested to 40 and 80. Since the results suggested that N/P 40 gave the best transfection efficiency and lowest cytotoxicity, it is worth investigating at N/P ratios lower than 40. It is possible that at lower N/P ratios lower cytotoxicity may be achieved thus leading to higher transgene expression. Since PGAA synthesis was inspired by the chemistry and function of chitosan and PEI, it is reasonable to compare transfection efficiency and cytotoxicity among these three polymers. Moreover, since we know that using CpG-free pDNA results in an increase in transgene expression, one could incorporate CpG-free plasmids into PGAApp formulations to further improve transfection efficiencies. To date, PGAA or Glycofect ^{TM} has been tested in various cell lines such as human oral squamous cell carcinoma (HCS-3) [206], human dermal fibroblasts (HDFn) [207] and rat mesenchymal stem cells (RMSC) [207]. To the best of our knowledge, there has been no in vivo study using PGAA as a vector.

Chapter 4 was dedicated to the potential use of high-content screening (HCS) in the gene delivery field. High-content screening (HCS) has gained interest in cellular

imaging because of its ability to provide statistically significant data from multiple parameters simultaneously in cell-based assays. HCS was used to measure transfection efficiencies and cytotoxicities of polyplexes made from fluorescently labeled polyethylenimine (PEI) and pDNA encoding EGFP. The results generated using HCS were confirmed using more conventional and labor-intensive methods. Our findings suggest that HCS has the potential to be used as a tool in the field of gene delivery. Nowadays, where there are many cationic polymers and modified forms of cationic polymers synthesized, it is convenient to have an automated system that can evaluate transfection efficiency and cytotoxicity of these polymers. Moreover, the optimization of the transfecting conditions and formulations such as polymer molecular weight, N/P ratios and order of mixing, could be done simultaneously using HCS.

For the first time, a relationship between transfected cells and the number of polyplexes in the cytoplasm was shown. Four to five polyplexes were found in the cytoplasm of successfully transfected cells, whilst non-transfected cells harbored, on average, less than one polyplex within the cytoplasm. HCS can not only simultaneously measure transfection efficiency and cytotoxicity of various non-viral gene vectors; it can also be used to track these vectors through various subcellular compartments.

In summary, the research goal was to develop polyplex formulations made from cationic polymers that mediate optimal transfection efficiencies and low cytotoxicities. We found that pDNA composition was important. We also introduced a new system to gene delivery field (high-content screening) with the hope that this could help to identify the trafficking pathways of various non-viral gene delivery vehicles as well as cellular barriers to optimal transgene expression, thereby aiding in the designing of successful gene delivery systems in the future.

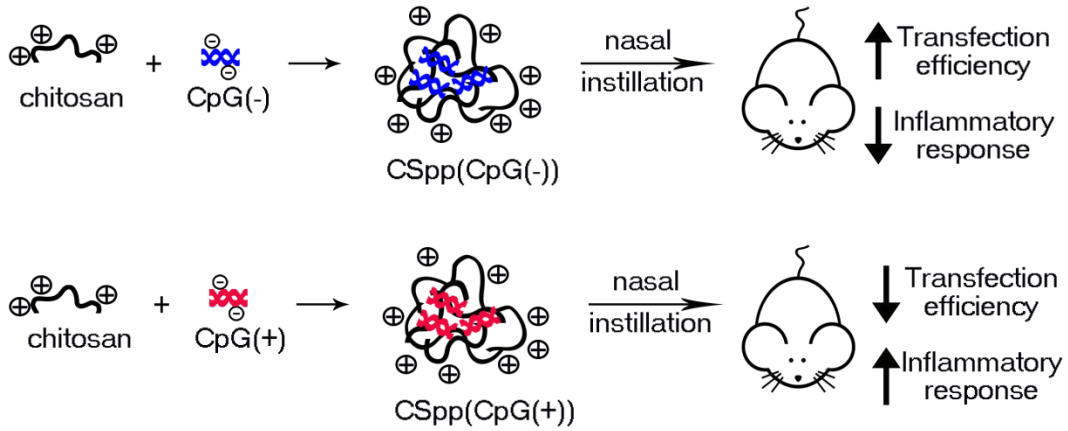

Figure 5-1 Schematic represents the results obtained from the Chapter 2. When compared with CSpp(CpG(+)), nasal instillation of CSpp(CpG(-)) to mice lungs showed higher transfection efficiency. In addition, CSpp(CpG(-)) elicited milder inflammatory responses in mice.

REFERENCES

1. Ramamoorth, M.; Narvekar, A., Non Viral Vectors in Gene Therapy- An Overview. *Journal of clinical and diagnostic research : JCDR* **2015,** 9, (1), GE01-GE06.

2. Glover, D. J.; Lipps, H. J.; Jans, D. A., Towards safe, non-viral therapeutic gene expression in humans. *Nat Rev Genet* **2005,** 6, (4), 299-310.

3. Nayerossadat, N.; Maedeh, T.; Ali, P. A., Viral and nonviral delivery systems for gene delivery. *Advanced biomedical research* **2012,** 1, 27.

4. Mueller, C.; Flotte, T. R., Gene therapy for cystic fibrosis. *Clinical reviews in allergy & immunology* **2008,** 35, (3), 164-78.

5. Flotte, T. R., Recombinant adeno-associated virus vectors for cystic fibrosis gene therapy. *Current opinion in molecular therapeutics* **2001,** 3, (5), 497-502.

6. Boucher, R. C.; Knowles, M. R.; Johnson, L. G.; Olsen, J. C.; Pickles, R.; Wilson, J. M.; Engelhardt, J.; Yang, Y.; Grossman, M., Gene therapy for cystic fibrosis using E1-deleted adenovirus: a phase I trial in the nasal cavity. The University of North Carolina at Chapel Hill. *Human gene therapy* **1994,** 5, (5), 615-39.

7. Prickett, M.; Jain, M., Chapter 16 - Gene Therapy in Cystic Fibrosis. In *Translating Gene Therapy to the Clinic*, Franklin, J. L., Ed. Academic Press: Boston, 2015; pp 247-260.

8. Chuah, M. K.; Evens, H.; VandenDriessche, T., Gene therapy for hemophilia. *Journal of thrombosis and haemostasis : JTH* **2013,** 11 Suppl 1, 99-110.

9. Chuah, M. K.; Nair, N.; VandenDriessche, T., Recent progress in gene therapy for hemophilia. *Human gene therapy* **2012,** 23, (6), 557-65.

10. Chuah, M. K.; Collen, D.; Vandendriessche, T., Preclinical and clinical gene therapy for haemophilia. *Haemophilia : the official journal of the World Federation of Hemophilia* **2004,** 10 Suppl 4, 119-25.

11. Olowoyeye, A.; Okwundu, C. I., Gene therapy for sickle cell disease. *The Cochrane database of systematic reviews* **2012,** 11, Cd007652.

12. Rubanyi, G. M., The future of human gene therapy. *Molecular Aspects of Medicine* **2001,** 22, (3), 113-142.

13. Amer, M., Gene therapy for cancer: present status and future perspective. *Molecular and Cellular Therapies* **2014,** 2, (1), 27.

14. Das, S. K.; Menezes, M. E.; Bhatia, S.; Wang, X.-Y.; Emdad, L.; Sarkar, D.; Fisher, P. B., Gene Therapies for Cancer: Strategies, Challenges and Successes. *Journal of Cellular Physiology* **2015,** 230, (2), 259-271.

15. Cross, D.; Burmester, J. K., Gene therapy for cancer treatment: past, present and future. *Clinical medicine & research* **2006,** 4, (3), 218-27.

16. Scholl, S. M.; Michaelis, S.; McDermott, R., Gene Therapy Applications to Cancer Treatment. *Journal of Biomedicine and Biotechnology* **2003,** 2003, (1), 35-47.

17. Gould, D. J.; Favorov, P., Vectors for the treatment of autoimmune disease. *Gene Ther* **0000,** 10, (10), 912-927.

18. Seroogy, C. M.; Fathman, C. G., The application of gene therapy in autoimmune diseases. *Gene Ther* **2000,** 7, (1), 9-13.

19. Nanou, A.; Azzouz, M., Gene therapy for neurodegenerative diseases based on lentiviral vectors. *Progress in brain research* **2009,** 175, 187-200.

20. Ralph, G. S.; Binley, K.; Wong, L. F.; Azzouz, M.; Mazarakis, N. D., Gene therapy for neurodegenerative and ocular diseases using lentiviral vectors. *Clinical science (London, England : 1979)* **2006,** 110, (1), 37-46.

21. Madonna, R.; Cadeddu, C.; Deidda, M.; Giricz, Z.; Madeddu, C.; Mele, D.; Monte, I.; Novo, G.; Pagliaro, P.; Pepe, A.; Spallarossa, P.; Tocchetti, C. G.; Varga, Z. V.; Zito, C.; Geng, Y. J.; Mercuro, G.; Ferdinandy, P., Cardioprotection by gene therapy: A review paper on behalf of the Working Group on Drug Cardiotoxicity and

Cardioprotection of the Italian Society of Cardiology. *International journal of cardiology* **2015,** 191, 203-210.

22. Wolfram, J. A.; Donahue, J. K., Gene therapy to treat cardiovascular disease. *Journal of the American Heart Association* **2013,** 2, (4), e000119.

23. Baker, A. H., Designing gene delivery vectors for cardiovascular gene therapy. *Progress in biophysics and molecular biology* **2004,** 84, (2-3), 279-99.

24. Waehler, R.; Russell, S. J.; Curiel, D. T., Engineering targeted viral vectors for gene therapy. *Nat Rev Genet* **2007,** 8, (8), 573-587.

25. Young, L. S.; Searle, P. F.; Onion, D.; Mautner, V., Viral gene therapy strategies: from basic science to clinical application. *The Journal of Pathology* **2006,** 208, (2), 299-318.

26. Boeckle, S.; Wagner, E., Optimizing targeted gene delivery: chemical modification of viral vectors and synthesis of artificial virus vector systems. *Aaps j* **2006,** 8, (4), E731-42.

27. Boulaiz, H.; Marchal, J. A.; Prados, J.; Melguizo, C.; Aranega, A., Non-viral and viral vectors for gene therapy. *Cellular and molecular biology (Noisy-le-Grand, France)* **2005,** 51, (1), 3-22.

28. Yi, Y.; Jong Noh, M.; Hee Lee, K., Current Advances in Retroviral Gene Therapy. *Curr. Gene Ther.* **2011,** 11, (3), 218-228.

29. Sadelain, M., Insertional oncogenesis in gene therapy: how much of a risk? *Gene Ther* **0000,** 11, (7), 569-573.

30. Friedmann, T.; Roblin, R., Gene therapy for human genetic disease? *Science (New York, N.Y.)* **1972,** 175, (4025), 949-55.

31. Ginn, S. L.; Alexander, I. E.; Edelstein, M. L.; Abedi, M. R.; Wixon, J., Gene therapy clinical trials worldwide to 2012 – an update. *The journal of gene medicine* **2013,** 15, (2), 65-77.

32. Yla-Herttuala, S., Endgame: glybera finally recommended for approval as the first gene therapy drug in the European union. *Molecular therapy : the journal of the American Society of Gene Therapy* **2012,** 20, (10), 1831-2.

33. Gaudet, D.; de Wal, J.; Tremblay, K.; Dery, S.; van Deventer, S.; Freidig, A.; Brisson, D.; Methot, J., Review of the clinical development of alipogene tiparvovec gene therapy for lipoprotein lipase deficiency. *Atherosclerosis. Supplements* **2010,** 11, (1), 55-60.

34. Ferreira, V.; Twisk, J.; Kwikkers, K.; Aronica, E.; Brisson, D.; Methot, J.; Petry, H.; Gaudet, D., Immune Responses to Intramuscular Administration of Alipogene Tiparvovec (AAV1-LPL(S447X)) in a Phase II Clinical Trial of Lipoprotein Lipase Deficiency Gene Therapy. *Hum. Gene Ther.* **2014,** 25, (3), 180-188.

35. Burnett, J. R.; Hooper, A. J., Alipogene tiparvovec, an adeno-associated virus encoding the Ser(447)X variant of the human lipoprotein lipase gene for the treatment of patients with lipoprotein lipase deficiency. *Current opinion in molecular therapeutics* **2009,** 11, (6), 681-91.

36. Yla-Herttuala, S., Endgame: Glybera Finally Recommended for Approval as the First Gene Therapy Drug in the European Union. *Molecular therapy : the journal of the American Society of Gene Therapy* **2012,** 20, (10), 1831-1832.

37. Ylä-Herttuala, S., Endgame: Glybera Finally Recommended for Approval as the First Gene Therapy Drug in the European Union. *Mol. Ther.* **2012,** 20, (10), 1831-1832.

38. Edelstein, M. L.; Abedi, M. R.; Wixon, J.; Edelstein, R. M., Gene therapy clinical trials worldwide 1989-2004-an overview. *The journal of gene medicine* **2004,** 6, (6), 597-602.

39. Ginn, S. L.; Alexander, I. E.; Edelstein, M. L.; Abedi, M. R.; Wixon, J., Gene therapy clinical trials worldwide to 2012 - an update. *The journal of gene medicine* **2013,** 15, (2), 65-77.

40. Douglas, K. L., Toward development of artificial viruses for gene therapy: a comparative evaluation of viral and non-viral transfection. *Biotechnology progress* **2008,** 24, (4), 871-83.

41. Zhang, J.; Li, X.; Lou, L.; Li, X.; Jia, Y.; Jin, Z.; Zhu, Y., Non-viral Gene Therapy. In *Intracellular Delivery: Fundamentals and Applications*, Prokop, A., Ed. Springer Netherlands: Springer Science, 2011; pp 599-699.

42. van Gaal, E. V. B.; van Eijk, R.; Oosting, R. S.; Kok, R. J.; Hennink, W. E.; Crommelin, D. J. A.; Mastrobattista, E., How to screen non-viral gene delivery systems in vitro? *Journal of Controlled Release* **2011,** 154, (3), 218-232.

43. Al-Dosari, M. S.; Gao, X., Nonviral Gene Delivery: Principle, Limitations, and Recent Progress. *The AAPS Journal* **2009,** 11, (4), 671-681.

44. Thomas, M.; Klibanov, A. M., Non-viral gene therapy: polycation-mediated DNA delivery. *Applied microbiology and biotechnology* **2003,** 62, (1), 27-34.

45. Medina-Kauwe, L. K.; Xie, J.; Hamm-Alvarez, S., Intracellular trafficking of nonviral vectors. *Gene Ther* **2005,** 12, (24), 1734-51.

46. Evans, C. W.; Fitzgerald, M.; Clemons, T. D.; House, M. J.; Padman, B. S.; Shaw, J. A.; Saunders, M.; Harvey, A. R.; Zdyrko, B.; Luzinov, I.; Silva, G. A.; Dunlop, S. A.; Iyer, K. S., Multimodal Analysis of PEI-Mediated Endocytosis of Nanoparticles in Neural Cells. *ACS Nano* **2011,** 5, (11), 8640-8648.

47. Rémy-Kristensen, A.; Clamme, J.-P.; Vuilleumier, C.; Kuhry, J.-G.; Mély, Y., Role of endocytosis in the transfection of L929 fibroblasts by polyethylenimine/DNA complexes. *Biochimica et Biophysica Acta (BBA) - Biomembranes* **2001,** 1514, (1), 21-32.

48. Khalil, I. A.; Kogure, K.; Akita, H.; Harashima, H., Uptake pathways and subsequent intracellular trafficking in nonviral gene delivery. *Pharmacological reviews* **2006,** 58, (1), 32-45.

49. Boussif, O.; Lezoualc'h, F.; Zanta, M. A.; Mergny, M. D.; Scherman, D.; Demeneix, B.; Behr, J. P., A versatile vector for gene and oligonucleotide transfer into cells in culture and in vivo: polyethylenimine. *Proc Natl Acad Sci U S A* **1995,** 92, (16), 7297-301.

50. Akinc, A.; Thomas, M.; Klibanov, A. M.; Langer, R., Exploring polyethylenimine-mediated DNA transfection and the proton sponge hypothesis. *The journal of gene medicine* **2005,** 7, (5), 657-63.

51. Kichler, A.; Leborgne, C.; Coeytaux, E.; Danos, O., Polyethylenimine-mediated gene delivery: a mechanistic study. *The journal of gene medicine* **2001,** 3, (2), 135-44.

52. Sonawane, N. D.; Szoka, F. C., Jr.; Verkman, A. S., Chloride accumulation and swelling in endosomes enhances DNA transfer by polyamine-DNA polyplexes. *J Biol Chem* **2003,** 278, (45), 44826-31.

53. Benjaminsen, R. V.; Mattebjerg, M. A.; Henriksen, J. R.; Moghimi, S. M.; Andresen, T. L., The possible "proton sponge " effect of polyethylenimine (PEI) does not include change in lysosomal pH. *Mol. Ther.* **2013,** 21, (1), 149-57.

54. Bieber, T.; Meissner, W.; Kostin, S.; Niemann, A.; Elsasser, H. P., Intracellular route and transcriptional competence of polyethylenimine-DNA complexes. *Journal of controlled release : official journal of the Controlled Release Society* **2002,** 82, (2-3), 441-54.

55. Won, Y.-Y.; Sharma, R.; Konieczny, S. F., Missing Pieces in Understanding the Intracellular Trafficking of Polycation/DNA Complexes. *Journal of Controlled Release* **2009,** 139, (2), 88-93.

56. Pichon, C.; Billiet, L.; Midoux, P., Chemical vectors for gene delivery: uptake and intracellular trafficking. *Current Opinion in Biotechnology* **2010,** 21, (5), 640-645.

57. Suh, J.; Wirtz, D.; Hanes, J., Efficient active transport of gene nanocarriers to the cell nucleus. *Proceedings of the National Academy of Sciences of the United States of America* **2003,** 100, (7), 3878-3882.

58. Maeshima, K.; Iino, H.; Hihara, S.; Imamoto, N., Nuclear size, nuclear pore number and cell cycle. *Nucleus* **2011,** 2, (2), 113-118.

59. Gerace, L., Nuclear export signals and the fast track to the cytoplasm. *Cell* **1995,** 82, (3), 341-4.

60. Schaffert, D.; Wagner, E., Gene therapy progress and prospects: synthetic polymer-based systems. *Gene Ther* **2008,** 15, (16), 1131-1138.

61. Lemkine, G. F.; Demeneix, B. A., Polyethylenimines for in vivo gene delivery. *Current opinion in molecular therapeutics* **2001,** 3, (2), 178-82.

62. Lai, W. F., In vivo nucleic acid delivery with PEI and its derivatives: current status and perspectives. *Expert review of medical devices* **2011,** 8, (2), 173-85.

63. Cho, C.-S., Design and Development of Degradable Polyethylenimines for Delivery of DNA and Small Interfering RNA: An Updated Review. *ISRN Materials Science* **2012,** 2012, 24.

64. Tong, H.; Qin, S.; Fernandes, J. C.; Li, L.; Dai, K.; Zhang, X., Progress and prospects of chitosan and its derivatives as non-viral gene vectors in gene therapy. *Current gene therapy* **2009,** 9, (6), 495-502.

65. Mansouri, S.; Lavigne, P.; Corsi, K.; Benderdour, M.; Beaumont, E.; Fernandes, J. C., Chitosan-DNA nanoparticles as non-viral vectors in gene therapy: strategies to improve transfection efficacy. *European journal of pharmaceutics and biopharmaceutics : official journal of Arbeitsgemeinschaft fur Pharmazeutische Verfahrenstechnik e.V* **2004,** 57, (1), 1-8.

66. Tiera, M. J.; Winnik, F. O.; Fernandes, J. C., Synthetic and natural polycations for gene therapy: state of the art and new perspectives. *Current gene therapy* **2006,** 6, (1), 59-71.

67. Tiera, M. J.; Shi, Q.; Winnik, F. M.; Fernandes, J. C., Polycation-based gene therapy: current knowledge and new perspectives. *Current gene therapy* **2011,** 11, (4), 288-306.

68. Guang Liu, W.; De Yao, K., Chitosan and its derivatives--a promising non-viral vector for gene transfection. *Journal of controlled release : official journal of the Controlled Release Society* **2002,** 83, (1), 1-11.

69. Kean, T.; Thanou, M., Biodegradation, biodistribution and toxicity of chitosan. *Advanced drug delivery reviews* **2010,** 62, (1), 3-11.

70. Huang, M.; Fong, C. W.; Khor, E.; Lim, L. Y., Transfection efficiency of chitosan vectors: effect of polymer molecular weight and degree of deacetylation. *Journal of controlled release : official journal of the Controlled Release Society* **2005,** 106, (3), 391-406.

71. Mao, H. Q.; Roy, K.; Troung-Le, V. L.; Janes, K. A.; Lin, K. Y.; Wang, Y.; August, J. T.; Leong, K. W., Chitosan-DNA nanoparticles as gene carriers: synthesis, characterization and transfection efficiency. *Journal of controlled release : official journal of the Controlled Release Society* **2001,** 70, (3), 399-421.

72. Jiang, H. L.; Kim, T. H.; Kim, Y. K.; Park, I. Y.; Cho, M. H.; Cho, C. S., Efficient gene delivery using chitosan-polyethylenimine hybrid systems. *Biomedical materials (Bristol, England)* **2008,** 3, (2), 025013.

73. Schwartz, D. A.; Quinn, T. J.; Thorne, P. S.; Sayeed, S.; Yi, A. K.; Krieg, A. M., CpG motifs in bacterial DNA cause inflammation in the lower respiratory tract. *Journal of Clinical Investigation* **1997,** 100, (1), 68-73.

74. Knuefermann, P.; Baumgarten, G.; Koch, A.; Schwederski, M.; Velten, M.; Ehrentraut, H.; Mersmann, J.; Meyer, R.; Hoeft, A.; Zacharowski, K.; Grohé, C., CpG oligonucleotide activates Toll-like receptor 9 and causes lung inflammation in vivo. *Respiratory Research* **2007,** 8, (1), 72-72.

75. Krieg, A. M., CpG motifs in bacterial DNA and their immune effects. *Annual review of immunology* **2002,** 20, 709-60.

76. Scheule, R. K., The role of CpG motifs in immunostimulation and gene therapy. *Advanced drug delivery reviews* **2000,** 44, (2-3), 119-34.

77. Reineke, T. M., Poly(glycoamidoamine)s: Cationic glycopolymers for DNA delivery. *Journal of Polymer Science Part A: Polymer Chemistry* **2006,** 44, (24), 6895-6908.

78. Liu, Y.; Reineke, T. M., Poly(glycoamidoamine)s for gene delivery: stability of polyplexes and efficacy with cardiomyoblast cells. *Bioconjugate chemistry* **2006,** 17, (1), 101-8.

79. Liu, Y.; Reineke, T. M., Degradation of Poly(glycoamidoamine) DNA Delivery Vehicles: Polyamide Hydrolysis at Physiological Conditions Promotes DNA Release. *Biomacromolecules* **2010,** 11, (2), 316-325.

80. Liu, Y.; Reineke, T. M., Hydroxyl Stereochemistry and Amine Number within Poly(glycoamidoamine)s Affect Intracellular DNA Delivery. *Journal of the American Chemical Society* **2005,** 127, (9), 3004-3015.

81. De Smedt, S. C.; Demeester, J.; Hennink, W. E., Cationic polymer based gene delivery systems. *Pharmaceutical research* **2000,** 17, (2), 113-26.

82. Lechardeur, D.; Lukacs, G. L., Intracellular barriers to non-viral gene transfer. *Current gene therapy* **2002,** 2, (2), 183-94.

83. Haney, S. A.; LaPan, P.; Pan, J.; Zhang, J., High-content screening moves to the front of the line. *Drug Discovery Today* **2006,** 11, (19–20), 889-894.

84. Zanella, F.; Lorens, J. B.; Link, W., High content screening: seeing is believing. *Trends in biotechnology* **2010,** 28, (5), 237-245.

85. Nagpal, K.; Singh, S. K.; Mishra, D. N., Chitosan nanoparticles: a promising system in novel drug delivery. *Chemical & pharmaceutical bulletin* **2010,** 58, (11), 1423-30.

86. Shukla, S. K.; Mishra, A. K.; Arotiba, O. A.; Mamba, B. B., Chitosan-based nanomaterials: A state-of-the-art review. *Int. J. Biol. Macromol.* **2013,** 59, (0), 46-58.

87. Varshosaz, J., The promise of chitosan microspheres in drug delivery systems. *Expert opinion on drug delivery* **2007,** 4, (3), 263-73.

88. Guang Liu, W.; De Yao, K., Chitosan and its derivatives—a promising non-viral vector for gene transfection. *Journal of Controlled Release* **2002,** 83, (1), 1-11.

89. Lai, W. F.; Lin, M. C., Nucleic acid delivery with chitosan and its derivatives. *Journal of controlled release : official journal of the Controlled Release Society* **2009,** 134, (3), 158-68.

90. Saranya, N.; Moorthi, A.; Saravanan, S.; Devi, M. P.; Selvamurugan, N., Chitosan and its derivatives for gene delivery. *International journal of biological macromolecules* **2011,** 48, (2), 234-8.

91. Richardson, S. C.; Kolbe, H. V.; Duncan, R., Potential of low molecular mass chitosan as a DNA delivery system: biocompatibility, body distribution and ability to complex and protect DNA. *International journal of pharmaceutics* **1999,** 178, (2), 231-43.

92. Kiang, T.; Wen, J.; Lim, H. W.; Leong, K. W., The effect of the degree of chitosan deacetylation on the efficiency of gene transfection. *Biomaterials* **2004,** 25, (22), 5293-301.

93. Ren, D.; Yi, H.; Wang, W.; Ma, X., The enzymatic degradation and swelling properties of chitosan matrices with different degrees of N-acetylation. *Carbohydr. Res.* **2005,** 340, (15), 2403-10.

94. Zhang, H.; Neau, S. H., In vitro degradation of chitosan by a commercial enzyme preparation: effect of molecular weight and degree of deacetylation. *Biomaterials* **2001,** 22, (12), 1653-8.

95. Kulish, E. I.; Volodina, V. P.; Kolesov, S. V.; Zaikov, G. E., Enzymatic degradation of chitosan films by collagenase. *Polym. Sci. Ser. B* **2006,** 48, (5), 244-246.

96. Muzzarelli, R. A., Human enzymatic activities related to the therapeutic administration of chitin derivatives. *Cell. Mol. Life Sci.* **1997,** 53, (2), 131-40.

97. Koping-Hoggard, M.; Tubulekas, I.; Guan, H.; Edwards, K.; Nilsson, M.; Varum, K. M.; Artursson, P., Chitosan as a nonviral gene delivery system. Structure-property relationships and characteristics compared with polyethylenimine in vitro and after lung administration in vivo. *Gene Ther* **2001,** 8, (14), 1108-21.

98. Okamoto, H.; Nishida, S.; Todo, H.; Sakakura, Y.; Iida, K.; Danjo, K., Pulmonary gene delivery by chitosan-pDNA complex powder prepared by a supercritical carbon dioxide process. *Journal of pharmaceutical sciences* **2003,** 92, (2), 371-80.

99. Nydert, P.; Dragomir, A.; Hjelte, L., Chitosan as a carrier for non-viral gene transfer in a cystic-fibrosis cell line. *Biotechnology and applied biochemistry* **2008,** 51, (Pt 4), 153-7.

100. Mohammadi, Z.; Dorkoosh, F. A.; Hosseinkhani, S.; Gilani, K.; Amini, T.; Najafabadi, A. R.; Tehrani, M. R., In vivo transfection study of chitosan-DNA-FAP-B nanoparticles as a new non viral vector for gene delivery to the lung. *International journal of pharmaceutics* **2011,** 421, (1), 183-8.

101. Kong, X.; Hellermann, G. R.; Zhang, W.; Jena, P.; Kumar, M.; Behera, A.; Behera, S.; Lockey, R.; Mohapatra, S. S., Chitosan Interferon-gamma Nanogene Therapy for Lung Disease: Modulation of T-Cell and Dendritic Cell Immune Responses. *Allergy, asthma, and clinical immunology : official journal of the Canadian Society of Allergy and Clinical Immunology* **2008,** 4, (3), 95-105.

102. Okamoto, H.; Shiraki, K.; Yasuda, R.; Danjo, K.; Watanabe, Y., Chitosan-interferon-beta gene complex powder for inhalation treatment of lung metastasis in mice. *Journal of controlled release : official journal of the Controlled Release Society* **2011,** 150, (2), 187-95.

103. Jiang, H. L.; Cui, P. F.; Xie, R. L.; Cho, C. S., Chemical modification of chitosan for efficient gene therapy. *Advances in food and nutrition research* **2014,** 73, 83-101.

104. Singh, B.; Choi, Y. J.; Park, I. K.; Akaike, T.; Cho, C. S., Chemical modification of chitosan with pH-sensitive molecules and specific ligands for efficient DNA transfection and siRNA silencing. *Journal of nanoscience and nanotechnology* **2014,** 14, (1), 564-76.

105. Lavertu, M.; Methot, S.; Tran-Khanh, N.; Buschmann, M. D., High efficiency gene transfer using chitosan/DNA nanoparticles with specific combinations of molecular weight and degree of deacetylation. *Biomaterials* **2006,** 27, (27), 4815-24.

106. Romoren, K.; Pedersen, S.; Smistad, G.; Evensen, O.; Thu, B. J., The influence of formulation variables on in vitro transfection efficiency and physicochemical properties of chitosan-based polyplexes. *International journal of pharmaceutics* **2003,** 261, (1-2), 115-27.

107. Kim, T. H.; Kim, S. I.; Akaike, T.; Cho, C. S., Synergistic effect of poly(ethylenimine) on the transfection efficiency of galactosylated chitosan/DNA complexes. *Journal of controlled release : official journal of the Controlled Release Society* **2005,** 105, (3), 354-66.

108. Zhao, Q. Q.; Chen, J. L.; Han, M.; Liang, W. Q.; Tabata, Y.; Gao, J. Q., Combination of poly(ethylenimine) and chitosan induces high gene transfection efficiency and low cytotoxicity. *Journal of bioscience and bioengineering* **2008,** 105, (1), 65-8.

109. Jiang, H. L.; Kim, Y. K.; Arote, R.; Jere, D.; Quan, J. S.; Yu, J. H.; Choi, Y. J.; Nah, J. W.; Cho, M. H.; Cho, C. S., Mannosylated chitosan-graft-polyethylenimine as a

gene carrier for Raw 264.7 cell targeting. *International journal of pharmaceutics* **2009,** 375, (1-2), 133-9.

110. Jiang, H. L.; Kwon, J. T.; Kim, E. M.; Kim, Y. K.; Arote, R.; Jere, D.; Jeong, H. J.; Jang, M. K.; Nah, J. W.; Xu, C. X.; Park, I. K.; Cho, M. H.; Cho, C. S., Galactosylated poly(ethylene glycol)-chitosan-graft-polyethylenimine as a gene carrier for hepatocyte-targeting. *Journal of controlled release : official journal of the Controlled Release Society* **2008,** 131, (2), 150-7.

111. Chen, H.; Cui, S.; Zhao, Y.; Zhang, C.; Zhang, S.; Peng, X., Grafting chitosan with polyethylenimine in an ionic liquid for efficient gene delivery. *PloS one* **2015,** 10, (4), e0121817.

112. Kean, T.; Thanou, M., Biodegradation, biodistribution and toxicity of chitosan. *Advanced drug delivery reviews* **2010,** 62, (1), 3-11.

113. Mukhopadhyay, P.; Bhattacharya, S.; Nandy, A.; Bhattacharyya, A.; Mishra, R.; Kundu, P. P., Assessment of in vivo chronic toxicity of chitosan and its derivates used as oral insulin carriers. *Toxicology Research* **2015,** 4, (2), 281-290.

114. Buschmann, M. D.; Merzouki, A.; Lavertu, M.; Thibault, M.; Jean, M.; Darras, V., Chitosans for delivery of nucleic acids. *Adv. Drug Del. Rev.* **2013,** 65, (9), 1234-1270.

115. Mansouri, S.; Lavigne, P.; Corsi, K.; Benderdour, M.; Beaumont, E.; Fernandes, J. C., Chitosan-DNA nanoparticles as non-viral vectors in gene therapy: strategies to improve transfection efficacy. *European Journal of Pharmaceutics and Biopharmaceutics* **2004,** 57, (1), 1-8.

116. Enriquez de Salamanca, A.; Diebold, Y.; Calonge, M.; Garcia-Vazquez, C.; Callejo, S.; Vila, A.; Alonso, M. J., Chitosan nanoparticles as a potential drug delivery system for the ocular surface: toxicity, uptake mechanism and in vivo tolerance. *Investigative ophthalmology & visual science* **2006,** 47, (4), 1416-25.

117. Mohammadi, Z.; Abolhassani, M.; Dorkoosh, F. A.; Hosseinkhani, S.; Gilani, K.; Amini, T.; Najafabadi, A. R.; Tehrani, M. R., Preparation and evaluation of chitosan-DNA-FAP-B nanoparticles as a novel non-viral vector for gene delivery to the lung epithelial cells. *International journal of pharmaceutics* **2011,** 409, (1-2), 307-13.

118. Sato, T.; Ishii, T.; Okahata, Y., In vitro gene delivery mediated by chitosan. effect of pH, serum, and molecular mass of chitosan on the transfection efficiency. *Biomaterials* **2001,** 22, (15), 2075-80.

119. Rajesh Kumar, S.; Ishaq Ahmed, V. P.; Parameswaran, V.; Sudhakaran, R.; Sarath Babu, V.; Sahul Hameed, A. S., Potential use of chitosan nanoparticles for oral delivery of DNA vaccine in Asian sea bass (Lates calcarifer) to protect from Vibrio (Listonella) anguillarum. *Fish & Shellfish Immunology* **2008,** 25, (1–2), 47-56.

120. Corsi, K.; Chellat, F.; Yahia, L.; Fernandes, J. C., Mesenchymal stem cells, MG63 and HEK293 transfection using chitosan-DNA nanoparticles. *Biomaterials* **2003,** 24, (7), 1255-64.

121. Krieg, A. M.; Yi, A. K.; Matson, S.; Waldschmidt, T. J.; Bishop, G. A.; Teasdale, R.; Koretzky, G. A.; Klinman, D. M., CpG motifs in bacterial DNA trigger direct B-cell activation. *Nature* **1995,** 374, (6522), 546-9.

122. Yew, N. S.; Zhao, H.; Wu, I. H.; Song, A.; Tousignant, J. D.; Przybylska, M.; Cheng, S. H., Reduced inflammatory response to plasmid DNA vectors by elimination and inhibition of immunostimulatory CpG motifs. *Molecular therapy : the journal of the American Society of Gene Therapy* **2000,** 1, (3), 255-62.

123. Hyde, S. C.; Pringle, I. A.; Abdullah, S.; Lawton, A. E.; Davies, L. A.; Varathalingam, A.; Nunez-Alonso, G.; Green, A. M.; Bazzani, R. P.; Sumner-Jones, S. G.; Chan, M.; Li, H.; Yew, N. S.; Cheng, S. H.; Boyd, A. C.; Davies, J. C.; Griesenbach, U.; Porteous, D. J.; Sheppard, D. N.; Munkonge, F. M.; Alton, E. W.; Gill, D. R., CpG-

free plasmids confer reduced inflammation and sustained pulmonary gene expression. *Nature biotechnology* **2008,** 26, (5), 549-51.

124. Lesina, E.; Dames, P.; Rudolph, C., The effect of CpG motifs on gene expression and clearance kinetics of aerosol administered polyethylenimine (PEI)-plasmid DNA complexes in the lung. *Journal of controlled release : official journal of the Controlled Release Society* **2010,** 143, (2), 243-50.

125. Lesina, E.; Dames, P.; Flemmer, A.; Hajek, K.; Kirchner, T.; Bittmann, I.; Rudolph, C., CpG-free plasmid DNA prevents deterioration of pulmonary function in mice. *European journal of pharmaceutics and biopharmaceutics : official journal of Arbeitsgemeinschaft fur Pharmazeutische Verfahrenstechnik e.V* **2010,** 74, (3), 427-34.

126. Qian, R. Q.; Glanville, R. W. Methods for purifying chitosan. US 2004/0118778 A1, 2005.

127. Abbas, A. O. M. Chitosan for biomedical application. The University of Iowa, Iowa Research Online, 2010.

128. Thorne, P. S., Inhalation toxicology models of endotoxin- and bioaerosol-induced inflammation. *Toxicology* **2000,** 152, (1-3), 13-23.

129. Healey, A.; Furtado, A.; Cooper, T.; Henry, R. J., Protocol: a simple method for extracting next-generation sequencing quality genomic DNA from recalcitrant plant species. *Plant methods* **2014,** 10, 21.

130. Mao, H.-Q.; Roy, K.; Troung-Le, V. L.; Janes, K. A.; Lin, K. Y.; Wang, Y.; August, J. T.; Leong, K. W., Chitosan-DNA nanoparticles as gene carriers: synthesis, characterization and transfection efficiency. *Journal of Controlled Release* **2001,** 70, (3), 399-421.

131. Intra, J.; Salem, A. K., Characterization of the transgene expression generated by branched and linear polyethylenimine-plasmid DNA nanoparticles in vitro and after

intraperitoneal injection in vivo. *Journal of controlled release : official journal of the Controlled Release Society* **2008,** 130, (2), 129-38.

132. Southam, D. S.; Dolovich, M.; O'Byrne, P. M.; Inman, M. D., Distribution of intranasal instillations in mice: effects of volume, time, body position, and anesthesia. *Am J Physiol Lung Cell Mol Physiol* **2002,** 282, (4), L833-9.

133. Adamcakova-Dodd, A.; Stebounova, L. V.; O'Shaughnessy, P. T.; Kim, J. S.; Grassian, V. H.; Thorne, P. S., Murine pulmonary responses after sub-chronic exposure to aluminum oxide-based nanowhiskers. *Part Fibre Toxicol* **2012,** 9, 22.

134. Gautam, A.; Densmore, C. L.; Waldrep, J. C., Pulmonary cytokine responses associated with PEI-DNA aerosol gene therapy. *Gene Ther* **2001,** 8, (3), 254-7.

135. Manthorpe, M.; Cornefert-Jensen, F.; Hartikka, J.; Felgner, J.; Rundell, A.; Margalith, M.; Dwarki, V., Gene therapy by intramuscular injection of plasmid DNA: studies on firefly luciferase gene expression in mice. *Human gene therapy* **1993,** 4, (4), 419-31.

136. Stammberger, U.; Uduehi, A. N.; Kubisa, B.; Roth, T.; Schmid, R. A., Non-viral gene delivery to atelectatic and ventilated lungs. *The Annals of thoracic surgery* **2002,** 73, (2), 432-6.

137. Hornung, R. W.; Reed, L. D., Estimation of Average Concentration in the Presence of Nondetectable Values. *Applied Occupational and Environmental Hygiene* **1990,** 5, (1), 46-51.

138. Hollinger, J. O., *An introduction to biomaterials*. 2nd ed.; CRC Press/Taylor & Francis: Boca Raton, FL, 2012; p xix, 624 p.

139. Brigham, K. L.; Meyrick, B., Endotoxin and lung injury. *The American review of respiratory disease* **1986,** 133, (5), 913-27.

140. Rudbach, J. A.; Milner, K. C., Reaction of endotoxin and surfactants. 3. Effect of sodium lauryl sulfate on the structure and pyrogenicity of endotoxin. *Canadian journal of microbiology* **1968,** 14, (11), 1173-8.

141. Oroszlan, S. I.; Mora, P. T., DISSOCIATION AND RECONSTITUTION OF AN ENDOTOXIN. *Biochemical and biophysical research communications* **1963,** 12, 345-9.

142. Williams, K. L., *Endotoxins : pyrogens, LAL testing and depyrogenation*. 3rd ed.; Informa Healthcare: New York, 2007; p ix, 419 p.

143. Dynamic Light Scattering Common Terms Defined. http://www.biophysics.bioc.cam.ac.uk/wp-content/uploads/2011/02/DLS_Terms_defined_Malvern.pdf (04/16),

144. Hsu, E. C.; Fleet, C.; Cheung, A.; Gao, J. High concentration chitosan-nucleic acid polyplex compositions. US 2011/0039917 A1, 2011.

145. Davies, L. A.; McLachlan, G.; Sumner-Jones, S. G.; Ferguson, D.; Baker, A.; Tennant, P.; Gordon, C.; Vrettou, C.; Baker, E.; Zhu, J.; Alton, E. W.; Collie, D. D.; Porteous, D. J.; Hyde, S. C.; Gill, D. R., Enhanced lung gene expression after aerosol delivery of concentrated pDNA/PEI complexes. *Molecular therapy : the journal of the American Society of Gene Therapy* **2008,** 16, (7), 1283-90.

146. Apo-ONE Homogeneous Caspase-3/7 Assay Instructions For Use of Products G7790, G7791 and G7792. https://www.promega.com/~/media/files/resources/protocols/technical%20bulletins/0/apo one%20homogeneous%20caspase%203%207%20assay%20protocol.pdf (05/11/2015),

147. Stowe, D. F.; Camara, A. K., Mitochondrial reactive oxygen species production in excitable cells: modulators of mitochondrial and cell function. *Antioxidants & redox signaling* **2009,** 11, (6), 1373-414.

148. Malich, G.; Markovic, B.; Winder, C., The sensitivity and specificity of the MTS tetrazolium assay for detecting the in vitro cytotoxicity of 20 chemicals using human cell lines. *Toxicology* **1997,** 124, (3), 179-92.

149. Droemann, D.; Albrecht, D.; Gerdes, J.; Ulmer, A. J.; Branscheid, D.; Vollmer, E.; Dalhoff, K.; Zabel, P.; Goldmann, T., Human lung cancer cells express functionally active Toll-like receptor 9. *Respir Res* **2005,** 6, 1.

150. Barnie, P. A.; Zhang, P.; Lu, P.; Chen, X.; Su, Z.; Wang, S.; Xu, H., CpG-oligodeoxynucleotides suppress the proliferation of A549 lung adenocarcinoma cells via toll-like receptor 9 signaling and upregulation of Runt-related transcription factor 3 expression. *Biomed Rep* **2014,** 2, (3), 374-377.

151. Drent, M.; Cobben, N. A.; Henderson, R. F.; Wouters, E. F.; van Dieijen-Visser, M., Usefulness of lactate dehydrogenase and its isoenzymes as indicators of lung damage or inflammation. *The European respiratory journal* **1996,** 9, (8), 1736-42.

152. Kawai, T.; Akira, S., TLR signaling. *Cell Death Differ* **2006,** 13, (5), 816-25.

153. Hsu, E. C.; Fleet, C.; Cheung, A.; Gao, J. High Concentration Chitosan-Nucleic Acid Polyplex Compositions. US 2011/0039917 A1, 2011.

154. Jiang, D.; Salem, A. K., Optimized dextran-polyethylenimine conjugates are efficient non-viral vectors with reduced cytotoxicity when used in serum containing environments. *International journal of pharmaceutics* **2012,** 427, (1), 71-9.

155. Kim, N.; Jiang, D.; Jacobi, A. M.; Lennox, K. A.; Rose, S. D.; Behlke, M. A.; Salem, A. K., Synthesis and characterization of mannosylated pegylated polyethylenimine as a carrier for siRNA. *International journal of pharmaceutics* **2012,** 427, (1), 123-33.

156. Intra, J.; Salem, A. K., Rational design, fabrication, characterization and in vitro testing of biodegradable microparticles that generate targeted and sustained transgene expression in HepG2 liver cells. *Journal of drug targeting* **2011,** 19, (6), 393-408.

157. Moghimi, S. M.; Symonds, P.; Murray, J. C.; Hunter, A. C.; Debska, G.; Szewczyk, A., A two-stage poly(ethylenimine)-mediated cytotoxicity: implications for gene transfer/therapy. *Molecular therapy : the journal of the American Society of Gene Therapy* **2005,** 11, (6), 990-995.

158. Lungwitz, U.; Breunig, M.; Blunk, T.; Gopferich, A., Polyethylenimine-based non-viral gene delivery systems. *European journal of pharmaceutics and biopharmaceutics : official journal of Arbeitsgemeinschaft fur Pharmazeutische Verfahrenstechnik e.V* **2005,** 60, (2), 247-66.

159. Yue, J.; Wu, J.; Liu, D.; Zhao, X.; Lu, W. W., BMP2 gene delivery to bone mesenchymal stem cell by chitosan-g-PEI nonviral vector. *Nanoscale Research Letters* **2015,** 10, 203.

160. Wongrakpanich, A.; Adamcakova-Dodd, A.; Xie, W.; Joshi, V. B.; Mapuskar, K. A.; Geary, S. M.; Spitz, D. R.; Thorne, P. S.; Salem, A. K., The Absence of CpG in Plasmid DNA–Chitosan Polyplexes Enhances Transfection Efficiencies and Reduces Inflammatory Responses in Murine Lungs. *Mol. Pharm.* **2014,** 11, (3), 1022-1031.

161. Hagiwara, K.; Anastasia, R.; Nakata, M.; Sato, T., Physicochemical properties of pDNA/chitosan complexes as gene delivery systems. *Current drug discovery technologies* **2011,** 8, (4), 329-39.

162. Ingle, N. P.; Malone, B.; Reineke, T. M., Poly(glycoamidoamine)s: a broad class of carbohydrate-containing polycations for nucleic acid delivery. *Trends in biotechnology* **2011,** 29, (9), 443-53.

163. McLendon, P. M.; Buckwalter, D. J.; Davis, E. M.; Reineke, T. M., Interaction of poly(glycoamidoamine) DNA delivery vehicles with cell-surface glycosaminoglycans leads to polyplex internalization in a manner not solely dependent on charge. *Molecular pharmaceutics* **2010,** 7, (5), 1757-68.

164. Liu, Y.; Wenning, L.; Lynch, M.; Reineke, T. M., New poly(d-glucaramidoamine)s induce DNA nanoparticle formation and efficient gene delivery into mammalian cells. *Journal of the American Chemical Society* **2004,** 126, (24), 7422-3.

165. Liu, Y.; Reineke, T. M., Hydroxyl stereochemistry and amine number within poly(glycoamidoamine)s affect intracellular DNA delivery. *Journal of the American Chemical Society* **2005,** 127, (9), 3004-15.

166. Thomas, P.; Smart, T. G., HEK293 cell line: a vehicle for the expression of recombinant proteins. *Journal of pharmacological and toxicological methods* **2005,** 51, (3), 187-200.

167. Zhang, X.; Edwards, J. P.; Mosser, D. M., The Expression of Exogenous Genes in Macrophages: Obstacles and Opportunities. *Methods in molecular biology (Clifton, N.J.)* **2009,** 531, 123.

168. T009-Tehnical Bulletin 260/280 and 260/230 Ratios. http://www.nanodrop.com/Library/T009-NanoDrop%201000-&-NanoDrop%208000-Nucleic-Acid-Purity-Ratios.pdf (04/18/2015),

169. Tang, X. W.; Liao, C.; Li, Y.; Xie, X. M.; Huang, Y. L., [Modified guanidine hydrochloride method for DNA extraction from cord blood used in HLA genotyping]. *Zhongguo shi yan xue ye xue za zhi / Zhongguo bing li sheng li xue hui = Journal of experimental hematology / Chinese Association of Pathophysiology* **2006,** 14, (2), 363-5.

170. Ingle, N. P.; Malone, B.; Reineke, T. M., Poly(glycoamidoamine)s: a broad class of carbohydrate-containing polycations for nucleic acid delivery. *Trends in biotechnology* **2011,** 29, (9), 443-453.

171. Rejman, J.; Bragonzi, A.; Conese, M., Role of Clathrin- and Caveolae-Mediated Endocytosis in Gene Transfer Mediated by Lipo- and Polyplexes. *Molecular therapy : the journal of the American Society of Gene Therapy* **2005,** 12, (3), 468-474.

172. McLendon, P. M.; Fichter, K. M.; Reineke, T. M., Poly(glycoamidoamine) vehicles promote pDNA uptake through multiple routes and efficient gene expression via caveolae-mediated endocytosis. *Molecular pharmaceutics* **2010,** 7, (3), 738-50.

173. Zanella, F.; Lorens, J. B.; Link, W., High content screening: seeing is believing. *Trends in biotechnology* **2010,** 28, (5), 237-45.

174. Buchser, W.; Collins, M.; Garyantes, T.; Guha, R.; Haney, S.; Lemmon, V.; Li, Z.; Trask, O. J., Assay Development Guidelines for Image-Based High Content Screening, High Content Analysis and High Content Imaging. In *Assay Guidance Manual*, Sittampalam, G. S.; Coussens, N. P.; Nelson, H.; Arkin, M.; Auld, D.; Austin, C.; Bejcek, B.; Glicksman, M.; Inglese, J.; Lemmon, V.; Li, Z.; McGee, J.; McManus, O.; Minor, L.; Napper, A.; Riss, T.; Trask, O. J.; Weidner, J., Eds. Bethesda (MD), 2004.

175. Abraham, V. C.; Taylor, D. L.; Haskins, J. R., High content screening applied to large-scale cell biology. *Trends Biotechnol.* **2004,** 22, (1), 15-22.

176. Giuliano, K. A.; Haskins, J. R.; Taylor, D. L., Advances in high content screening for drug discovery. *Assay and drug development technologies* **2003,** 1, (4), 565-77.

177. Nichols, A., High content screening as a screening tool in drug discovery. *Methods Mol Biol* **2007,** 356, 379-87.

178. de Raad, M.; Teunissen, E. A.; Lelieveld, D.; Egan, D. A.; Mastrobattista, E., High-content screening of peptide-based non-viral gene delivery systems. *Journal of controlled release : official journal of the Controlled Release Society* **2012,** 158, (3), 433-42.

179. Verma, I. M.; Weitzman, M. D., Gene therapy: twenty-first century medicine. *Annual review of biochemistry* **2005,** 74, 711-38.

180. Ramamoorth, M.; Narvekar, A., Non viral vectors in gene therapy- an overview. *Journal of clinical and diagnostic research : JCDR* **2015,** 9, (1), Ge01-6.

181. Mali, S., Delivery systems for gene therapy. *Indian journal of human genetics* **2013,** 19, (1), 3-8.

182. Nayerossadat, N.; Maedeh, T.; Ali, P. A., Viral and nonviral delivery systems for gene delivery. *Advanced biomedical research* **2012,** 1, 27.

183. Ojea-Jimenez, I.; Tort, O.; Lorenzo, J.; Puntes, V. F., Engineered nonviral nanocarriers for intracellular gene delivery applications. *Biomedical materials (Bristol, England)* **2012,** 7, (5), 054106.

184. Wang, W.; Li, W.; Ma, N.; Steinhoff, G., Non-viral gene delivery methods. *Current pharmaceutical biotechnology* **2013,** 14, (1), 46-60.

185. Wang, D.; Gao, G., State-of-the-art human gene therapy: part I. Gene delivery technologies. *Discovery medicine* **2014,** 18, (97), 67-77.

186. Jin, S.; Ye, K., Nanoparticle-mediated drug delivery and gene therapy. *Biotechnology progress* **2007,** 23, (1), 32-41.

187. Luo, D.; Saltzman, W. M., Synthetic DNA delivery systems. *Nature biotechnology* **2000,** 18, (1), 33-7.

188. Godbey, W. T.; Wu, K. K.; Mikos, A. G., Poly(ethylenimine) and its role in gene delivery. *Journal of Controlled Release* **1999,** 60, (2–3), 149-160.

189. de Bruin, K.; Ruthardt, N.; von Gersdorff, K.; Bausinger, R.; Wagner, E.; Ogris, M.; Brauchle, C., Cellular dynamics of EGF receptor-targeted synthetic viruses. *Molecular therapy : the journal of the American Society of Gene Therapy* **2007,** 15, (7), 1297-305.

190. Godbey, W. T.; Wu, K. K.; Mikos, A. G., Tracking the intracellular path of poly(ethylenimine)/DNA complexes for gene delivery. *Proc Natl Acad Sci U S A* **1999,** 96, (9), 5177-81.

191. Akita, H.; Ito, R.; Khalil, I. A.; Futaki, S.; Harashima, H., Quantitative three-dimensional analysis of the intracellular trafficking of plasmid DNA transfected by a

nonviral gene delivery system using confocal laser scanning microscopy. *Molecular therapy : the journal of the American Society of Gene Therapy* **2004,** 9, (3), 443-51.

192. Clamme, J. P.; Krishnamoorthy, G.; Mely, Y., Intracellular dynamics of the gene delivery vehicle polyethylenimine during transfection: investigation by two-photon fluorescence correlation spectroscopy. *Biochimica et biophysica acta* **2003,** 1617, (1-2), 52-61.

193. Kircheis, R.; Wightman, L.; Wagner, E., Design and gene delivery activity of modified polyethylenimines. *Adv. Drug Del. Rev.* **2001,** 53, (3), 341-358.

194. Neu, M.; Fischer, D.; Kissel, T., Recent advances in rational gene transfer vector design based on poly(ethylene imine) and its derivatives. *The journal of gene medicine* **2005,** 7, (8), 992-1009.

195. Itaka, K.; Harada, A.; Yamasaki, Y.; Nakamura, K.; Kawaguchi, H.; Kataoka, K., In situ single cell observation by fluorescence resonance energy transfer reveals fast intra-cytoplasmic delivery and easy release of plasmid DNA complexed with linear polyethylenimine. *The journal of gene medicine* **2004,** 6, (1), 76-84.

196. Intra, J.; Salem, A. K., Characterization of the transgene expression generated by branched and linear polyethylenimine-plasmid DNA nanoparticles in vitro and after intraperitoneal injection in vivo. *Journal of controlled release : official journal of the Controlled Release Society* **2008,** 130, (2), 129-138.

197. Instrumentation, Operetta. http://www.wistar.org/our-science/shared-facilities/molecular-screening-facility/instrumentation (05/06/2015),

198. D'Mello, S.; Salem, A. K.; Hong, L.; Elangovan, S., Characterization and evaluation of the efficacy of cationic complex mediated plasmid DNA delivery in human embryonic palatal mesenchyme cells. *J Tissue Eng Regen Med* **2014**.

199. Berridge, M. V.; Herst, P. M.; Tan, A. S., Tetrazolium dyes as tools in cell biology: new insights into their cellular reduction. *Biotechnology annual review* **2005,** 11, 127-52.

200. Remy-Kristensen, A.; Clamme, J. P.; Vuilleumier, C.; Kuhry, J. G.; Mely, Y., Role of endocytosis in the transfection of L929 fibroblasts by polyethylenimine/DNA complexes. *Biochimica et biophysica acta* **2001,** 1514, (1), 21-32.

201. Rajendra, Y.; Kiseljak, D.; Baldi, L.; Wurm, F. M.; Hacker, D. L., Transcriptional and post-transcriptional limitations of high-yielding, PEI-mediated transient transfection with CHO and HEK-293E cells. *Biotechnology progress* **2015,** 31, (2), 541-9.

202. Mozley, O. L.; Thompson, B. C.; Fernandez-Martell, A.; James, D. C., A mechanistic dissection of polyethylenimine mediated transfection of CHO cells: to enhance the efficiency of recombinant DNA utilization. *Biotechnology progress* **2014,** 30, (5), 1161-70.

203. Liu, C.; Dalby, B.; Chen, W.; Kilzer, J. M.; Chiou, H. C., Transient transfection factors for high-level recombinant protein production in suspension cultured mammalian cells. *Molecular biotechnology* **2008,** 39, (2), 141-53.

204. Subrizi, A.; Yliperttula, M.; Tibaldi, L.; Schacht, E.; Dubruel, P.; Joliot, A.; Urtti, A., Optimized transfection protocol for efficient in vitro non-viral polymeric gene delivery to human retinal pigment epithelial cells (ARPE-19). **2009**.

205. Lindberg, M. F.; Le Gall, T.; Carmoy, N.; Berchel, M.; Hyde, S. C.; Gill, D. R.; Jaffrès, P.-A.; Lehn, P.; Montier, T., Efficient in vivo transfection and safety profile of a CpG-free and codon optimized luciferase plasmid using a cationic lipophosphoramidate in a multiple intravenous administration procedure. *Biomaterials* **2015,** 59, (0), 1-11.

206. Gebremedhin, S.; Singh, A.; Koons, S.; Bernt, W.; Konopka, K.; Duzgunes, N., Gene delivery to carcinoma cells via novel non-viral vectors: Nanoparticle tracking analysis and suicide gene therapy. *European Journal of Pharmaceutical Sciences* **2014,** 60, (0), 72-79.

207. Kizjakina, K.; Bryson, J. M.; Grandinetti, G.; Reineke, T. M., Cationic glycopolymers for the delivery of pDNA to human dermal fibroblasts and rat mesenchymal stem cells. *Biomaterials* **2012,** 33, (6), 1851-1862.